DEVELOPMENT, VALIDATION, AND IMPLEMENTATION OF NIR CALIBRATION MODELS IN A COMMERCIAL CONTINUOUS MANUFACTURING PROCESS

By
Jenny M. Vargas Irizarry

A dissertation submitted in partial fulfillment of the requirements for the degree of

DOCTOR OF PHILOSOPHY

in

Applied Chemistry

UNIVERSITY OF PUERTO RICO

MAYAGÜEZ CAMPUS

2017

_____	_____
Rodolfo J. Romañach, Ph.D. President, Graduate Committee	Date
_____	_____
Manel Alcalà, Ph.D. Member, Graduate Committee	Date
_____	_____
Rafael Méndez, Ph.D. Member, Graduate Committee	Date
_____	_____
Félix R. Román, Ph.D. Member, Graduate Committee	Date
_____	_____
Jessica Torres, Ph.D. Member, Graduate Committee	Date
_____	_____
Paul Sundaram, Ph.D. Representative, Graduate Studies	Date
_____	_____
Enrique Meléndez, Ph.D. Director, Chemistry Department	Date

ABSTRACT

Near infrared spectroscopy is a very promising non-invasive technique since it allows the use of calibration models to monitor physical and chemical properties of raw materials, intermediate products (blend), and the end product (tablets) without sample preparation. In this investigation, near infrared (NIR) spectroscopy and chemometric models were used as in-line techniques integrated to a closed-loop control system that provides drug concentration results in real time. The use of NIR chemometric modelling for continuous manufacturing (CM) processes, such as the one discussed in this study, allows the manufacture of large quantities of product in a short time while maintaining all necessary controls to ensure high quality of the end product.

The first investigation presented in this dissertation focuses on the use of chemometric models and variographic analysis to evaluate the analytical and sampling errors of the predicted API concentration of blends produced during a pharmaceutical CM process. An NIR calibration model was developed using blends prepared in lab scale equipment. The model was validated with blends prepared using lab scale, pilot plant, and CM processes. Variographic analysis was performed to blends and tablets prepared using the CM process.

The second investigation presented in this dissertation focuses on the integration of PAT and CM in a CGMP regulated pharmaceutical plant. This study shows the application of CM and chemometric modelling for the commercial manufacturing of a pharmaceutical product. Two NIR chemometric models were developed, validated, and implemented for the identification and quantification of blends produced during a commercial CM process. The calibration and validation sets were prepared using the CM process, thus including sample and process variations into the models. All blend spectra were collected in-line, during the manufacturing process. An original approach is suggested for the calculation of the standard error of prediction (SEP) acceptance criteria. Variographic analysis of a 28-hour commercial run was performed.

The third investigation presented in this dissertation focuses on testing the robustness of an NIR calibration model for the prediction of drug concentration in core tablets during a CM process. The robustness evaluation was performed by exploring how the NIR spectra and predictions were affected when tablets were: (1) exposed to the environment for prolonged times; (2) protected from the environment; and (3) experiencing their “relaxation” phase (elastic recovery). An NIR calibration model was developed with tablets prepared using lab-scale equipment. Two

optimizations were performed to the NIR calibration model based on: (1) spectral range and (2) calibration sample set. The inclusion of tablets representative of the CM process to the NIR calibration model proved to be an efficient way of including inherent process variations, thus increasing the robustness of the model.

RESUMEN

La espectroscopia de infrarrojo cercano es una técnica no invasiva muy prometedora ya que permite el uso de modelos de calibración para monitorear propiedades físicas y químicas de materiales, productos intermediarios (mezclas) y del producto final (tabletas) la necesidad de hacer preparación de muestras. En esta investigación, la espectroscopia de infrarrojo cercano y modelos quemométricos fueron utilizados como técnicas en línea integradas a un sistema de control cerrado que provee resultados de la concentración de droga en tiempo real. El uso de infrarrojo cercano con modelos quemométricos para procesos de manufactura continua, como los discutidos en esta disertación, permiten la manufactura de grandes cantidades de productos en un corto tiempo manteniendo todos los controles necesarios para asegurar la alta calidad del producto final.

La primera investigación presentada en esta disertación se enfocó en el uso de modelos quemométricos y análisis variográfico para evaluar los errores analíticos y de muestreo de la predicción de concentración de droga de mezclas producidas durante un proceso farmacéutico de manufactura continua. Un modelo de calibración de infrarrojo cercano fue desarrollado con mezclas preparadas utilizando equipo de laboratorio. El modelo fue validado con mezclas preparadas utilizando equipo de laboratorio, una planta piloto, y un proceso de manufactura continua. El análisis variográfico fue realizado a mezclas y tabletas preparadas utilizando el proceso de manufactura continua.

La segunda investigación presentada en esta disertación se enfocó en la integración de PAT y manufactura continua en una planta farmacéutica regulada (CGMP). Este estudio mostró la aplicación de manufactura continua y modelaje quemométrico para la manufactura comercial de un producto farmacéutico. Dos modelos quemométricos de infrarrojo cercano fueron desarrollados, validados e implementados para la identificación y cuantificación de mezclas producidas durante un proceso comercial de manufactura continua. Los conjuntos de calibración y validación fueron preparados utilizando el proceso de manufactura continua, incluyendo así variaciones de muestra y proceso a los modelos. Todos los espectros de las mezclas fueron tomados en línea, durante el proceso de manufactura. Un acercamiento original fue sugerido para calcular el criterio de aceptación para el error estándar de predicción (SEP

por sus siglas en ingles). El análisis variográfico fue realizado para una corrida comercial de 28 horas de duración.

La tercera investigación presentada en esta disertación se enfocó en comprobar la robustez del modelo quemométrico para la predicción de la concentración de droga en tabletas durante el proceso de manufactura continua. La evaluación de robustez se llevó a cabo explorando como se afectaron los espectros de infrarrojo cercano y las predicciones cuando las tabletas: (1) fueron expuestas al ambiente por un tiempo prolongado; (2) fueron protegidas del ambiente; y (3) estuvieron en su fase de relajación (recuperación elástica). Un modelo de calibración de infrarrojo cercano fue desarrollado con tabletas preparadas utilizando equipo de laboratorio. Dos optimizaciones fueron realizadas al modelo de calibración de infrarrojo cercano basadas en: (1) el rango espectral y (2) el conjunto de calibración. La inclusión de tabletas representativas del proceso de manufactura continua al modelo de calibración de infrarrojo cercano probó ser una manera eficiente de incluir variaciones del proceso, lo que a su vez aumento la robustez del modelo.

To my two angels Nefty and Gael,
You are the engine of my life.
Without your support,
None of this would have been possible

El que puede tener paciencia puede tener lo que quiera
-Benjamín Franklin

“He that can have patience can have what he will”
-Benjamin Franklin

ACKNOWLEDGEMENTS

I am eternally grateful for my husband and son (Nefty and Gael) who have only been supportive and encouraging through all this process, from the beginning. I only got encouraging words and strength from you. I will be forever indebted for your patience. To my family, Jenny, Israel, Carmen, and Rali, who have always been supportive.

I want to express my gratitude to my PhD advisor, Dr. Rodolfo Romañach. Thank you for your guidance, support, patience, and motivation. This experience has shaped my personal and professional life. I would like to extend my gratitude to my graduate committee members Dra. Jessica Torres, Dr. Manel Alcalà, Dr. Félix R. Román, and Dr. Rafael Méndez for their availability and suggestions throughout my studies.

I want to thank Janssen Ortho LLC, Gurabo, especially Eric Sanchez, for the opportunity of completing an internship at their facilities. This experience enriched my professional career significantly. Eric, thank you for believing in me, for your support, and your trust. I also want to thank my colleagues at Janssen who made the transition from the university to the work place easier. I am very grateful.

TABLE OF CONTENTS

List of Tables

List of Figures

Chapter 1

1 Introduction

1.1 Motivation

The work presented in this dissertation resulted as part of the collaboration between the University of Puerto Rico, Mayaguez Campus (UPRM) and Janssen Ortho LLC at Gurabo, PR.

In pharmaceutical procedures, the quality of the final drug product is assured as long as critical process parameters (CPPs) and critical quality attributes (CQAs) are maintained within established limits [1]. Traditionally the quality verification of the product is performed off-line after the batch has been completed (batch process). Therefore, if the product is not in compliance with its specifications, the complete batch is lost. Continuous manufacturing offers the flexibility of monitoring the manufacturing process from beginning to end, decreasing the probability of losing a complete batch due to specification failure of the product during the quality verification, after batch completion.

Traditionally, a batch process is performed during several separate steps. It may be noted that CM involves the merging of several process steps to make one whole continuous process. This merge of several steps could complicate the manufacturing process. However, if CQA and CPP parameters are monitored and maintained within specifications, CM can be successful. The use of process analytical technology (PAT) helps to understand and control the manufacturing process [2]. Implementation of PAT in a CM process will assure the manufacture of high quality drug products at low costs [3]. Multivariate data analysis (chemometric modelling), NIR spectrometers (in-line spectra acquisition), and process control tools are PAT techniques that can be combined to monitor a CM process.

In this investigation, NIR and chemometric models were used as an in-line techniques integrated to a closed-loop control system that provides API concentration results (NIR

predictions) in real time. The use of NIR chemometric modelling for CM processes, such as the one discussed in this study, allows the manufacture of large quantities of product in a short time while maintaining all necessary controls to ensure high quality of the end product [4, 5]. This research includes the investigation performed for the implementation of the first FDA approved CM line for a pharmaceutical company in Puerto Rico. This investigation and subsequent approval serves as a basis for other companies worldwide to begin making changes in their manufacturing processes which will eventually lead to a revolution in the pharmaceutical industry. This approved change from a batch process to a CM process included the complete development, validation, and implementation of blend and tablet monitoring processes to achieve real time release testing (RTRt). This study will influence further investigations related to implementation of continuous manufacturing in pharmaceutical processes.

1.2 Scope

The scope of this dissertation is to develop, validate, and implement multivariate calibration models using NIR spectroscopy to assure the desired product quality of the end product during a continuous manufacturing process in an FDA regulated pharmaceutical company.

1.3 Goal

The overall goal of this dissertation is the implementation of NIR calibration models to identify and determine the concentration of the active pharmaceutical ingredient (API) in blends and tablets. Part of this research was performed within the Engineering Research Center for Structured Organic Particulate Systems (ERC-CSOPS) while the other part was performed at the recently FDA approved CM line at Janssen, Puerto Rico [6-10].

The objectives of this investigation were to (1) analyze accuracy and precision of NIR predictions to assure the implementation of a robust calibration model; (2) evaluate spectra acquisition parameters for blends and tablets in diffuse reflectance and transmittance mode; (3) evaluate process parameters that could affect NIR predictions; (4) use alternative statistical tools such as the distance to the model in the X-space (DModX) and the Hotelling's T^2Range (T^2R) to evaluate robustness of the calibration models; (5) incorporate theory of sampling for blend acquisition since sampling could affect the NIR results; (6) evaluate analytical and sampling errors of blends and tablets in the NIR predictions of the API using variographic analysis; and (7) compare blends and tablets results since blends could be affected by segregation and thus, tablet NIR spectra could be affected.

1.4 References

1. Yu LX. Pharmaceutical quality by design: product and process development, understanding, and control. Pharmaceutical research. 2008;25(4):781-91.

2. Food U, Administration D. PAT guidance for industry–a framework for innovative pharmaceutical development, manufacturing and quality assurance. US Department of Health and Human Services. Food and Drug Administration, Center for drug evaluation and research, Center for veterinary medicine, Office of regulatory affairs, Rockville, MD. 2004.

3. McAuliffe MAP, O'Mahony GE, Blackshields CA, Collins JA, Egan DP, Kiernan L et al. The Use of PAT and Off-line Methods for Monitoring of Roller Compacted Ribbon and Granule Properties with a View to Continuous Processing. Organic Process Research & Development. 2015;19(1):158-66.

4. Märk J, Andre M, Karner M, Huck CW. Prospects for multivariate classification of a pharmaceutical intermediate with near-infrared spectroscopy as a process analytical technology (PAT) production control supplement. European Journal of Pharmaceutics and Biopharmaceutics. 2010;76(2):320-7.

5. Shaibu A, Yang Y, Cho BR, Choi Y, Shin S, editors. Process analytical technology (PAT) initiatives in improving pharmaceutical quality by design. IIE Annual Conference. Proceedings; 2008: Institute of Industrial Engineers-Publisher.

6. Brennan Z. FDA Allows First Switch From Batch to Continuous Manufacturing for HIV Drug. In: Regularoty affairs professionals society. http://raps.org/Regulatory-Focus/News/2016/04/12/24739/FDA-Allows-First-Switch-From-Batch-to-Continuous-Manufacturing-for-HIV-Drug/. 2016. Accessed July 23, 2016.

7. Yu L. Continuous Manufacturing Has a Strong Impact on Drug Quality. In: FDA Voice. http://blogs.fda.gov/fdavoice/index.php/2016/04/continuous-manufacturing-has-a-strong-impact-on-drug-quality/. 2016. Accessed July 23, 2016.

8. Gray N. In first, FDA approves Janssen's switch to continuous manufacturing for HIV drug. In: BioPharma Dive. http://www.biopharmadive.com/news/in-first-fda-approves-janssens-switch-to-continuous-manufacturing-for-hiv/417460/. 2016. Accessed July 23, 2016.

9. Langhauser K. Janssen's Historic FDA Approval. The FDA has approved -- for the first time in history -- a manufacturer's production method change from "batch" to continuous manufacturing. In: Pharmaceutical Manufacturing. http://www.pharmamanufacturing.com/articles/2016/janssens-historic-fda-approval/. 2016. Accessed July 23, 2016.

10. MacDonald G. Janssen working on other continuous processes post US FDA OK for Prezista. In: in-Pharma Technologist. http://www.in-

pharmatechnologist.com/Processing/Janssen-working-on-other-continuous-processes-post-US-FDA-OK-for-Prezista?utm_source=copyright&utm_medium=OnSite&utm_campaign=copyright. 2016. Accessed July 23, 2016.

Chapter 2

2 Background

2.1 Summary

Pharmaceutical companies are transforming the manufacture of drug products. FDA regulated facilities are investigating the modification of drug preparation by implementing continuous manufacturing (CM) processes using process analytical technology (PAT) and quality by design (QbD) approaches [1]. The pharmaceutical sector has intensified their research towards implementing CM processes as a substitute to the current batch process [1-5]. This increase in investigations has led to a deeper understanding of what is continuous manufacturing and how it is affected by different process parameters.

Implementation of CM as a commercial pharmaceutical process is bound to increase efficiency (release time) and improve the financial (production cost), environmental (waste and footprint), and operational aspects (less, smaller equipment). CM can also improve the agility, flexibility, and robustness of manufacturing [2, 6, 7]. The implementation of CM involves the monitoring of critical quality attributes (CQAs), such as drug concentration, using process analytical technology linked to a control system [8-13]. PAT systems provide real time results allowing the monitoring and control of the CM process. A CM process produces large data sets which require the use of multivariate data analysis (chemometric models). Multivariate data analysis combined with PAT techniques such as near infrared spectroscopy (NIRS), have been previously used to develop models for the identification and assay of solids to determine the quality of the end product [8, 14, 15]. The use of NIR has increased since the implementation of CM usually involves performing in-line and at-line analysis of the processes (e.g. blends, tablets) [16]. Therefore the implementation of CM integrated with PAT in pharmaceutical industries is expected to provide high quality products at lower manufacturing costs [17]. The studies presented in this dissertation include the use of the same concepts (NIR, PAT, CM, chemometric models) but applied to a commercial CM run.

2.2 Process Analytical Technology (PAT)

Process analytical technology (PAT) is considered by the FDA as "*a system for designing, analyzing, and controlling manufacturing through timely measurements (e.g. during processing) of critical quality and performance attributes of raw and in-process materials and processes, with the goal of ensuring final product quality*" [18]. The objective of PAT is to improve the understanding and control of manufacturing processes by efficiently designing processes in which quality of the final product is achieved as the result of the design. The quality of the product is ensured through the design of the manufacturing process rather than just testing after production. There must be a complete understanding beforehand of how materials and process parameters affect the quality of the final product to achieve this type of process.

Pharmaceutical processes involve several steps (unit operations) focused on performing specific tasks to ensure high quality of the final product. Powder mixing is a key unit operation for tablet manufacturing. Content uniformity, a CQA, is directly linked to blend homogeneity [19]. Therefore, powder blending and homogeneity should be closely monitored and controlled to ensure the quality of the tablets produced. The use of near infrared spectroscopy (NIRS) to monitor blends is widely accepted since this technique allows a non-invasive, fast in-line analysis of blends without sample preparation.

2.3 Near Infrared Spectroscopy (NIRS)

Near infrared (NIR) is one of the most commonly used spectroscopic methods in the pharmaceutical industry [20-29]. This method offers essential information on chemical and physical properties of materials and is fast, non-invasive, and non-destructive. NIR spectroscopy shows absorption bands in the wavenumber region from about 4000 up to 12500 cm^{-1} (800 – 2500 nm) (**Figure 2.1**) [30, 31]. This spectral region covers mainly overtones and combination bands of molecular vibrations that modulate the dipole moment of molecules with X-H bonds (e.g. organic compounds such as CH, OH, and NH).

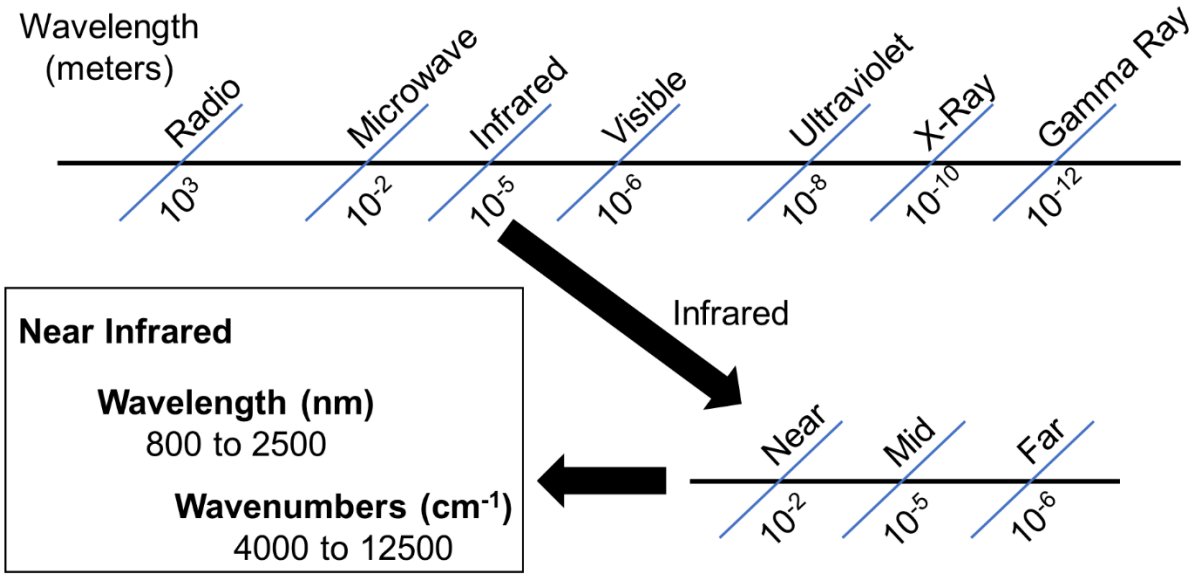

Figure 2.1 Electromagnetic spectrum with the infrared region defined

Combination bands are formed due to the combination of two or more fundamental frequencies and are usually 10 times weaker (lower intensity) than the original fundamental band. Overtones occurs when the vibrational mode is excited from the fundamental or ground energy level (υ = 0) to a higher energy level (υ = 2), known as the first overtone. This excitation could also occur from the fundamental energy level (v = 0) to an even higher energy level (υ = 3), thus producing what is known as a second overtone. However, probability of occurrence decreases as the excitation from the

fundamental to a higher energy level increases (v = n; n = 2, 3, 4, etc.). Overtones tend to be 20 to 100 times weaker (lower intensity) than their fundamental band. The molecular vibrations that produce overtones and combination bands require more energy for the vibration to go from one energy level to the next. The absorptions observed in the NIR region are at a higher state of excitement and thus, require more energy than the fundamental absorption band. Fundamental frequencies obey Hooke's Law (Eq. 1).

$$\nu = \frac{1}{2\pi}\sqrt{\frac{k}{\mu}} \qquad \text{Eq. 1}$$

Where v is the vibrational frequency, k is the classical force constant, and μ is the reduced mass of the two atoms given by Eq. 2.

$$\mu = \frac{m_1 m_2}{m_1 + m_2} \qquad \text{Eq. 2}$$

These fundamental vibrations are described by the harmonic oscillator (**Figure 2.2**) model where transitions are allowed for energy changes of ±1. This quantum model defines the possible energy levels for a specific vibration as:

$$E_\nu = \left(\nu + \frac{1}{2}\right) h\nu \qquad \text{Eq. 3}$$

Where ν is the quantum number of the vibrational frequency and v is the fundamental frequency of the vibration (Eq. 1).

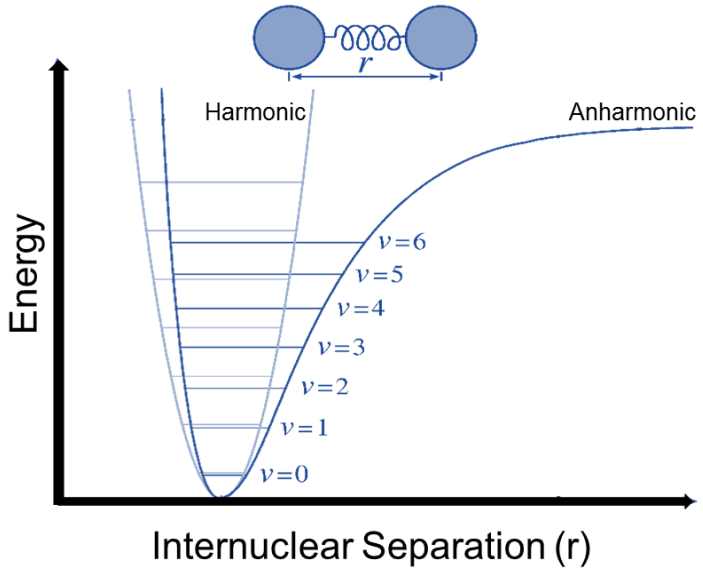

Figure 2.2 Representation of the harmonic and anharmonic oscillators

Molecular vibrations have been observed to occur with energy changes greater than ±1 (e.g. overtones). These energy changes (Δn = ±2, ±3, etc.) cannot be explained by the harmonic oscillator model. Anharmonicity (**Figure 2.2**) explains the occurrence of these energy changes, thus allowing the existence of the overtones observed in NIR. Energy levels in the anharmonic oscillator are not equally spaced as they get slightly closer as the energy increases [31]. This phenomenon is described by the anharmonic equation (Eq. 4).

$$E_v = \left(v + \frac{1}{2}\right) h\omega_e - \left(v + \frac{1}{2}\right)^2 \omega_e\chi_e + \left(v + \frac{1}{2}\right)^3 \omega_e y_e + \cdots \qquad \text{Eq. 4}$$

Where ω_e is the vibrational frequency (Eq. 1) and $\omega_e\chi_e$ is the anharmonicity constant.

NIR spectral differences are due to the differences observed in the intensity and position of overtones and combination bands [32]. In addition, differences in resonance, crystallinity, particle size, and temperature, among others, also have an influence on the

molecular spectral differences observed in NIR. Therefore, NIR spectra is dependent of the physical and chemical properties of the material [33].

Spectra of solids can be recorded in reflectance or transmittance. NIR diffuse reflectance is a technique widely used to analyze powders (**Figure 2.3**) [34]. When light is directed to a solid sample, it is reflected. The reflected light will endure specular or diffuse reflection. The specular reflection is the light reflected in a single angle (“mirror style”) while the diffused reflection light has uniform remission at all angles [35].

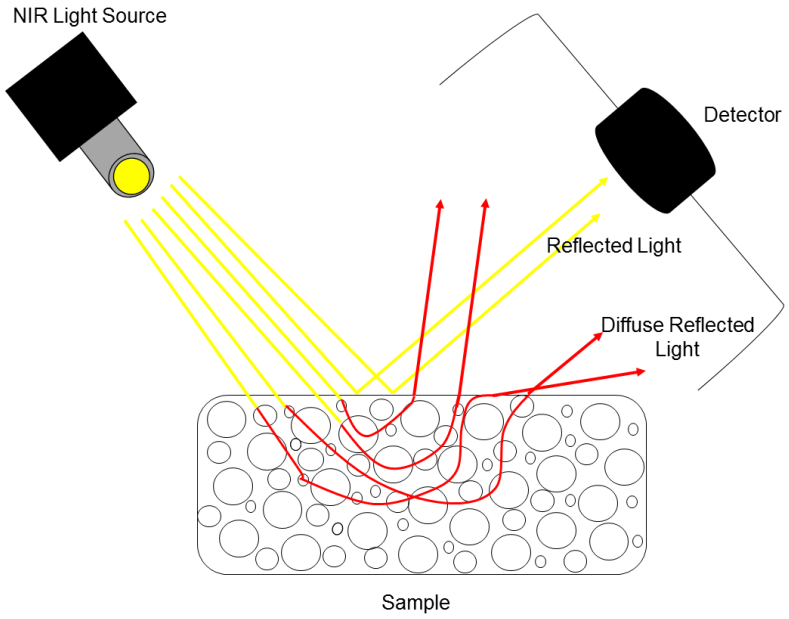

Figure 2.3 Schematic diagram of light scattering from a solid sample

NIR diffuse reflectance is based on the diffuse component since the specular component gives no information on the composition of the material [33]. The diffuse reflected signal is reduced due to absorption and scattering [30]. Scattering is related to differences in particle size, has a multiplicative effect on the absorbed light, and combines with other additive effects (e.g. shifts in baseline and chemical absorption) [33]. The multiplicative effect is explained by the Kubelka-Munck theory and can also be seen in the absorbance equation (Eq. 5) [36].

$$A = \log\left(\frac{1}{R}\right) \quad \text{Eq. 5}$$

The additive effect adopts the idea of theoretical models such as Kubelka-Munck and Beer-Lambert which assume that all or a constant part of the reflected light is detected [36]. However, most instruments used for diffuse reflectance only detect a fraction (1/c) of the reflected light. Therefore,

$$I_{detected} = \left(\frac{1}{c}\right)(I_{reflected}) \quad \text{Eq. 6}$$

$$A_{detected} = -log(R_{detected}) = -log\left(\frac{I_{detected}}{I_o}\right)$$
$$= \log c + log\left(\frac{I_o}{I_{reflected}}\right) = c' + A \quad \text{Eq. 7}$$

An additive baseline (additive effect in the absorbance values) is caused if c′ = log(c) is dependent upon the sample [36].

In transmittance spectra (**Figure 2.4**), the amount of light scattered through a sample is measured. Transmittance is defined by Eq. 8.

$$T = \left(\frac{I}{I_o}\right) \quad \text{Eq. 8}$$

Where *T* is the transmittance, *I* is the transmitted light, and I_o is the incident light. Transmittance will vary between 0 and 1. A transmittance of 1 indicates that no light was absorbed. Absorbance is calculated using Eq. 9.

$$A = 2 - \log \%T \quad \text{Eq. 9}$$

Where *A* is the absorbance and *T* is the transmittance.

The emitted radiation penetrates the sample and interacts with a greater portion of it, compared to diffuse reflectance where light penetrates only a few millimeters before being reflected [37].

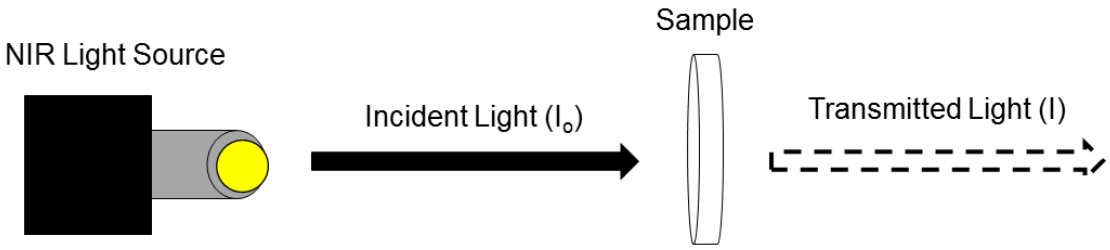

Figure 2.4 Schematic diagram of transmittance NIR

NIR spectroscopy has been a widely used method since it is non-invasive, requires no sample preparation and can determine physical and chemical parameters simultaneously in a rapid, non-destructive way [20, 28]. NIR allows the determination of physical and chemical parameters without sample preparation which greatly reduces costs [20-26]. Understanding of NIR spectroscopy has increased during recent years. Researchers are now able to differentiate between the effects of physical properties and the spectral variation related to the quantified analytes [38, 39]. NIR is currently being used to monitor and control continuous manufacturing processes [3, 40-42].

NIR has become an important technique in the implementation of modern control strategies using in-line measurements [16]. In addition, the use of this method with multivariate data analysis (chemometric modelling) has allowed the development of models to identify and quantify solids used to determine the quality of the end product [8, 14, 15]. The implementation of chemometric models in CM processes using NIR allows the manufacture of large quantities of product in less time while maintaining all necessary controls ensuring high quality of the end product [8, 43].

2.4 Literature Review

Implementation of CM processes using NIR and PAT is an efficient alternative of drug manufacture to substitute the batch process [1, 2, 40]. The implementation of a CM process is bound to improve the financial, environmental, and operational aspects because this process reduces the equipment space, material, waste and release time [2, 7]. Previous studies have also demonstrated how continuous manufacturing can increase the efficiency of the process by reducing the space needed for manufacturing (less and smaller equipment) and eliminating the relocation of material from room to room or from one facility to another [44-47].

Continuous manufacturing involves the monitoring of quality attributes such as API concentration, using process analytical technology (PAT). The use of multivariate data analysis such as chemometric modelling, allows the development of models to determine API concentration of blends and tablets prepared during a CM process, in real time (in-line analysis). Previous studies have described the development and validation of NIR methods to monitor blending in CM [3, 40, 48]. Sulub et al. demonstrated the use off-line PLS calibration approach to quantitatively monitor the concentration of API in real-time from laboratory scale to production scale [49].

NIR calibration models have been successfully used in previous studies where drug concentration of powder mixtures and homogeneity characterization were performed in a blend with four components [48, 50]. However, pharmaceutical blends contain more than two components. Studies have also indicated the importance of including process and sample variations to the developed model [51]. Blanco et al. demonstrated that preparation differences (laboratory, production, production-doped) influences the spectra and accuracy of the predictions. Furthermore, results showed the spectral differences to be related to scattering due to physical differences between the samples [52].

This dissertation describes the efforts performed to evaluate how sample preparation (laboratory, pilot plant, and CM scale) of blends and tablets affects the model outcome (NIR predictions of the API concentration). The effects of changes in environmental conditions and process variability were also evaluated. In addition, variographic analysis

was used to evaluate sampling and analytical errors in the NIR predictions. This work also includes different approaches to identify, study, and classify the spectra variability associated with physical parameters of blends (e.g. particle size) and tablets (e.g. hardness).

2.5 References

1. Anderson NG. Using Continuous Processes to Increase Production. Organic Process Research & Development. 2012;16(5):852-69.

2. Byrn S, Futran M, Thomas H, Jayjock E, Maron N, Meyer RF et al. Achieving continuous manufacturing for final dosage formation: challenges and how to meet them. May 20-21, 2014 Continuous Manufacturing Symposium. Journal of pharmaceutical sciences. 2015;104(3):792-802.

3. Martínez L, Peinado A, Liesum L, Betz G. Use of near-infrared spectroscopy to quantify drug content on a continuous blending process: Influence of mass flow and rotation speed variations. European Journal of Pharmaceutics and Biopharmaceutics. 2013;84(3):606-15.

4. Shi ZQ, McGhehey KC, Leavesley IM, Manley LF. On-line monitoring of blend uniformity in continuous drug product manufacturing process-The impact of powder flow rate and the choice of spectrometer: Dispersive vs. FT. J Pharm Biomed Anal. 2016;118:259-66. doi:10.1016/j.jpba.2015.11.005.

5. Colón YM, Vargas J, Sánchez E, Navarro G, Romañach RJ. Assessment of Robustness for a Near-Infrared Concentration Model for Real-Time Release Testing in a Continuous Manufacturing Process. J Pharm Innov. 2017;12(1):14-25. doi:10.1007/s12247-016-9265-6.

6. Lee SL, O'Connor TF, Yang X, Cruz CN, Chatterjee S, Madurawe RD et al. Modernizing pharmaceutical manufacturing: from batch to continuous production. Journal of Pharmaceutical Innovation. 2015;10(3):191-9.

7. Allison G, Cain YT, Cooney C, Garcia T, Bizjak TG, Holte O et al. Regulatory and quality considerations for continuous manufacturing. May 20–21, 2014 Continuous Manufacturing Symposium. Journal of pharmaceutical sciences. 2015;104(3):803-12.

8. Märk J, Andre M, Karner M, Huck CW. Prospects for multivariate classification of a pharmaceutical intermediate with near-infrared spectroscopy as a process analytical technology (PAT) production control supplement. European Journal of Pharmaceutics and Biopharmaceutics. 2010;76(2):320-7.

9. Wu H, Tawakkul M, White M, Khan MA. Quality-by-design (QbD): an integrated multivariate approach for the component quantification in powder blends. International journal of pharmaceutics. 2009;372(1-2):39-48.

10. Bakeev KA. Process Analytical Technology: Spectroscopic Tools and Implementation Strategies for the Chemical and Pharmaceutical Industries. Blackwell: Oxford, UK. 2005.

11. Helmdach L, Feth MP, Minnich C, Ulrich J. Application of ATR-MIR spectroscopy in the pilot plant—Scope and limitations using the example of Paracetamol

crystallizations. Chemical Engineering and Processing: Process Intensification. 2013;70:184-97.

12. Yu LX. Pharmaceutical quality by design: product and process development, understanding, and control. Pharmaceutical research. 2008;25(4):781-91.

13. Román-Ospino AD, Singh R, Ierapetritou M, Ramachandran R, Méndez R, Ortega-Zuñiga C et al. Near infrared spectroscopic calibration models for real time monitoring of powder density. Int J Pharm. 2016;512(1):61-74. doi:http://dx.doi.org/10.1016/j.ijpharm.2016.08.029.

14. Olsen BA, Borer MW, Perry FM, Forbes RA. Screening for counterfeit drugs using near-infrared spectroscopy. Pharmaceutical technology. 2002;26(6):62-71.

15. Sánchez MS, Bertran E, Sarabia LA, Ortiz MC, Blanco M, Coello J. Quality control decisions with near infrared data. Chemometrics and Intelligent Laboratory Systems. 2000;53(1–2):69-80.

16. Bu D, Wan B, McGeorge G. A discussion on the use of prediction uncertainty estimation of NIR data in partial least squares for quantitative pharmaceutical tablet assay methods. Chemometrics and Intelligent Laboratory Systems. 2013;120:84-91.

17. McAuliffe MAP, O'Mahony GE, Blackshields CA, Collins JA, Egan DP, Kiernan L et al. The Use of PAT and Off-line Methods for Monitoring of Roller Compacted Ribbon and Granule Properties with a View to Continuous Processing. Organic Process Research & Development. 2015;19(1):158-66.

18. Food and Drug Administration. PAT guidance for industry–a framework for innovative pharmaceutical development, manufacturing and quality assurance. US Department of Health and Human Services. Food and Drug Administration, Center for drug evaluation and research, Center for veterinary medicine, Office of regulatory affairs, Rockville, MD. 2004.

19. Corredor CC, Lozano R, Bu X, McCann R, Dougherty J, Stevens T et al. Analytical method quality by design for an on-line near-infrared method to monitor blend potency and uniformity. Journal of Pharmaceutical Innovation. 2015;10(1):47-55.

20. Blanco M, Bautista M, Alcala M. Preparing calibration sets for use in pharmaceutical analysis by NIR spectroscopy. Journal of pharmaceutical sciences. 2008;97(3):1236-45.

21. Meza CP, Santos MA, Romanach RJ. Quantitation of drug content in a low dosage formulation by transmission near infrared spectroscopy. AAPS PharmSciTech. 2006;7(1):E29.

22. Blanco M, Cruz J, Bautista M. Development of a univariate calibration model for pharmaceutical analysis based on NIR spectra. Analytical and bioanalytical chemistry. 2008;392(7-8):1367-72.

23. Laasonen M, Harmia-Pulkkinen T, Simard C, Räsänen M, Vuorela H. Development and Validation of a Near-Infrared Method for the Quantitation of Caffeine in Intact Single Tablets. Analytical Chemistry. 2003;75(4):754-60.

24. Blanco M, Alcalá M. Content uniformity and tablet hardness testing of intact pharmaceutical tablets by near infrared spectroscopy. Analytica Chimica Acta. 2006;557(1-2):353-9.

25. Blanco M, Peguero A. Influence of physical factors on the accuracy of calibration models for NIR spectroscopy. Journal of pharmaceutical and biomedical analysis. 2010;52(1):59-65.

26. Isaksson T, Næs T. Selection of Samples for Calibration in Near-Infrared Spectroscopy. Part II: Selection Based on Spectral Measurements. Applied spectroscopy. 1990;44(7):1152-8.

27. Iyer M, Morris H, Drennen III J. Solid dosage form analysis by near infrared spectroscopy: comparison of reflectance and transmittance measurements including the determination of effective sample mass. Journal of Near Infrared Spectroscopy. 2002;10(4):233-45.

28. Blanco M, Cruz J, Bautista M. Development of a univariate calibration model for pharmaceutical analysis based on NIR spectra. Analytical and bioanalytical chemistry. 2008;392(7-8):1367-72.

29. Blanco M, Alcalá M. Content uniformity and tablet hardness testing of intact pharmaceutical tablets by near infrared spectroscopy: a contribution to process analytical technologies. Analytica Chimica Acta. 2006;557(1):353-9.

30. Bakeev KA. Process analytical technology: spectroscopic tools and implementation strategies for the chemical and pharmaceutical industries. John Wiley & Sons; 2010.

31. Burns DA, Ciurczak EW. Handbook of Near-Infrared Analysis, Second Edition. Taylor & Francis; 2001.

32. Griffiths PR, De Haseth JA. Fourier transform infrared spectrometry. John Wiley & Sons; 2007.

33. Blanco M, Coello J, Iturriaga H, Maspoch S, De La Pezuela C. Effect of data preprocessing methods in near-infrared diffuse reflectance spectroscopy for the determination of the active compound in a pharmaceutical preparation. Applied spectroscopy. 1997;51(2):240-6.

34. Berntsson O, Danielsson L-G, Johansson M, Folestad S. Quantitative determination of content in binary powder mixtures using diffuse reflectance near infrared spectrometry and multivariate analysis. Analytica chimica acta. 2000;419(1):45-54.

35. Dahm DJ, Dahm KD. The physics of near-infrared scattering. Near-Infrared Technology in the Agricultural and Food Industries. 2001;2.

36. Naes T, Isaksson T, Fearn T, Davies T. A user friendly guide to multivariate calibration and classification. NIR publications; 2002.

37. Sanchez-Paternina A, Roman-Ospino AD, Martinez M, Mercado J, Alonso C, Romanach RJ. Near infrared spectroscopic transmittance measurements for pharmaceutical powder mixtures. Journal of pharmaceutical and biomedical analysis. 2016;123:120-7.

38. Romañach R, Román-Ospino A, Alcalà M. A Procedure for Developing Quantitative Near Infrared (NIR) Methods for Pharmaceutical Products. In: Ierapetritou MG, Ramachandran R, editors. Process Simulation and Data Modeling in Solid Oral Drug Development and Manufacture. Methods in Pharmacology and Toxicology: Springer New York; 2016. p. 133-58.

39. Romañach R. Near infrared spectroscopy: from feasibility to implementation in the pharmaceutical industry. NIR news. 2016;27(1):33-8.

40. Colón YM, Florian MA, Acevedo D, Méndez R, Romañach RJ. Near infrared method development for a continuous manufacturing blending process. Journal of Pharmaceutical Innovation. 2014;9(4):291-301.

41. Singh R, Velazquez C, Sahay A, Karry KM, Muzzio FJ, Ierapetritou MG et al. Advanced Control of Continuous Pharmaceutical Tablet Manufacturing Processes. In: Ierapetritou MG, Ramachandran R, editors. Process Simulation and Data Modeling in Solid Oral Drug Development and Manufacture. Methods in Pharmacology and Toxicology, 2016. p. 191-224.

42. Shi Z, McGhehey KC, Leavesley IM, Manley LF. On-line monitoring of blend uniformity in continuous drug product manufacturing process—The impact of powder flow rate and the choice of spectrometer: Dispersive vs. FT. Journal of pharmaceutical and biomedical analysis. 2016;118:259-66.

43. Shaibu A, Yang Y, Cho BR, Choi Y, Shin S, editors. Process analytical technology (PAT) initiatives in improving pharmaceutical quality by design. IIE Annual Conference. Proceedings; 2008: Institute of Industrial Engineers-Publisher.

44. Allison G, Cain YT, Cooney C, Garcia T, Bizjak TG, Holte O et al. Regulatory and Quality Considerations for Continuous Manufacturing. Journal of pharmaceutical sciences. 2015;104(3):803-12.

45. Schaber SD, Gerogiorgis DI, Ramachandran R, Evans JMB, Barton PI, Trout BL. Economic Analysis of Integrated Continuous and Batch Pharmaceutical Manufacturing: A Case Study. Industrial & Engineering Chemistry Research. 2011;50(17):10083-92.

46. Mollan Jr MJ, Lodaya M. Continuous processing in pharmaceutical manufacturing. American Pharmaceutical Review. 2004.

47. McKenzie P, Kiang S, Tom J, Rubin AE, Futran M. Can pharmaceutical process development become high tech? AIChE Journal. 2006;52(12):3990-4.

48. Vanarase AU, Alcalà M, Rozo JIJ, Muzzio FJ, Romañach RJ. Real-time monitoring of drug concentration in a continuous powder mixing process using NIR spectroscopy. Chemical Engineering Science. 2010;65(21):5728-33.

49. Sulub Y, Wabuyele B, Gargiulo P, Pazdan J, Cheney J, Berry J et al. Real-time on-line blend uniformity monitoring using near-infrared reflectance spectrometry: a noninvasive off-line calibration approach. Journal of pharmaceutical and biomedical analysis. 2009;49(1):48-54.

50. Koller DM, Posch A, Hörl G, Voura C, Radl S, Urbanetz N et al. Continuous quantitative monitoring of powder mixing dynamics by near-infrared spectroscopy. Powder technology. 2011;205(1):87-96.

51. Pierna JAF, Chauchard F, Preys S, Roger JM, Galtier O, Baeten V et al. How to build a robust model against perturbation factors with only a few reference values: A chemometric challenge at 'Chimiométrie 2007'. Chemometrics and Intelligent Laboratory Systems. 2011;106(2):152-9.

52. Blanco M, Coello J, Iturriaga H, Maspoch S, Pou N. Influence of the procedure used to prepare the calibration sample set on the performance of near infrared spectroscopy in quantitative pharmaceutical analyses. Analyst. 2001;126(7):1129-34.

Chapter 3

3 Evaluation of Analytical and Sampling Errors in the Prediction of the Active Pharmaceutical Ingredient Concentration in Blends and Tablets from a Continuous Manufacturing Process

Published online in the Journal of Pharmaceutical Innovation, 2017, 12 (2), 155–167.

Jenny M. Vargas, Andrés D. Román-Ospino, Eric Sánchez, Rodolfo J. Romañach

3.1 Introduction

Current pharmaceutical procedures involve the preparation of tablets using a batch process. The quality of tablets is evaluated off-line after batch completion. Tablets are prepared using heterogeneous blend mixtures. However, the blend is not monitored or tested throughout the traditional batch manufacturing process. The use of continuous manufacturing (CM) together with process analytical technology (PAT) techniques such as near infrared spectroscopy (NIRS) allows the monitoring of blend mixtures before tablet compression.

The FDA recently approved, the conversion of a commercial drug batch process into a continuous manufacturing process with integrated real-time release testing (RTRt) using near infrared (NIR) spectroscopy [1-5]. NIR spectroscopy is one of the most commonly used techniques in the pharmaceutical industry because it is fast, non-invasive, non-destructive and offers chemical and physical information of materials [6-13]. The use of NIR in continuous manufacturing allows the in-line analysis and monitoring of blends during the process.

Continuous manufacturing can be designed to improve the quality of the product and decrease manufacturing costs [14-17]. Implementation of continuous manufacturing increases the efficiency of the manufacturing process by eliminating the relocation of material and reduces the manufacturing space needed by using less and smaller equipment. Therefore, the implementation of continuous manufacturing integrated with PAT techniques in pharmaceutical industries is expected to provide high quality products at lower manufacturing costs [18].

This chapter presents the use of chemometric modelling and variographic analysis to evaluate the analytical and sampling error of the predicted API concentration of blends produced during a pharmaceutical continuous manufacturing (CM) process.

Previous investigations have shown the development of NIR calibration to predict drug concentration in batch processes [8, 9, 19-28]. However, these studies have not evaluated the analytical and sampling errors of blends obtained from a CM process using

variographic analysis. This study includes the use of an NIR calibration model to predict the API concentration of CM blends and tablets and the evaluation of analytical and sampling errors using variographic analysis. A continuous mixing system including a sensing interface coupled with three NIR spectrometers was used to monitor the blending process after achieving steady state [29, 30]. Blends were evaluated with the use of variographic analysis to determine the optimal sampling frequency and evaluate sampling error [31].

3.2 Materials and Methods

3.2.1. Materials

Prosolv® (JRS Pharma) silicified micro cellulose (SMCC) (filler) was chosen as the main excipient (approximately 48% w/w). Crospovidone NF/PH EUR (disintegrant), Screen Colloidal silicon dioxide (glidant), and Magnesium Stearate NF/EP (lubricant) were included as minor excipients along with a cohesive API.

3.2.2. Preparation of the Calibration Set

The calibration set was prepared in a lab-scale equipment by mixing placebo (composed of Prosolv®, crospovidone, and colloidal), API, and magnesium stearate in fixed quantities. A total of five placebos were prepared. The weights used to prepare the placebos were obtained by performing a full factorial D-Optimal Design of Experiment (DoE). Prosolv®, crospovidone, and colloidal were the only excipients included in the DoE. The target level for these excipients in the DoE was from 70% to 130% of their target concentrations, except for the colloidal silicon dioxide (set to zero in two of the placebos). Raw materials were individually weighed and placed in appropriate bottles. After, each placebo was placed in individual small plastic bags and transferred to 2.2 L polyethylene bottles; they were mixed inside a 16-qt PK Shell V-blender. Each placebo was individually mixed for 50 revolutions and aliquots were weighed to prepare the 33 calibration blends. The calibration blends were prepared in a concentration range spanning from 70% to 130% of the target API concentration. All 33 calibration blends were individually prepared by placing fixed quantities of the placebo (chosen randomly using https://www.random.org/), API and magnesium stearate in a plastic zippered bag and manually mixing for two minutes.

3.2.3. Preparation of the Validation Sets

Three validation sets were prepared and are described in **Table 3.1**. These validation sets included lab-scale, pilot plant, and CM prepared blends since each process entails distinctive characteristics of sample preparation (mixing, shear force, powder density, etc.). The validation sets prepared in lab-scale and pilot plant equipment were used to provide the preliminary evaluation of the calibration model while the CM plant was being built.

Table 3.1 Description of the validation sets concentrations, number of blends and samples, and spectral acquisition mode

Sample Preparation Mode	Blends Prepared	Concentration (% API target concentration)	Spectral Acquisition Mode	Number of Samples (n)
lab-scale	1	80	Static	10
pilot plant	1	100	Static	10
*CM	2	100	Dynamic	1800

*For the CM validation set, two runs were performed in which blend spectra were acquired. A total of 1800 spectra per run were acquired.

The validation set prepared in lab-scale was 80% of the API target concentration. Prosolv®, crospovidone, colloidal, magnesium stearate, and the API were weighed, placed in 2.2 L polyethylene bottles inside a 16-qt PK Shell V-blender and mixed for 50 revolutions. After mixing, each blend was stored in a sample container inside an Aluminum “Vapor-loc” bag.

The validation set prepared in the pilot plant had an API target concentration of 100%. Prosolv®, crospovidone, magnesium stearate, and the API were weighed and placed inside a Bohle 40L Mobile laboratory-scale blender for mixing. The blender was set at 20 rpm and materials were mixed for four minutes. Each blend was then stored in a sample container inside an Aluminum “Vapor-loc” bag.

Two blends were prepared during two CM process runs (CM-1 and CM-2) at specific target concentrations. Prosolv®, Crospovidone, and the API were transferred pneumatically from their original containers through a sieve into a vacuum receiver which

transferred the materials to maintain the proper level of powder in the volumetric feeder (100% for the API and to a constant throughput for the filler). Magnesium stearate was filled manually into the feeder (e.g. 5kg of lubricant every 16 hrs.).

3.2.4. Continuous Manufacturing Setup

The continuous manufacturing setup used for the preparation of the validation set is shown in **Figure 3.1**. The setup included four K-Tron (KT-20) Gravimetric Feeders marked F1, F2, F3, and F4. Feeders were calibrated and were qualified with three studies: the installation qualification (IQ), the operational qualification (OQ), and the performance qualification (PQ). The mass flow (feed rate) of the four feeders was monitored and controlled by the line control system during all CM runs. Mass flow values of the feeders were compared against established limits defined based on the product attributes (i.e. to maintain a blend API concentration between 90.0% and 110.0% of the API target concentration). Alarms are activated if any feeder is dispensing materials below or above the established limits and the CM line acts on whether to accept or reject the blend.

A Quadro Comil (In-line Quadro Comil U10) was used for de-lumping and a Glatt GCG 70 continuous blender was used for the blending of materials. **Figure 3.1** shows the continuous manufacturing setup including the three locations designed for the coupling of the three NIR spectrometers. The powder blend in the sensing interface is maintained at a specific level by the rotary valve which speed is moderated by a laser level sensor.

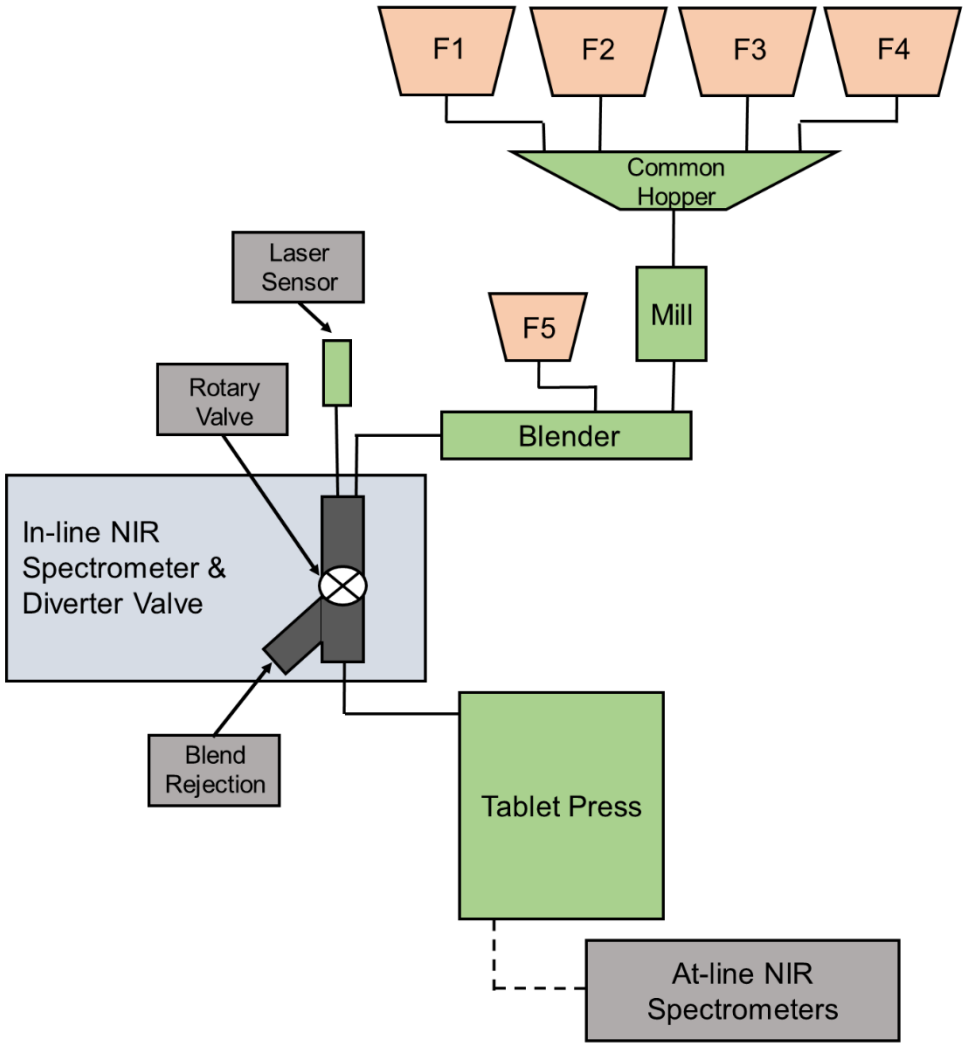

Figure 3.1 Diagram for the continuous manufacturing setup including the in-line NIR spectrometers location in the sensing interface.

3.2.5. Preparation of Tablets

Tablets were obtained from the two same continuous manufacturing runs used to prepare the blends validation set indicated above (Tab-CM-1 and Tab-CM-2). The tablets were prepared at an API target concentration of 100% following the CM process described above. After the blend reaching the sensing interface, it was directed to a Korsch XM-12 tablet press where the tablets were produced.

3.2.6. NIR Spectra Acquisition

All blend spectra acquisition was performed using three Bruker (Billerica, MA) FT-NIR spectrometers (M1, M2, and M3), controlled by the OVP (OPUS Validation Program) software Version 4.2. These Matrix-F spectrometers are used for process control and have a sensor head attached that allows the analysis of solids and powders in the spectral range of 12,000 - 4,000 cm^{-1}. The diffuse reflectance sensor head consists of two tungsten NIR light sources illuminating a 10-mm measurement area. All NIR spectra were obtained with a 16 cm^{-1} resolution and a total of 16 averaged scans (total scan time of 1.47 seconds). All three NIR spectrometers were calibrated and qualified.

Spectra acquisition for the calibration set and the validation sets prepared in lab-scale and pilot plant facilities was performed statically, at-line, as shown in **Figure 3.2**. Spectra were acquired after mixing was completed. Each blend sample was placed into a weighing tray (Fisher Scientific Company LLC, 1.62L x 1.62W x 0.31 in.) and five spectra were acquired in five different positions as indicated in **Figure 3.2**. The blend was then poured into a polyethylene bottle and then back again to the same weighing tray. Five more spectra were acquired in five different positions, for a total of ten spectra. A minimum of approximately 3.9 g of blend were deposited in the sample trays, each time. The calibration model was developed using 33 spectra (each spectrum was an average of the ten spectra acquired).

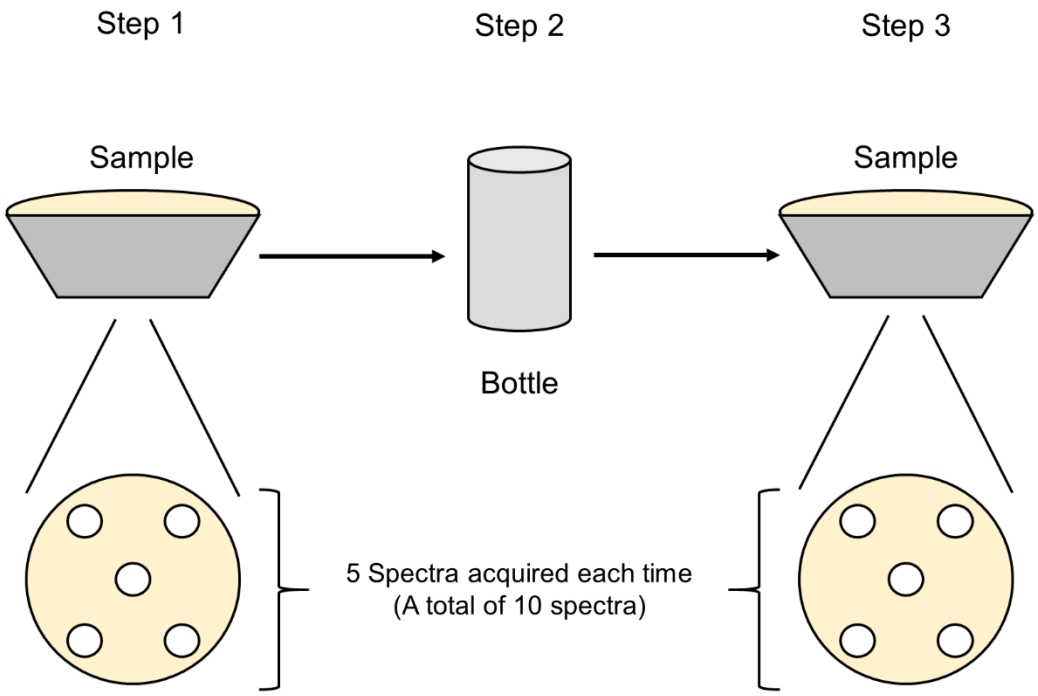

Figure 3.2 Representation of the static spectra acquisition setup for the calibration and validation sets prepared in lab-scale and pilot plant equipment.

Spectra of the validation set prepared using the continuous manufacturing line were acquired in-line, during two CM process runs. **Figure 3.3** shows the sensing interface setup where the three FT-NIR spectrometers were coupled for in-line spectra acquisition. The blended material passed from the blender (a) through a triangular sensing interface where spectra were collected by the three Bruker FT-NIR spectrometers (b-1, b-2, and b-3). A total of 1800 spectra were acquired per spectrometer for each of the two runs.

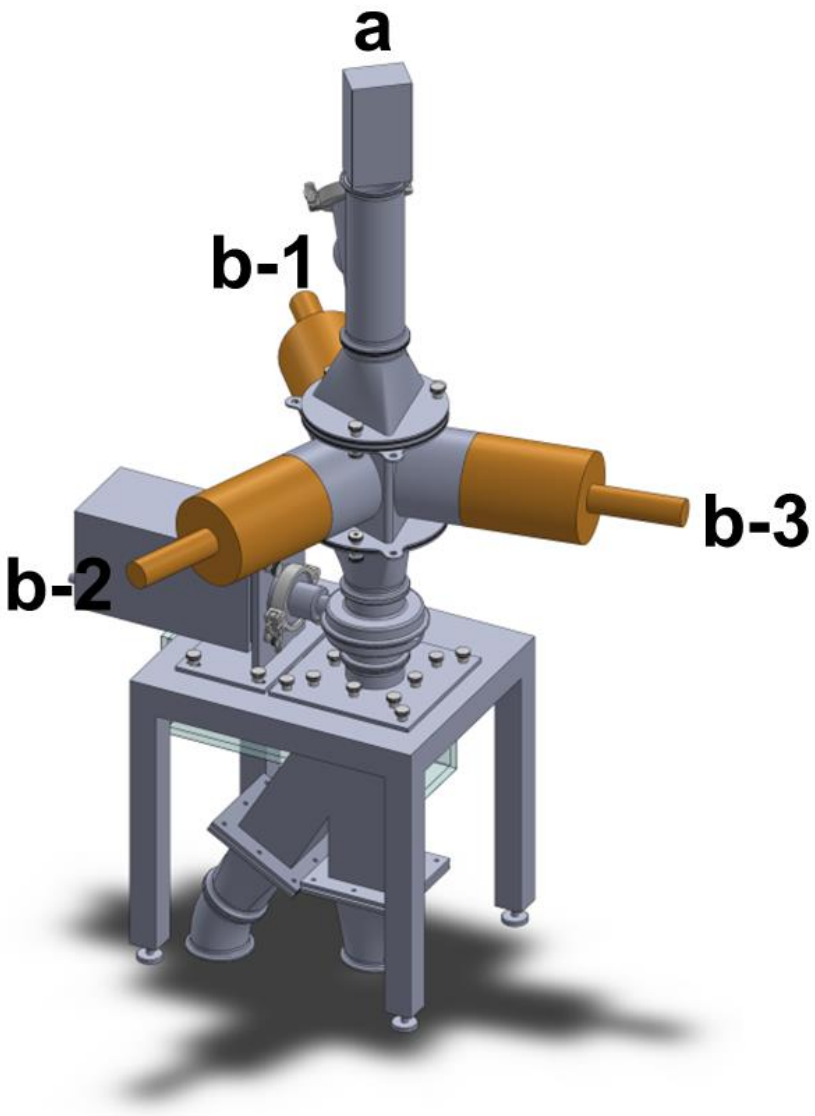

Figure 3.3 Sensing interface spectra acquisition setup: (a) shows where the material exits the blender and (b) shows the three spectrometers positions for spectra acquisition of the material flowing through the sensing interface

Sample mass was estimated for the NIR spectra acquired using the continuous manufacturing line as per equation (1) [32].

$$\boldsymbol{M = \rho \left[\pi \left(\frac{d}{2}\right)^2 + d\left(t_{acq} * V_{pow}\right)\right] H} \quad (1)$$

Where ρ is the bulk density of the blend (0.53 g/cm^3), d is the NIR beam diameter, t_{acq} is the time needed to acquire one NIR spectrum (16 scan average), V_{pow} is the linear velocity of the powder in the CM line, and H is the NIR beam depth of penetration. Sample mass was estimated to be approximately 37 mg per NIR spectrum (16 scan average). This estimated blend sample mass is considerably lower than the tablet mass (over 1000 mg).

Spectra of tablets prepared using the continuous manufacturing line were also collected. One Bruker Multi-Purpose Analyzer (MPA) NIR spectrometer was used to acquire the spectra of tablets. The system included an indium gallium arsenide (InGaAs) detector in the spectral range of 12500 - 5800 cm^{-1}. NIR spectra of tablets were collected using transmittance measurements at a resolution of 64 cm^{-1} with a total of 32 averaged scans (total scan time of 5.8 seconds).

3.2.7. NIR Calibration Model Development and Data Analysis

A Partial Least Squares (PLS) NIR calibration model was developed using Simca P+12 (Umetrics, NJ, USA). Different spectral regions and pretreatments (such as Standard Normal Variate, first derivative, second derivative, and combinations of SNV with the derivatives) were evaluated [33, 34].

The NIR calibration model was assessed in terms of precision (using the standard deviation) and predictive performance (using the root mean standard error). The predictive performance was evaluated for the cross validation (RMSECV - Eq. 2) [21, 35, 36]) and prediction sets (RMSEP - Eq. 3).

$$\boldsymbol{RMSECV} = \sqrt{\frac{\sum_{i=1}^{N}\left(\hat{y}_{CV,i} - y_i\right)^2}{N}} \tag{2}$$

$$\boldsymbol{RMSEP} = \sqrt{\frac{\sum_{i=1}^{Np}(\hat{y}_i - y_i)^2}{N}} \tag{3}$$

Where $\hat{y}_{CV,i}$ is the estimate for y_i based on the calibration equation with sample *i* deleted, $\hat{y}$ and y_i are the predicted and measured reference values for the test samples, and N is the number of samples.

Variograms were calculated using a code written in MATLAB 2013b (Eq. 4) (The MathWorks, Natick, MA). The sill, nugget effect (MPE), and corrected sill were calculated and verified against the variogram calculations in the recently approved DS-3077 [37].

$$\boldsymbol{V(j) = \frac{1}{2(Q_{total}-j)} \sum_{q=1}^{Q_{total}-j} (h_{q+j} - h_q)^2} \quad (4)$$

Where V(j) is the function of the distance between extracted increments (the lag which is defined as the inverse of the sampling frequency), Q_{total} is the total number of analytical results, *j* is the *lag* and *h* is the heterogeneity contribution of the analyte measured in each increment.

3.3 Results and Discussion

3.3.1. Development of the NIR Calibration Model

The spectral region used for the development of the NIR calibration model was chosen based on the comparison of the API and placebo spectra (**Figure 3.4**). Spectral differences were observed between the two spectra. Principal component analysis (PCA) was performed to evaluate the variation of the calibration set. **Figure 3.5** shows the PCA score plot for the 8956-6046 cm^{-1} spectral region. Standard normal variate (SNV) followed by first derivative (25-point window) were applied as pretreatments. Clusters are observed for the lowest, target, and highest API concentrations. The 1^{st} principal component (PC1) explains 81.2% of the variation in the chosen spectral region after pretreatment. **Figure 3.6** shows the pretreated spectra for the calibration set at low, middle, and high concentration levels (70%, 100%, 130% of API target concentration) in the selected spectral range (8956-6046 cm^{-1}).

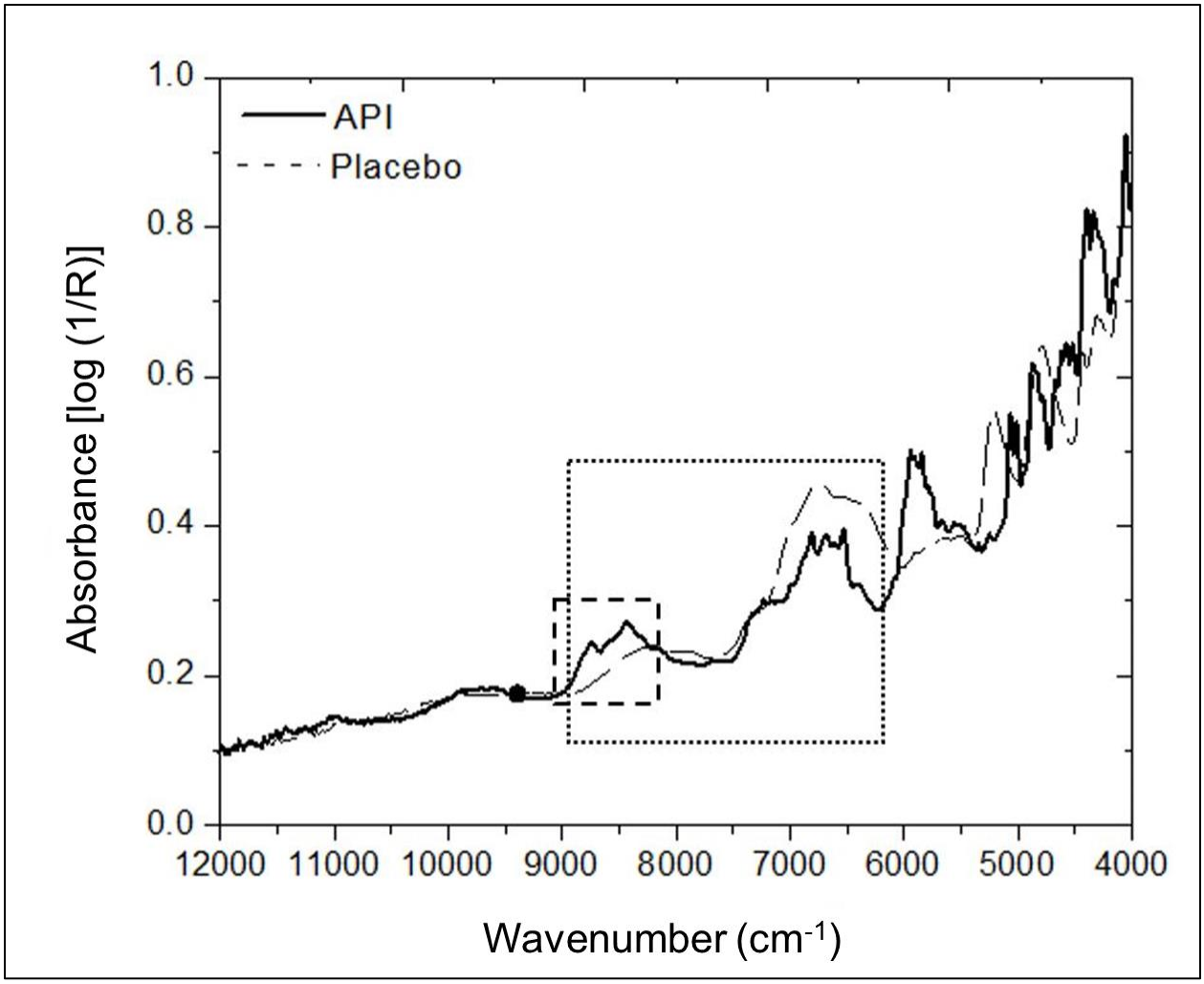

Figure 3.4 Pretreated NIR spectra of placebo and API. The selected area corresponds to the two spectral ranges evaluated: 8956 – 6046 cm^{-1} (dotted box) and 9044 – 8231 cm^{-1} (short lines box).

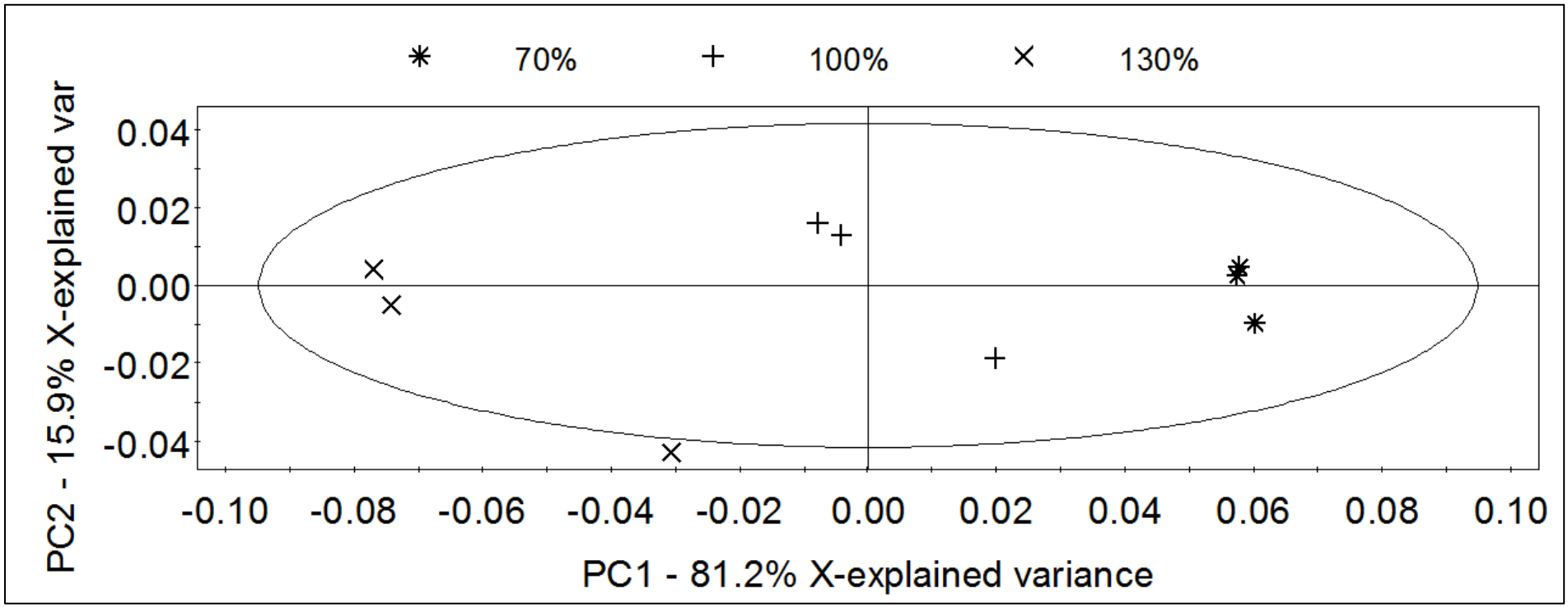

Figure 3.5 PCA scores plot of the target (100%), lowest (70%), and highest (130%) API target concentration levels for the calibration set. [Spectral pre-treatment: SNV+1st derivative (25 moving window); spectral range: 8956 cm^{-1} – 6046 cm^{-1}. PC1 explains 81.2% of the variation of the samples while PC2 explains 15.9%.

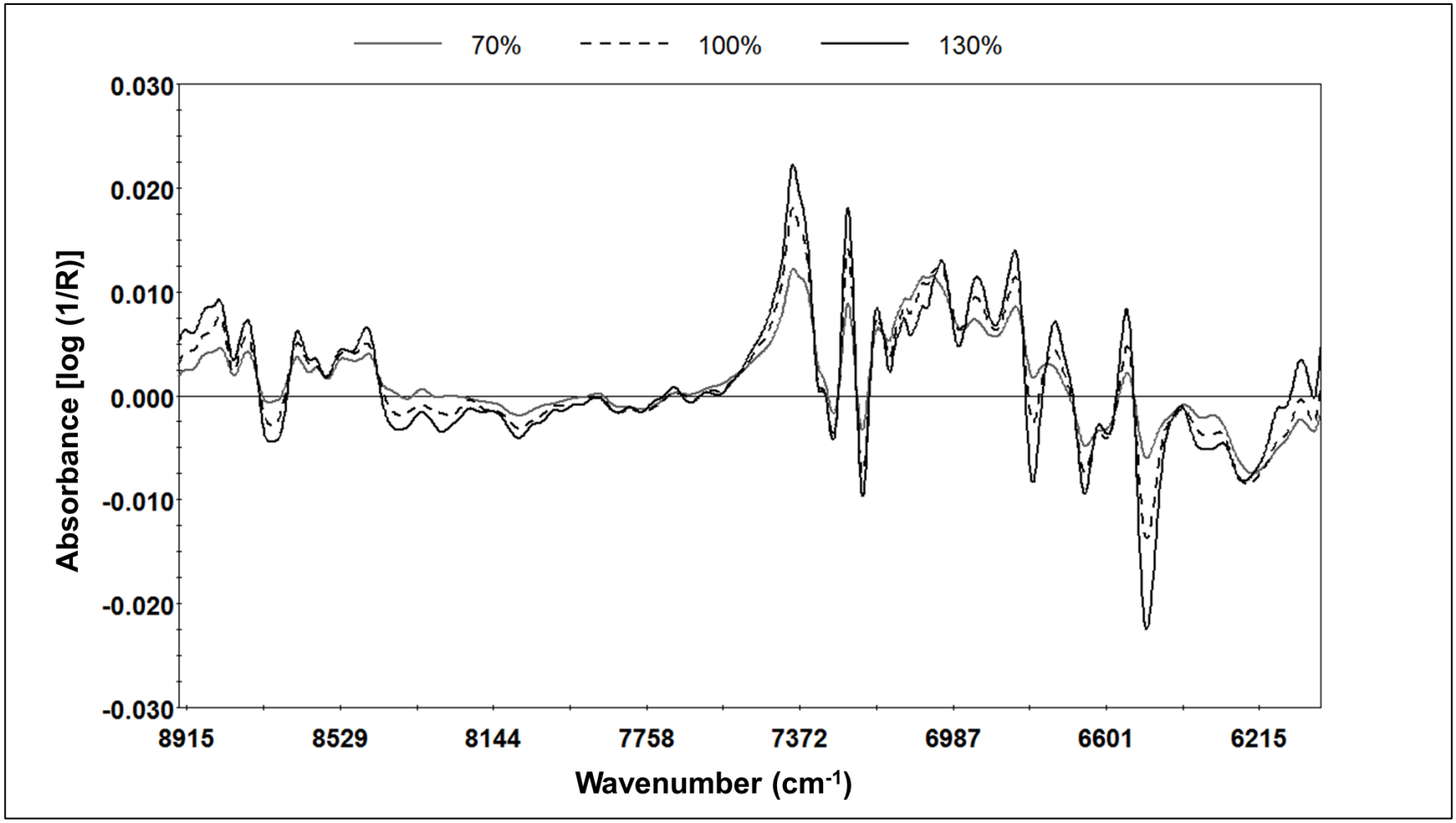

Figure 3.6 NIR spectra of calibration set developed in the spectral range 8956 – 6046 cm^{-1} using as pre-treatments SNV+1st derivative (25-point window)

The NIR calibration model was developed using 99 spectra (three NIR spectrometer – one averaged spectrum per spectrometer (n=10) – 33 concentration levels – three spectra per concentration level). Initial evaluation of the NIR model was performed using RMSECV (eq. 2) and the R2X values per PLS factor. **Table 3.2** shows the leave-one-out "cross validation" (CV) results, spectral ranges, PLS factors, and pretreatments evaluated that provided the best preliminary calibration models.

Table 3.2 Evaluation parameters for the preliminary NIR calibration models. All values are reported in terms of percent of API target concentration

NIR Calibration Model no.	Spectral Range (cm^{-1})	Pretreatment	PLS Factors	R2X (%)	RMSECV (%)
1	8956 - 6046	1st derivative (15 pts.)	1	70.0	2.91
			2	23.8	2.07
2		1st derivative (25 pts.)	1	76.8	2.81
			2	18.5	2.13
3		SNV+1st derivative (15 pts.)	1	77.6	5.76
			2	18.5	2.87
4		SNV+1st derivative (25 pts.)	1	81.2	5.32
			2	15.9	2.93
5	9044 - 8231	1st derivative (15 pts.)	1	72.5	2.67
			2	0.90	2.12
6		1st derivative (25 pts.)	1	82.4	2.55
			2	0.65	2.06
7		SNV+1st derivative (15 pts.)	1	75.6	4.91
			2	0.75	2.99
8		SNV+1st derivative (25 pts.)	1	85.7	4.70
			2	0.43	2.85

NIR near infrared, RM*SECV* root mean standard error of cross validation, *SNV* standard normal variate, *R2X* fraction of the x-variation modeled in the component

The spectral ranges analyzed (8956 – 6046 cm^{-1} and 9044 – 8231 cm^{-1}) avoid the inclusion of lower wavelengths with: high background noise associated with the use of a fiber optical probe [19], and less penetration of the radiation in the sample [13, 38, 39]. Higher frequencies are associated with more penetration of the radiation in the sample and thus, larger sampling mass. Both spectral ranges analyzed exclude the O-H combination band expected around 5200 cm^{-1} since the formulation includes a highly hygroscopic excipient. Both spectral ranges contain distinct API absorption bands (Refer to **Figure 3.4**). The preliminary NIR calibration models in the spectral range 8956 – 6046 cm^{-1} yield the highest $R^2X_{(cum)}$ (>90%). $R^2X_{(cum)}$ results for the spectral range 9044 – 8231 cm^{-1} are above 70%, also showing a very good cumulative fraction of the **X**-variation modeled in the component. All RMSECV values for both spectral ranges using two PLS factors are within the same range (NMT 3% API target concentration). The final selection of spectral range and pre-treatment for the NIR calibration model was also based on the results of the repeatability study. **Table 3.3** shows that repeatability varies according to the calibration model chosen (0.13 - 2.19% API target concentration). The selected calibration model no. 4 showed a repeatability of 0.14% with two PLS factors. These results are consistent with previous efforts that show that NIR methods are able to provide a repeatability in the range of 0.1 – 0.2% [32, 40].

The repeatability study indicates the short-term precision. It provides an estimate of minimum variation that may be expected from the NIR method, and thus the minimum variation expected of the continuous mixing process in this study. The NIR method monitors the performance of the entire continuous mixing process after steady state is achieved. Thus, the variation from the NIR method should be minimal and its thorough evaluation is essential to CM processes. The standard deviation from the NIR method should be minimal and the thorough evaluation of precision is essential for the monitoring of a continuous manufacturing process. Repeatability was calculated by obtaining six consecutive spectra without moving the sample.

Table 3.3 Repeatability assessment for the preliminary NIR calibration models. All values are reported in terms of percent of API target concentration

NIR Calibration Model no.	Spectral Range (cm^{-1})	SD (%) (*n=6*)
1	8956 - 6046	0.24
2		0.13
3		0.24
4		0.14
5	9044 - 8231	1.86
6		1.42
7		2.19
8		1.76

3.3.2. Prediction of the Validation Set Prepared in Lab-Scale

The NIR calibration model developed was first evaluated for performance, accuracy, and precision using a validation set prepared in lab-scale as described in **Table 3.1**. **Table 3.4** shows the results obtained for the NIR predictions of the validation set prepared in lab-scale equipment. The RMSEP results show the excellent predictions of drug concentration and excellent mixing, since the RMSEP encompasses both the accuracy and precision of the predictions [41].

RMSEP values were less than 0.83% of API target concentration. The low bias results (max. 0.57%) shows the excellent accuracy achieved by the NIR calibration model. The standard deviation varied from 0.41% to 0.82% of API target concentration.

Table 3.4 NIR predictions of the validation set prepared in lab-scale. All values are reported in terms of percent of API target concentration

NIR Spectrometer	Average NIR Prediction (%) (n=10)	Standard Deviation (%)	RMSEP (%)	Bias (%)
M1	79.78	0.41	0.61	0.47
M2	79.43	0.82	0.79	0.12
M3	79.88	0.64	0.83	0.57

3.3.3. Prediction of Validation Set Prepared in Pilot Plant Equipment

The NIR calibration model was also evaluated using a validation set prepared in a pilot plant, as described in **Table 3.1**. **Table 3.5** shows the results obtained.

Results showed the good predictive performance of the NIR calibration model for the validation set prepared in pilot plant. The highest RMSEP observed was 4.30% of API target concentration. Slightly higher predictions were expected since the preparation and spectra acquisition of the validation set prepared in pilot plant differed from the process used for the preparation and spectra acquisition of the calibration set.

Table 3.5 NIR predictions of the validation set prepared in pilot plant equipment. All values are reported in terms of percent of API target concentration

NIR Spectrometer	Average NIR Prediction (%.) (n=10)	Standard Deviation (%)	RMSEP (%)	Bias (%)
M1	96.62	1.18	3.56	3.38
M2	95.77	0.86	4.30	4.23
M3	96.46	0.88	3.64	3.54

3.3.4. Prediction of the Validation Set Prepared in a CM Process

The validation of the NIR calibration model also included the prediction of blends prepared using a continuous manufacturing line. The previous validation sets involved tumble blending. However, a continuous manufacturing process mixer includes a motor driver impeller along the entire length [42]. The impeller and blades force inter-particle collisions and shearing that may affect NIR spectra [43]. Therefore, the NIR calibration model developed was validated using two validation sets prepared in a CM line, as described in **Table 3.1**. These two validation sets were named CM-1 and CM-2, for clarity purposes. Three NIR spectrometers were installed in the CM line as shown in **Figure 3.3** and used for the in-line spectra acquisition of blends.

Figure 3.7 through **Figure 3.9** show the PCA scores plot for the validation sets (CM-1 and CM-2) prepared in a CM line using three NIR spectrometers (M1 – **Figure 3.7**, M2 – **Figure 3.8**, and M3 – **Figure 3.9**). The scores plots show that most of the spectra

obtained during the CM process are within the 95% confidence interval of the calibration model. Therefore, the NIR calibration model developed with laboratory prepared calibration samples includes some spectral variation observed in the blend spectra acquired in the CM line and thus, is expected to provide adequate predictions. **Table 3.6** shows the prediction results for the validation set prepared in a CM line using three NIR spectrometers (M1, M2, and M3). The RMSEP values for spectrometers M1 and M2 (1.57 – 3.69% of API target concentration) are generally two to four times the values reported for the validation set prepared in lab-scale equipment. However, RMSEP values for NIR spectrometer M3 ranged from 19.80 – 21.50% of target, showing extremely high prediction errors. M3 results were precise (SD NMT 1.63%) but not accurate (bias ≥ 19.74).

Table 3.6 NIR predictions of the validation set prepared in a CM process. All values are reported in terms of percent of target concentration

Sample Name	NIR Spectrometer	Average NIR Prediction (%)*	Standard Deviation (%)	RMSEP (%)	Bias (%)
CM-1	M1	101.67	0.97	1.93	1.67
	M2	103.60	0.84	3.69	3.60
	M3	119.74	1.63	19.80	19.74
CM-2	M1	101.19	1.02	1.57	1.19
	M2	103.16	0.85	3.27	3.16
	M3	121.44	1.58	21.50	21.44

*A total of 1800 predictions were used to obtain the average NIR predictions. Each spectrum analyzed a sample mass of approximately 37 mg.

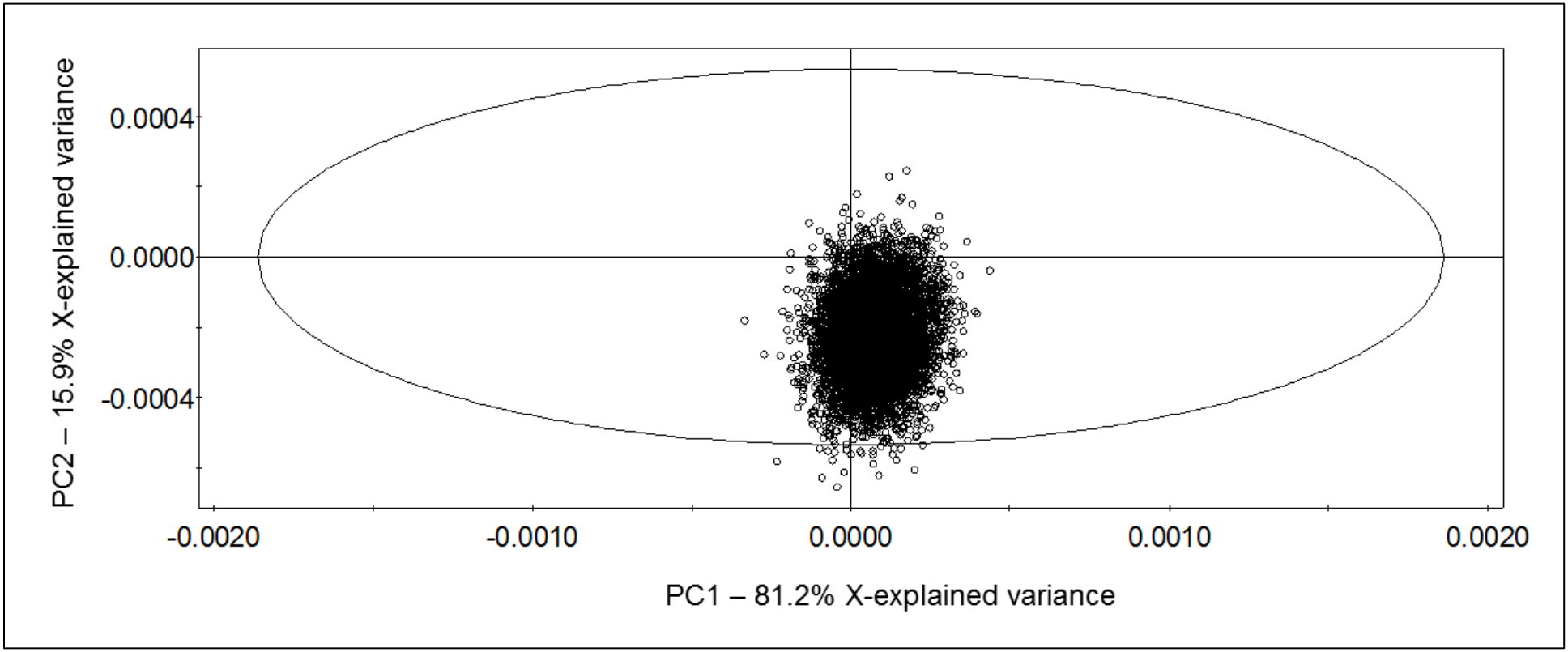

Figure 3.7 PCA scores plot of the validation set prepared in a CM process spectra obtained with NIR spectrometer M1

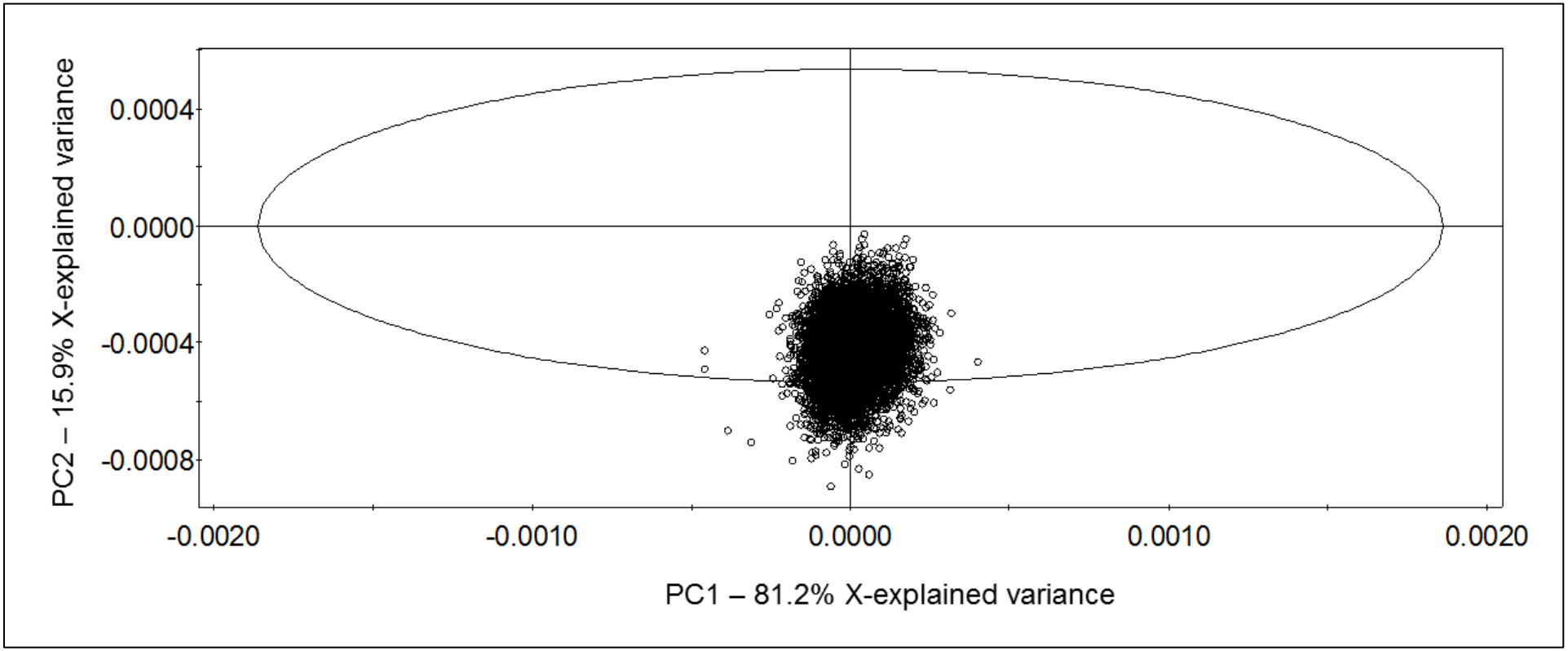

Figure 3.8 PCA scores plot of the validation set prepared in a CM process spectra obtained with NIR spectrometer M2

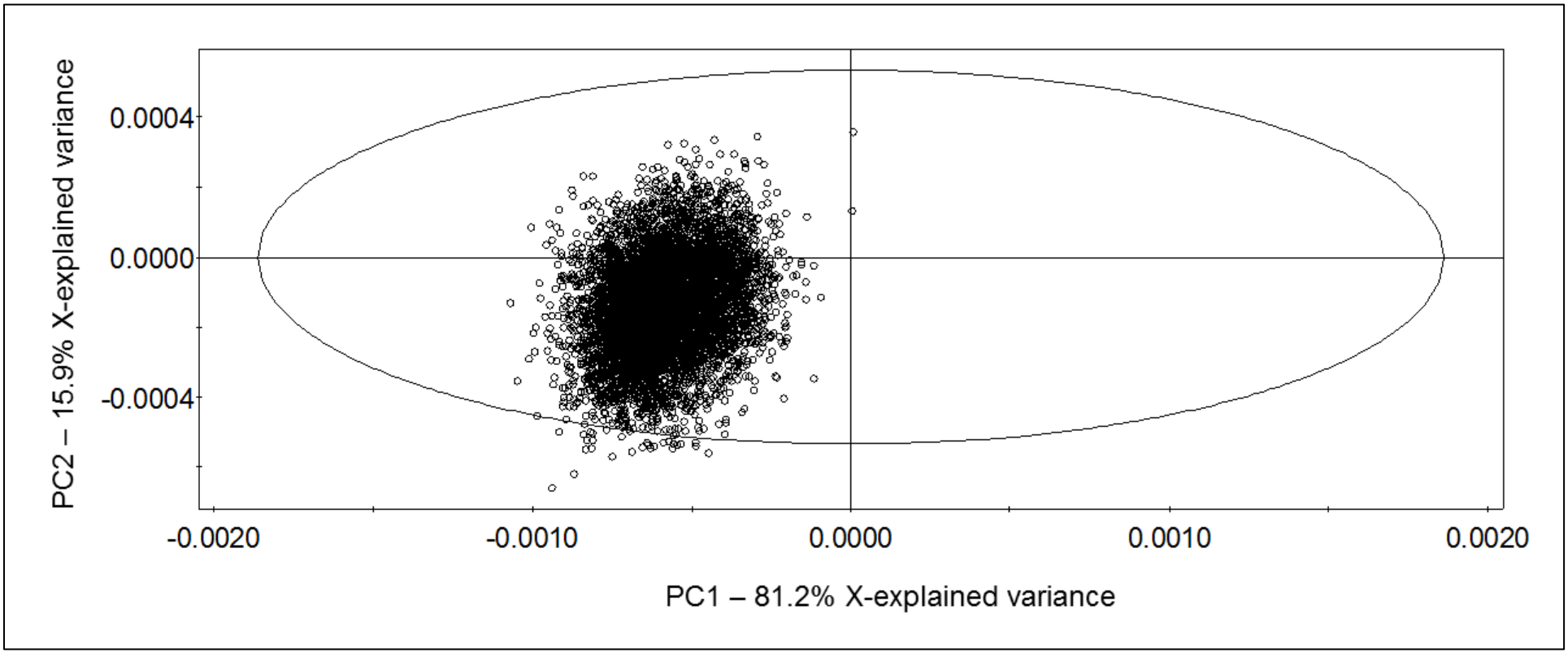

Figure 3.9 PCA scores plot of the validation set prepared in a CM process spectra obtained with NIR spectrometer M3

Considerable differences were observed between the results for M3 compared to the other two spectrometers (M1 and M2). The differences in the results between NIR spectrometers M1 and M2 and NIR spectrometer M3 did not appear to be related to instrument performance as all three instruments were calibrated and passed the qualifications performed (IQ, OQ, PQ, and OVP PQ). NIR spectrometer M3 was located in the sensing interface (**Figure 3.3**) just below the blender outlet which causes the blend to exert greater pressure on the material in front of this NIR spectrometer. The effect of probe location was evaluated through an experiment where the position of the three analyzers was changed to acquire blend spectra.

A CM run was performed at 90% API target concentration for the probe location study. Spectra were acquired in-line using all three NIR spectrometers coupled in the sensing interface. A rotation of the NIR probes was performed so that all NIR spectrometers acquired spectra in each of the three sensing interface positions (**Figure 3.3**). **Table 3.7** shows the results obtained for this evaluation, where most of the error is associated with the bias. Higher results were observed for all three NIR spectrometers in position b-2. Position b-2 in the sensing interface is right below the blender outlet and is where NIR spectrometer M3 is installed to acquire process spectra. NIR spectrometer M3 predictions yield the highest average NIR prediction, bias and standard deviation, regardless of the sensing interface position. NIR spectrometers M1 and M2 have similar results in all three sensing interface positions. These results indicate that sensing interface position b-2 affects the NIR predictions and that the results observed for NIR spectrometer M3 are because of internal instrument differences between M3 the other two instruments (M1 and M2). Therefore, NIR spectrometer M3 was not included in the variographic analysis.

After completing the investigation, NIR spectrometer M3 was sent to the vendor for further analysis. The spectrometer laser was replaced and after, the performance of the instrument improved.

Table 3.7 NIR predictions of NIR spectrometers in all three sensing interface positions. All values are reported in terms of percent of target concentration

Sensing Interface Position	NIR Spectrometer	Average NIR Prediction (%) (n = 53)	Standard Deviation (%)	Bias (%)	RMSEP (%)
1	M1	92.22	0.72	2.33	2.33
	M2	91.89	0.57	1.89	1.97
	M3	96.47	1.02	6.47	6.55
2	M1	99.56	0.69	9.56	9.59
	M2	98.41	0.71	8.41	8.43
	M3	105.36	1.07	15.36	15.40
3	M1	93.89	0.90	3.89	3.99
	M2	93.91	0.74	3.91	3.97
	M3	97.55	1.34	7.55	7.67

3.3.5. Evaluation of Total Sampling and Analytical Errors

Sampling and analytical errors were evaluated by performing a variographic analysis for two CM runs (CM-1 and CM-2). Variograms were calculated using the NIR predictions obtained achieving after steady state of the blend throughput in the CM line. Variographic analysis contributes to process understanding by elucidating the sources of errors.

The variogram plots the values of the variogram function V(j) as a function of the lag, or distance between concentration values which are reported in terms of percent of target concentration. A lag of one corresponds to the unit distance (time or distance) between two consecutive analytical results, while a lag of two characterizes the doubled inter-distance between measurements. A lag of 50 compares the first predicted concentration value to the fifty-first, and second to the fifty-second, until all concentration values that are fifty units apart are compared. Low V(j) values indicate that the concentration values are very similar; a low blend heterogeneity and the achievement of a good mixing. Larger V(j) values are often found with large lag values. At least 30 increments (composite samples) are necessary for a variogram. A higher number of increments was possible for this evaluation since sampling was performed using the NIR spectrometers in a sensing interface acquiring dynamic in-line spectra during a CM process.

The MPE (minimum practical error), the sill, and the corrected sill can be calculated from the variogram. MPE is an estimate of the total sampling error and the total analytical

error [44]. It is calculated by extrapolating V(j) to intercept the Y-axis, to estimate “lag 0” [45]. The sill gives information about the maximum heterogeneity between samples (total process variation) including sampling and analytical errors. The corrected sill represents the true process variation, or residual variance in the blend after subtracting the nugget effect (MPE) from the sill [44]. Therefore, the lower the corrected sill, the closer to reach the final state of blending.

Variographic analysis was performed for the individual and moving block (MB) predictions for the CM-1 and CM-2 runs (**Figure 3.10** through **Figure 3.13**). The moving block was performed by averaging every three NIR predictions (n=3), considering that the estimated sample mass analyzed by the FT-NIR spectrometers (~ 37 mg per NIR spectrum) was lower than the tablet mass (> 1000 mg). The estimated sample mass analyzed was about 111 mg for the moving block (three averaged NIR spectra). **Table 3.8** shows the sill, MPE and corrected sill values for the CM runs, for the individual and the MB predictions.

Table 3.8 Variographic analysis of the CM runs (individual and MB predictions)

Individual predictions	CM-1 M1	CM-2 M1	CM-1 M2	CM-2 M2
Sill	0.93	1.03	0.66	0.71
MPE	0.72	0.92	0.52	0.60
Corrected sill	0.21	0.10	0.14	0.11
Standard deviation (% label)	0.97	1.02	0.84	0.85
Individual predictions	**CM-1 M1**	**CM-2 M1**	**CM-1 M2**	**CM-2 M2**
Sill	0.43	0.39	0.30	0.29
MPE	0.06	0.08	0.05	0.06
Corrected sill	0.36	0.31	0.25	0.23
Standard deviation (% label)	0.66	0.63	0.59	0.55

The sill, nugget effect (MPE), and corrected sill were calculated for the variograms prepared using the individual and the MB predictions. Sill results for the variogram using the individual predictions ranged from 0.7 to 1.0 and for the MB were no more than 0.4, showing an improvement of the low residual variation of the blending process with the MB performed. The MPE was also greatly reduced with the MB (MB predictions 0.1;

individual predictions NMT 0.4). This improvement was expected as there is a larger composite sample from the three averaged spectra (MB). The range is short at around three lags. The fact that sill values are so close to the MPE values shows that the process can only be improved if the MPE is reduced.

Another evaluation of the results was done by calculating the “corrected sill”, directly related to the residual heterogeneity of the blend [44, 46]. This calculation was performed by subtracting the MPE from the sill for both the individual and the MB predictions (**Table 3.8**). Results showed a low and flat sill demonstrating that the variograms are showing a blend in the final state of mixing [44, 46].

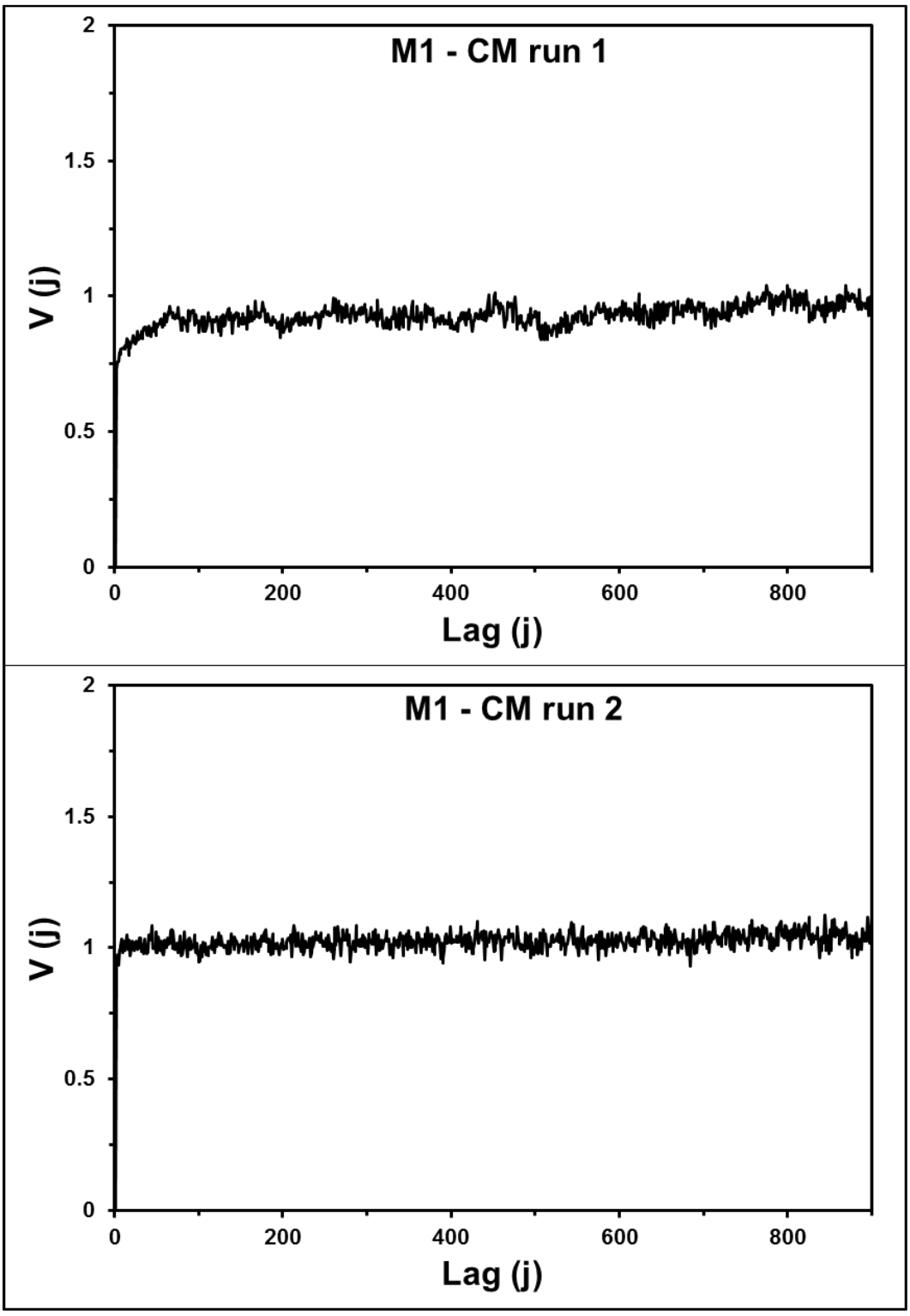

Figure 3.10 Variograms for the validation set prepared in a CM process using NIR spectrometer M1. Plots include variograms for the individual NIR predictions for two CM runs.

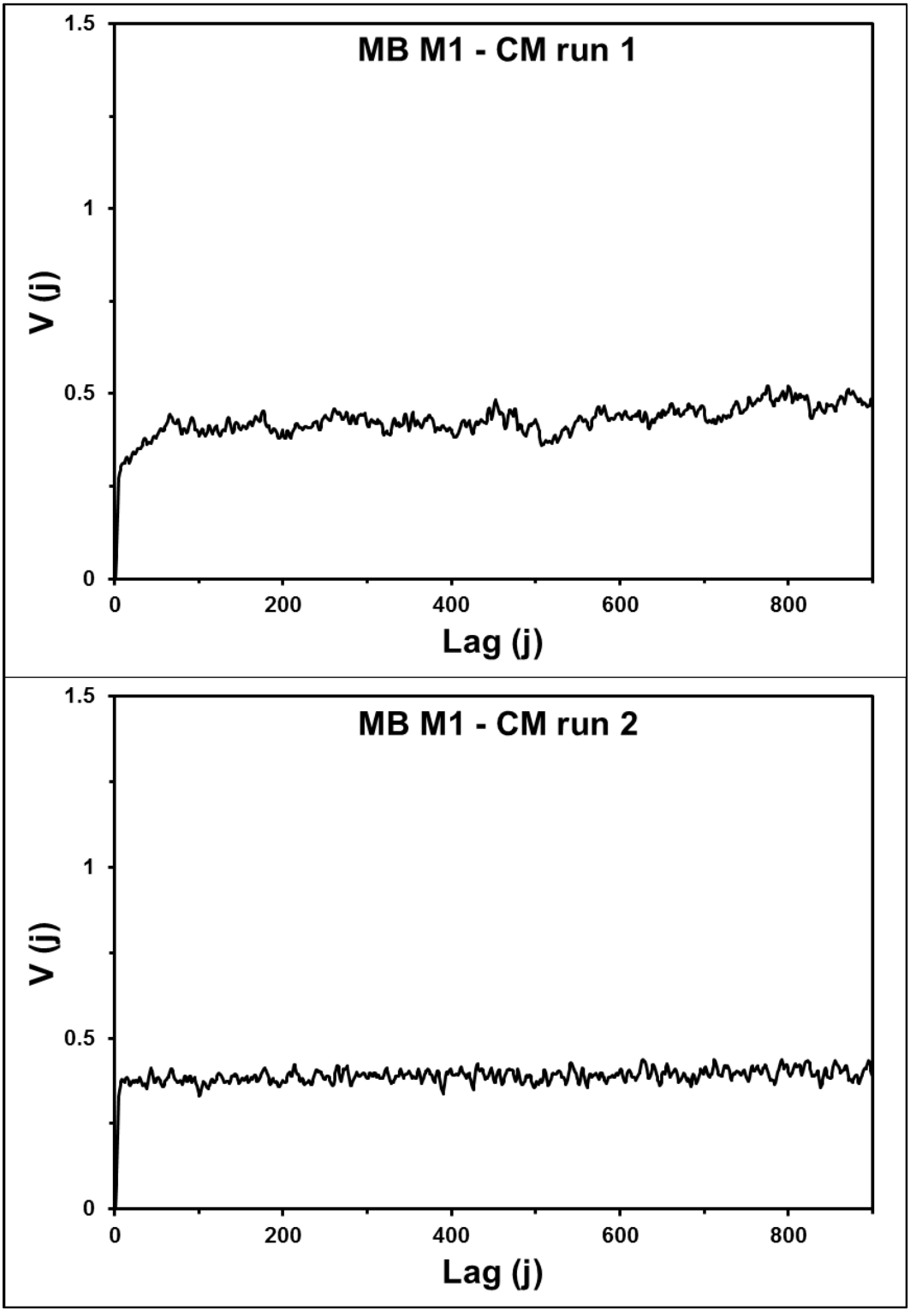

Figure 3.11 Variograms for the validation set prepared in a CM process using NIR spectrometer M1. Plots include variograms for the moving block NIR predictions for two CM runs.

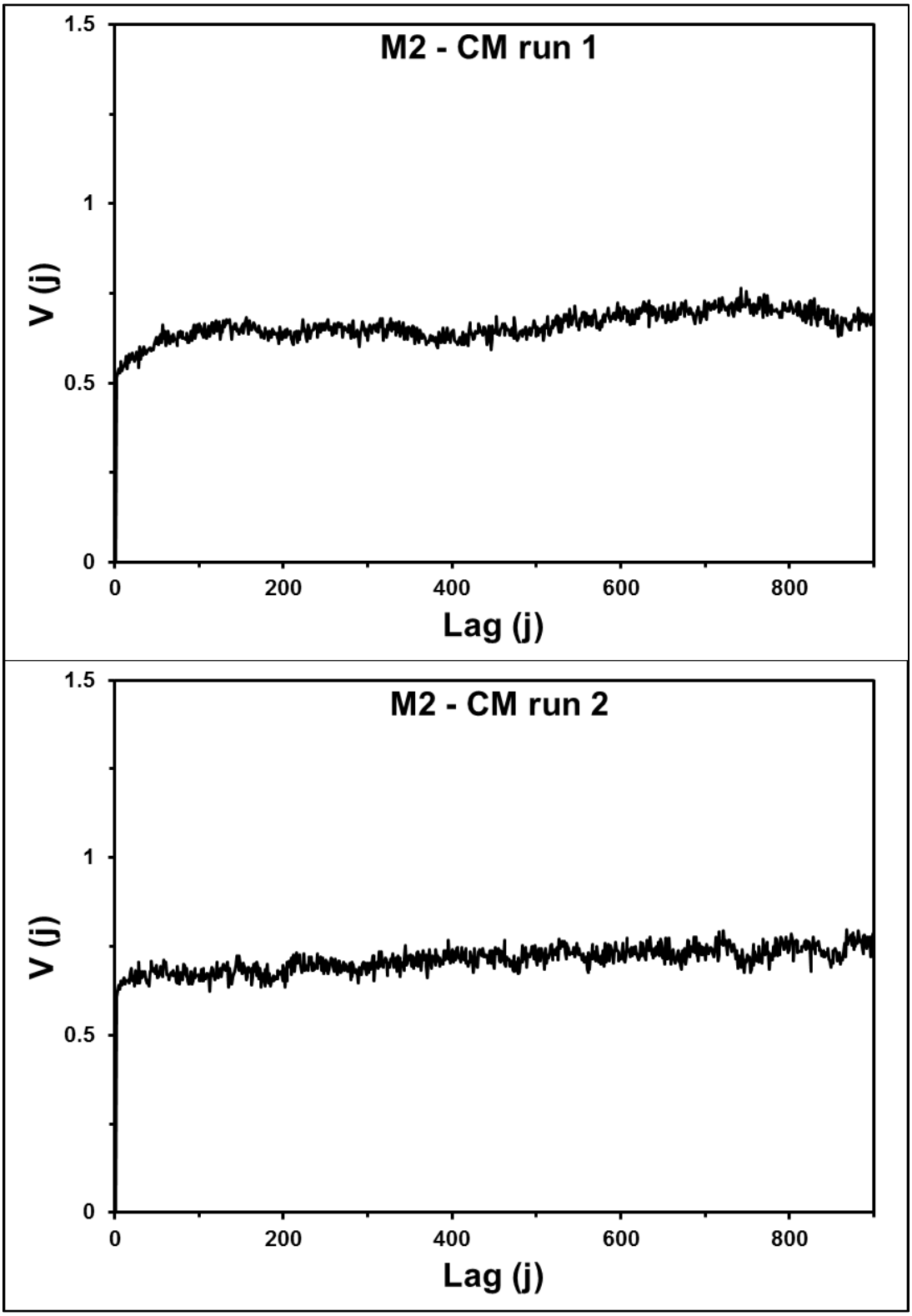

Figure 3.12 Variograms for the validation set prepared in a CM process using NIR spectrometer M2. Plots include variograms for the individual NIR predictions for two CM runs.

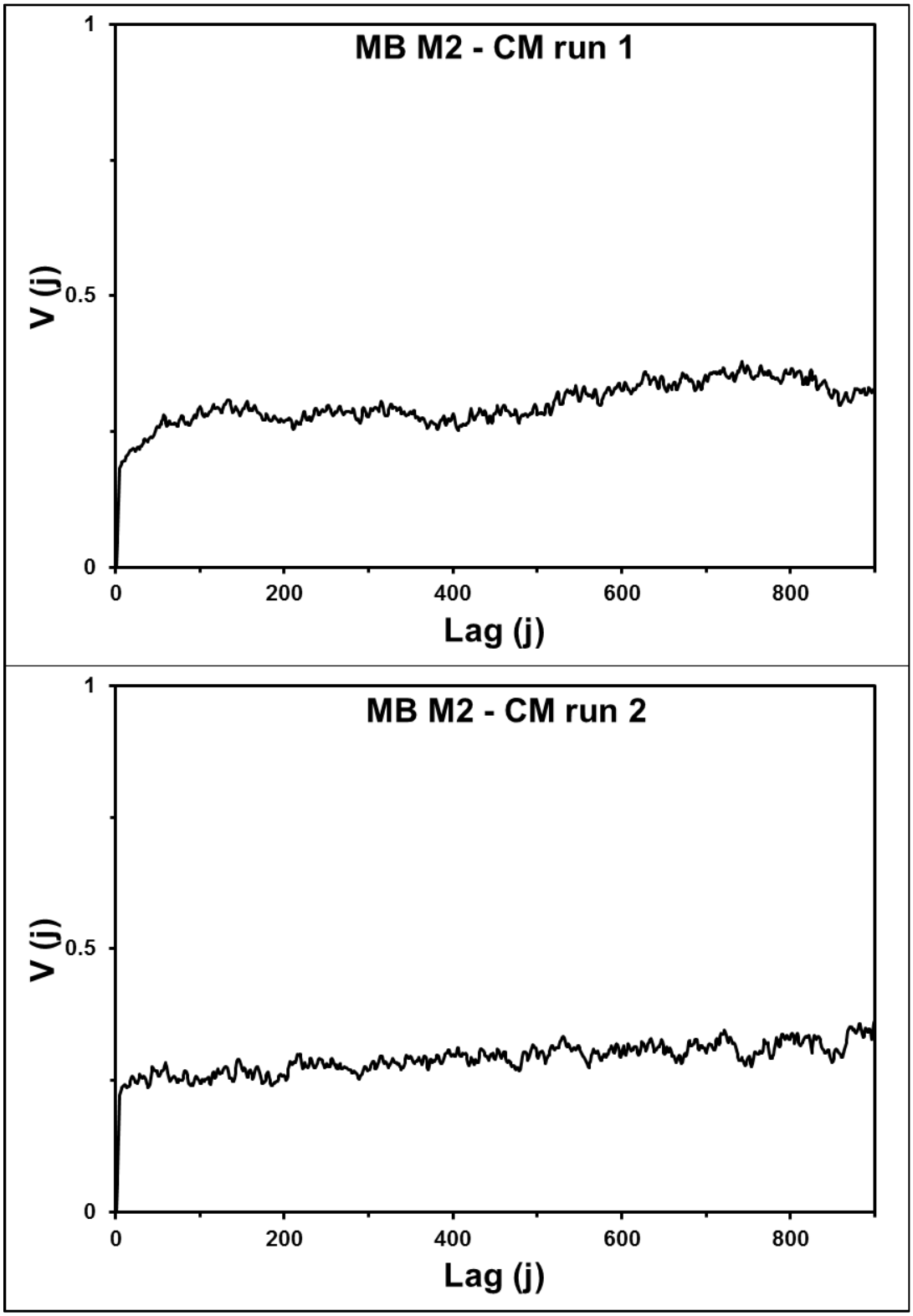

Figure 3.13 Variograms for the validation set prepared in a CM process using NIR spectrometer M2. Plots include variograms for the moving block NIR predictions for two CM runs.

Variograms were also calculated for tablets using the API concentrations predicted by the transmittance NIR calibration model. **Figure 3.14** shows the variograms obtained for the Tablet CM-1 and Tablet CM-2 runs. **Table 3.9** shows the tabulated analysis for the predictions of drug concentration in tablets, indicating relatively low heterogeneity in the tablets analyzed. A total of 60 tablets per CM run were evaluated.

Table 3.9 Variographic analysis of tablets produced from CM run

Individual predictions	CM-1 M1	CM-2 M1
Sill	0.16	0.17
MPE	0.17	0.14
Corrected sill	0.01	0.03
Standard deviation (% label)	0.41	0.41

Figure 3.14 (a) Variographic analysis of tablets obtained from the validation set prepared in a CM process (Tab-CM-1, Bruker FT-NIR spectrometer MPA1). The Nugget effect (MPE) is observed at V(j) = 0.2; (b) Variographic analysis of tablets obtained from the validation set prepared in a CM process (Tab-CM-2, Bruker FT-NIR spectrometer MPA1). The Nugget effect (MPE) is observed at V(j) = 0.1. Range = 0 for Tab-CM-1 and Tab-CM-2.

Variographic analysis of tablet results show the same value for the sill and MPE for the CM-1 run while there is a difference of 0.1 for the CM-2 run. The range is not observed for the variographic analysis of tablet drug concentration showing a process that cannot be improved. Lower sampling errors were obtained for tablets when compared to the blends individual prediction MPE results. The lower MPE was expected, since tablets were analyzed by NIR transmittance where a larger sample mass (composite sample) is analyzed. The sampling error for the MB predictions was found to be just as low as the sampling error obtained for tablets which might be directly related to analyzing a larger blend sample mass. Therefore, the use of the MB is recommended when analyzing blend results since sampling error is greatly reduced. These tablet results confirm the observations in the blends variograms which leads to conclude that the CM process evaluated is in control and blend spectra are being acquired when the blend is well mixed (final state of mixing).

3.4 Conclusion

Variographic analysis was successfully used to estimate the analytical and sampling errors in the NIR prediction of the API concentration of blends for a CM process. Different validation sets were used to evaluate the developed NIR model. These validation sets were prepared in different settings: laboratory scale, pilot plant scale, and in a CM facility. A high level of accuracy and precision was achieved. This study demonstrated that the calibration set must be prepared including the variation of the process that will be evaluated once the NIR model is implemented.

Variographic analysis was performed to blends and tablets obtained from two continuous manufacturing runs. Results showed that Sill and MPE values for the blends were similar indicative of a process that has little room for improvement. A low and flat sill were observed demonstrating low variation in the blends. This was confirmed with the V(j) and corrected sill values calculated. It was found that the sampling error for the variograms prepared using the moving block blend results was as low as the sampling error for tablets. Variographic analysis proved to be an excellent technique to evaluate the sampling error of blends produced in a continuous manufacturing process.

3.5 References

1. Yu L. Continuous Manufacturing Has a Strong Impact on Drug Quality. In: FDA Voice. http://blogs.fda.gov/fdavoice/index.php/2016/04/continuous-manufacturing-has-a-strong-impact-on-drug-quality/. 2016. Accessed July 23, 2016.

2. Gray N. In first, FDA approves Janssen's switch to continuous manufacturing for HIV drug. In: BioPharma Dive. http://www.biopharmadive.com/news/in-first-fda-approves-janssens-switch-to-continuous-manufacturing-for-hiv/417460/. 2016. Accessed July 23, 2016.

3. Brennan Z. FDA Allows First Switch From Batch to Continuous Manufacturing for HIV Drug. In: Regularoty affairs professionals society. http://raps.org/Regulatory-Focus/News/2016/04/12/24739/FDA-Allows-First-Switch-From-Batch-to-Continuous-Manufacturing-for-HIV-Drug/. 2016. Accessed July 23, 2016.

4. Langhauser K. Janssen's Historic FDA Approval. The FDA has approved -- for the first time in history -- a manufacturer's production method change from "batch" to continuous manufacturing. In: Pharmaceutical Manufacturing. http://www.pharmamanufacturing.com/articles/2016/janssens-historic-fda-approval/. 2016. Accessed July 23, 2016.

5. MacDonald G. Janssen working on other continuous processes post US FDA OK for Prezista. In: in-Pharma Technologist. http://www.in-pharmatechnologist.com/Processing/Janssen-working-on-other-continuous-processes-post-US-FDA-OK-for-Prezista?utm_source=copyright&utm_medium=OnSite&utm_campaign=copyright. 2016. Accessed July 23, 2016.

6. Blanco M, Bautista M, Alcala M. Preparing calibration sets for use in pharmaceutical analysis by NIR spectroscopy. Journal of pharmaceutical sciences. 2008;97(3):1236-45.

7. Meza CP, Santos MA, Romanach RJ. Quantitation of drug content in a low dosage formulation by transmission near infrared spectroscopy. AAPS PharmSciTech. 2006;7(1):E29.

8. Blanco M, Cruz J, Bautista M. Development of a univariate calibration model for pharmaceutical analysis based on NIR spectra. Analytical and bioanalytical chemistry. 2008;392(7-8):1367-72.

9. Laasonen M, Harmia-Pulkkinen T, Simard C, Räsänen M, Vuorela H. Development and Validation of a Near-Infrared Method for the Quantitation of Caffeine in Intact Single Tablets. Analytical Chemistry. 2003;75(4):754-60.

10. Blanco M, Alcalá M. Content uniformity and tablet hardness testing of intact pharmaceutical tablets by near infrared spectroscopy. Analytica Chimica Acta. 2006;557(1-2):353-9.

11. Blanco M, Peguero A. Influence of physical factors on the accuracy of calibration models for NIR spectroscopy. Journal of pharmaceutical and biomedical analysis. 2010;52(1):59-65.

12. Isaksson T, Næs T. Selection of Samples for Calibration in Near-Infrared Spectroscopy. Part II: Selection Based on Spectral Measurements. Applied spectroscopy. 1990;44(7):1152-8.

13. Iyer M, Morris H, Drennen III J. Solid dosage form analysis by near infrared spectroscopy: comparison of reflectance and transmittance measurements including the determination of effective sample mass. Journal of Near Infrared Spectroscopy. 2002;10(4):233-45.

14. Allison G, Cain YT, Cooney C, Garcia T, Bizjak TG, Holte O et al. Regulatory and Quality Considerations for Continuous Manufacturing. Journal of pharmaceutical sciences. 2015;104(3):803-12.

15. Schaber SD, Gerogiorgis DI, Ramachandran R, Evans JMB, Barton PI, Trout BL. Economic Analysis of Integrated Continuous and Batch Pharmaceutical Manufacturing: A Case Study. Industrial & Engineering Chemistry Research. 2011;50(17):10083-92.

16. Mollan Jr MJ, Lodaya M. Continuous processing in pharmaceutical manufacturing. American Pharmaceutical Review. 2004.

17. McKenzie P, Kiang S, Tom J, Rubin AE, Futran M. Can pharmaceutical process development become high tech? AIChE Journal. 2006;52(12):3990-4.

18. McAuliffe MAP, O'Mahony GE, Blackshields CA, Collins JA, Egan DP, Kiernan L et al. The Use of PAT and Off-line Methods for Monitoring of Roller Compacted Ribbon and Granule Properties with a View to Continuous Processing. Organic Process Research & Development. 2015;19(1):158-66.

19. Blanco M, Coello J, Eustaquio A, Iturriaga H, Maspoch S. Development and validation of a method for the analysis of a pharmaceutical preparation by near-infrared diffuse reflectance spectroscopy. Journal of pharmaceutical sciences. 1999;88(5):551-6.

20. Stordrange L, Malthe-Sørenssen D, Høyland OM. Development of a multivariate calibration model of an organic process by near infrared spectroscopy. J Process Anal Chem. 2001;6:6-20.

21. Swierenga H, Wülfert F, de Noord OE, de Weijer AP, Smilde AK, Buydens LMC. Development of robust calibration models in near infra-red spectrometric applications. Analytica Chimica Acta. 2000;411(1–2):121-35.

22. Blanco M, Alcalá M, González JM, Torras E. A process analytical technology approach based on near infrared spectroscopy: tablet hardness, content uniformity, and dissolution test measurements of intact tablets. Journal of pharmaceutical sciences. 2006;95(10):2137-44.

23. Despagne F, Massart DL, Chabot P. Development of a robust calibration model for nonlinear in-line process data. Analytical chemistry. 2000;72(7):1657-65.

24. Kim T, Hwang S, Hyun S. Development of a Continuous Manufacturing Process for Silica Sols via the Ion-exchange of a Waterglass. Industrial & Engineering Chemistry Research. 2008;47(18):6941-8.

25. Igne B, Zacour BM, Shi Z, Talwar S, Anderson CA, Drennen JK. Online Monitoring of Pharmaceutical Materials Using Multiple NIR Sensors—Part I: Blend Homogeneity. Journal of Pharmaceutical Innovation. 2011;6(1):47-59.

26. Xiang D, Berry J, Buntz S, Gargiulo P, Cheney J, Joshi Y et al. Robust calibration design in the pharmaceutical quantitative measurements with near-infrared (NIR) spectroscopy: Avoiding the chemometric pitfalls. Journal of pharmaceutical sciences. 2009;98(3):1155-66.

27. Shi Z, Cogdill RP, Short SM, Anderson CA. Process characterization of powder blending by near-infrared spectroscopy: blend end-points and beyond. Journal of pharmaceutical and biomedical analysis. 2008;47(4-5):738-45.

28. Liew CV, Karande AD, Heng PW. In-line quantification of drug and excipients in cohesive powder blends by near infrared spectroscopy. International journal of pharmaceutics. 2010;386(1-2):138-48.

29. Vanarase AU, Alcalà M, Jerez Rozo JI, Muzzio FJ, Romañach RJ. Real-time monitoring of drug concentration in a continuous powder mixing process using NIR spectroscopy. Chemical Engineering Science. 2010;65(21):5728-33.

30. Martínez L, Peinado A, Liesum L, Betz G. Use of near-infrared spectroscopy to quantify drug content on a continuous blending process: Influence of mass flow and rotation speed variations. European Journal of Pharmaceutics and Biopharmaceutics. 2013;84(3):606-15.

31. Wagner C, Esbensen KH. A critical review of sampling standards for solid biofuels – Missing contributions from the Theory of Sampling (TOS). Renewable and Sustainable Energy Reviews. 2012;16(1):504-17.

32. Colón YM, Florian MA, Acevedo D, Méndez R, Romañach RJ. Near Infrared Method Development for a Continuous Manufacturing Blending Process. Journal of Pharmaceutical Innovation. 2014;9(4):291-301.

33. Rinnan Å, Berg Fvd, Engelsen SB. Review of the most common pre-processing techniques for near-infrared spectra. TrAC Trends in Analytical Chemistry. 2009;28(10):1201-22.

34. Barnes RJ, Dhanoa MS, Lister SJ. Standard Normal Variate Transformation and De-trending of Near-Infrared Diffuse Reflectance Spectra. Applied spectroscopy. 1989;43(5):772-7.

35. Despagne F, Massart D-L, de Noord OE. Optimization of partial-least-squares calibration models by simulation of instrumental perturbations. Analytical Chemistry. 1997;69(16):3391-9.

36. Wülfert F. Temperature-robust multivariate calibration. Amsterdam: University of Amsterdam; 2004.

37. Esbensen K. DS 3077 Representative Sampling–Horizontal Standard. Danish Standards. www. ds. dk; 2013.

38. Blanco M, Coello J, Iturriaga H, Maspoch S, de la Pezuela C. Near-infrared spectroscopy in the pharmaceutical industry . Critical Review. Analyst. 1998;123(8):135R-50R.

39. Bellamy LJ, Nordon A, Littlejohn D. Real-time monitoring of powder mixing in a convective blender using non-invasive reflectance NIR spectrometry. Analyst. 2008;133(1):58-64. doi:10.1039/b713919e.

40. Sanchez-Paternina A, Roman-Ospino AD, Martinez M, Mercado J, Alonso C, Romanach RJ. Near infrared spectroscopic transmittance measurements for pharmaceutical powder mixtures. Journal of pharmaceutical and biomedical analysis. 2016;123:120-7.

41. Næs T, Isaksson T, Fearn T, Davies T. A User-Friendly Guide to Multivariate Calibration and Classification. Chichester, West Sussex: NIR Publications; 2002.

42. Osorio JG, Vanarase AU, Romañach RJ, Muzzio FJ. Continuous Powder Mixing. Pharmaceutical Blending and Mixing. John Wiley & Sons, Ltd; 2015. p. 101-27.

43. Hernandez E, Pawar P, Rodriguez S, Lysenko S, Muzzio FJ, Romanach RJ. Effect of Shear Applied During a Pharmaceutical Process on Near Infrared Spectra. Applied spectroscopy. 2016;70(3):455-66.

44. Esbensen KH, Román-Ospino AD, Sanchez A, Romañach RJ. Adequacy and verifiability of pharmaceutical mixtures and dose units by variographic analysis

(Theory of Sampling)–A call for a regulatory paradigm shift. International journal of pharmaceutics. 2016;499(1):156-74.

45. Harnby N. Chapter 2 - Characterization of powder mixtures. Mixing in the Process Industries (Second Edition). Oxford: Butterworth-Heinemann; 1992. p. 25-41.

46. Esbensen KH RR. Proper sampling, total measurement uncertainty, variographic analysis & fit-for-purpose acceptance levels for pharmaceutical mixing monitoring. InTOS forum 2015 Jun 9 (Vol. 5, No. 5, pp. 25-30).

Chapter 4

4 Process Analytical Technology in Continuous Manufacturing of a Commercial Pharmaceutical Product

Publication is in process of being submitted to the *International Journal of Pharmaceutics*

Jenny M. Vargas; Anthony Gonzalez, Eric Sanchez, Elvin Almodovar, Gustavo Classe, Yleana Colon, Sarah Nielsen, Vanessa Cardenas, Rodolfo J. Romañach

4.1 Introduction

This study describes the integration of process analytical technology (PAT) and continuous manufacturing (CM) within a cGMP regulated facility. Continuous manufacturing has been recognized as an innovation with significant potential to improve agility, flexibility, and robustness in the manufacture of pharmaceuticals [1]. CM together with PAT systems are used to analyze and control the manufacturing process to ensure high quality of the final drug product.

The implementation of CM reduces equipment space, material, waste, and release times thus improving the financial, environmental, and operational aspects [2-4]. The change from batch to continuous manufacturing eliminates the need to store and relocate intermediate products obtained during certain process steps avoiding segregation and degradation problems [1]. The change of a process from batch to continuous manufacturing was recently approved by the FDA and the PAT advances for this process are described in this study [5-9]. This study describes a significant advance by presenting a full continuous manufacturing run throughout 28 hours.

4.2 Materials and Methods

4.2.1. Materials

The formulation used for this study consisted of Prosolv® (JRS Pharma) silicified micro cellulose (SMCC), used as the major excipient; a cohesive API (> 50% LC concentration); crospovidone NF/PH EUR, and magnesium stearate NF/EP (lubricant).

4.2.2. Preparation of the Calibration and Validation Sets in the CM System

The calibration sample set (CSS) and validation sample sets (VSS) for the qualitative and the quantitative models were prepared using the CM process. Both sets of data were prepared on the same day and spectra were collected with the process in steady state. The CSS and VSS covered a concentration range spanning from 70% to 130% LC including five concentration levels (70%, 85%, 100%, 115%, and 130% LC). Two different API lot numbers were used during this CM run. Prosolv® and API concentrations were adjusted to achieve the desired concentration. Crospovidone and magnesium stearate were maintained at target concentration. A total of approximately 82 Kg were used to prepare the CSS and VSS. A second VSS (VSS2) was prepared at 95% and 105% LC. This VSS2 was used for the robustness evaluation. This validation set was prepared on a different day than the CSS and VSS using different API and excipient lot numbers.

The CSS and VSS sets were prepared using the same CM process and line as the commercial manufacturing process to be monitored (**Figure 4.1**). The CM line includes five K-tron gravimetric feeders. However, feeder #4 was not used since it is only used for formulations with at least five components. Gravimetric feeders for the API, Prosolv®, and crospovidone were automatically refilled using volumetric feeders. Magnesium stearate was manually refilled since this gravimetric feeder does not include a volumetric feeder. The CM process consisted of a pneumatic transfer of the API and excipients from containers to the volumetric feeders and then to the gravimetric feeders at specific rates, determined by a level sensor in each volumetric feeder. Volumetric feeders are used to refill the gravimetric feeders during refill cycles, initiated once the amount of material (API,

Prosolv®, crospovidone) in the gravimetric feeder reaches a minimum. Gravimetric feeders can operate as gravimetric (feeding process) and as volumetric (refill cycle). In gravimetric mode, loss in weight (LIW) control is used. LIW determines the rate at which the material is dispensed from the feeders since it updates the screw speed to maintain the mass flow rate. The gravimetric feeders and the mass flow are used for accurate material dispensing and as the reference method for the blends concentration, respectively.

The API and excipients pass from the gravimetric feeders to an in-line conical mill and then into an in-line continuous paddle blender. NIR spectroscopy is performed in the sensing interface, placed after the blender, as shown in **Figure 4.1**. Blend spectra are collected in-line as the powder flows from the blender to the tablet press. The level of the blend in the interface is controlled by the rotary valve and a level sensor. After the interface, the blended material passes through the diverter valve to the tablet press for tablet compaction or to the blend rejection port for waste.

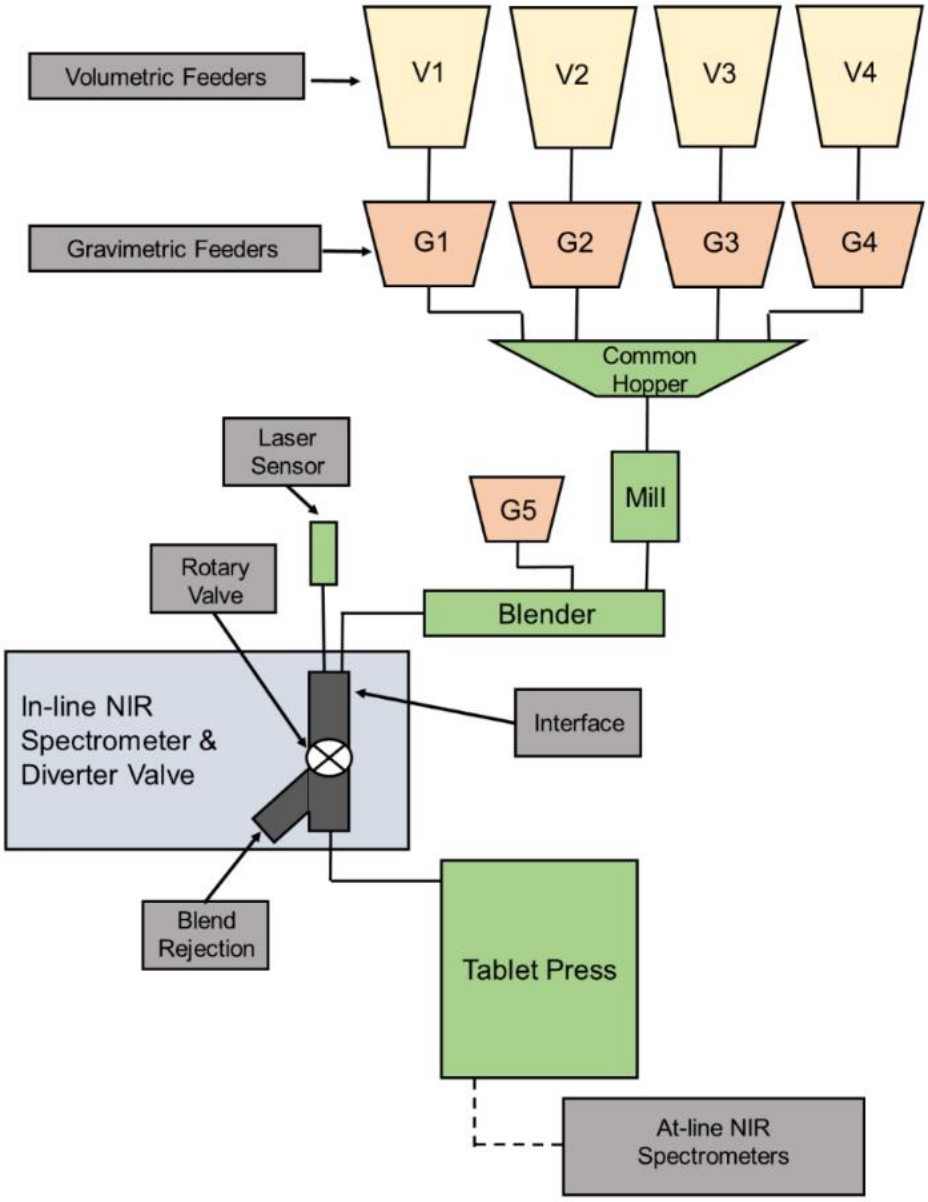

Figure 4.1 Continuous manufacturing line. The diagram includes the volumetric (V1, V2, V3, V4) and gravimetric feeders (G1, G2, G3, G4, G5), the continuous blender, the interface, and tablet press. The line throughput was maintained at 40 kg/hr for this study.

The feeder's calculated gravimetric concentrations were used as the reference method for the quantitative model. These concentrations were calculated using the feeder's mass flow and the residence time distribution (RTD). RTD correlates each blend spectrum with the mass flow data to calculate the concentration for each spectrum. Since

RTD gives the length of time a material spends in a system, it provided the length of time it takes the blend to flow from the feeders to the interface. The RTD was calculated to be 140 seconds for this specific line and product. The 140 seconds were subtracted from each spectrum time and then paired with the corresponding mass flow timed data. RTD must be calculated for each product used in the CM line since is dependent on the material properties.

4.2.3. Preparation of Challenge Blends for the Qualitative Model

Challenge blends were used to evaluate the specificity of the qualitative model and thus should be rejected by the model.

A total of six 100g challenge blends were prepared using Prosolv®, crospovidone, magnesium stearate, four APIs, and lactose. The four APIs (different from the API of the correct formulation) and lactose were chosen since they are common components used in the manufacturing site and might be used in the same CM line in the future. The preparation of the challenge blends at target concentration was performed by using the correct formulation excipients (crospovidone, Prosolv®, and magnesium stearate) and one of the four incorrect APIs. In addition, a placebo and a blend using the incorrect filler (lactose) were prepared.

All challenge blends were prepared using lab-scale equipment to avoid introducing incorrect materials to the cGMP continuous manufacturing line. Raw materials (APIs, Prosolv®, lactose, crospovidone, and magnesium stearate) were weighted and placed in individual bottles inside a Bohle (40 liters) LM-Bin blender for mixing at 20 rpm for four minutes. After mixing, blends were stored in suitable sample containers inside an Aluminum “Vapor-loc” bag.

4.2.4. NIR Spectral Acquisition

NIR spectra were acquired using the Bruker Matrix-FE FT-NIR spectrometer, emission series (Billerica, MA) controlled by the OVP (OPUS Validation Program) software Version 4.2. The Matrix-F spectrometer includes a diffuse reflectance probe with two tungsten NIR light sources and works in the spectral range of 12,000 - 4,000 cm^{-1}. A resolution of 16 cm^{-1} with 16 averaged scans were used for spectra acquisition. Each spectrum was acquired approximately every 5 seconds (16 scans = ~1.46 seconds plus file creation = ~3.54 seconds). Sample mass was calculated as 37 mg per NIR spectrum for 16 scans.

Spectra for the CSS and VSS were acquired in-line during CM runs. Material passed through the interface where diffuse reflectance spectra were collected using the NIR spectrometer [10]. A total of 60 CSS spectra were used for the qualitative model (five concentration levels, ten spectra per concentration level plus ten spectra from an additional API lot of the 100% API target concentration) while 125 CSS spectra were used for the quantitative model (five concentration levels, twenty-five spectra per concentration level plus twenty-five spectra from an additional API lot of the 100% API target concentration). Spectra for the challenge blends were acquired at-line with the Bruker NIR spectrometer. Six challenge blends were prepared and six samples (approximately 10-g per sample) were obtained per challenge blend prepared. Each 10-g sample was poured into a sample cup with a sapphire window bottom and placed on top of the NIR spectrometer. A total of 36 spectra (one spectrum per sample) were acquired for the challenge blends as indicated in **Table 4.1**.

4.2.5. Development and Validation of the Qualitative and Quantitative Models

Qualitative and quantitative multivariate models were developed and validated using the SIMCA-P+12 Software Prediction Engine from Umetrics [11-14]. The principal component analysis (PCA) algorithm was used to develop the qualitative model to determine whether the correct blend was prepared during the CM process. The quantitative model was developed using the partial least squares (PLS) algorithm and

was designed to predict API (drug) concentration of the blends. **Table 4.1** shows the number of spectra used for the CSS, VSS, and challenge blends for the development and validation of the quantitative and qualitative models.

Table 4.1 Summary of sample spectra used for the CSS, VSS, and challenge blends

Sample Set	Number of spectra in qualitative model	Number of spectra in quantitative model
CSS	60	150
VSS	310	310
Challenge blends	36	N/A

Specificity and robustness of the qualitative model were evaluated using the distance to the model in the X-space (DModX). DModX is defined as the residual (difference) between a sample and its projection into the calibration model (**Figure 4.2**). The DModX absolute values of the predicted observation were calculated as [15]:

$$\boldsymbol{S_i = sqrt\ (\sum e_{ik}{}^2\ /\ (K - A))} \quad (1)$$

Where **K** is the **X** variables, **A** is the absolute distance, and e_{ik} is the **X**-residuals of the observation ***i***.

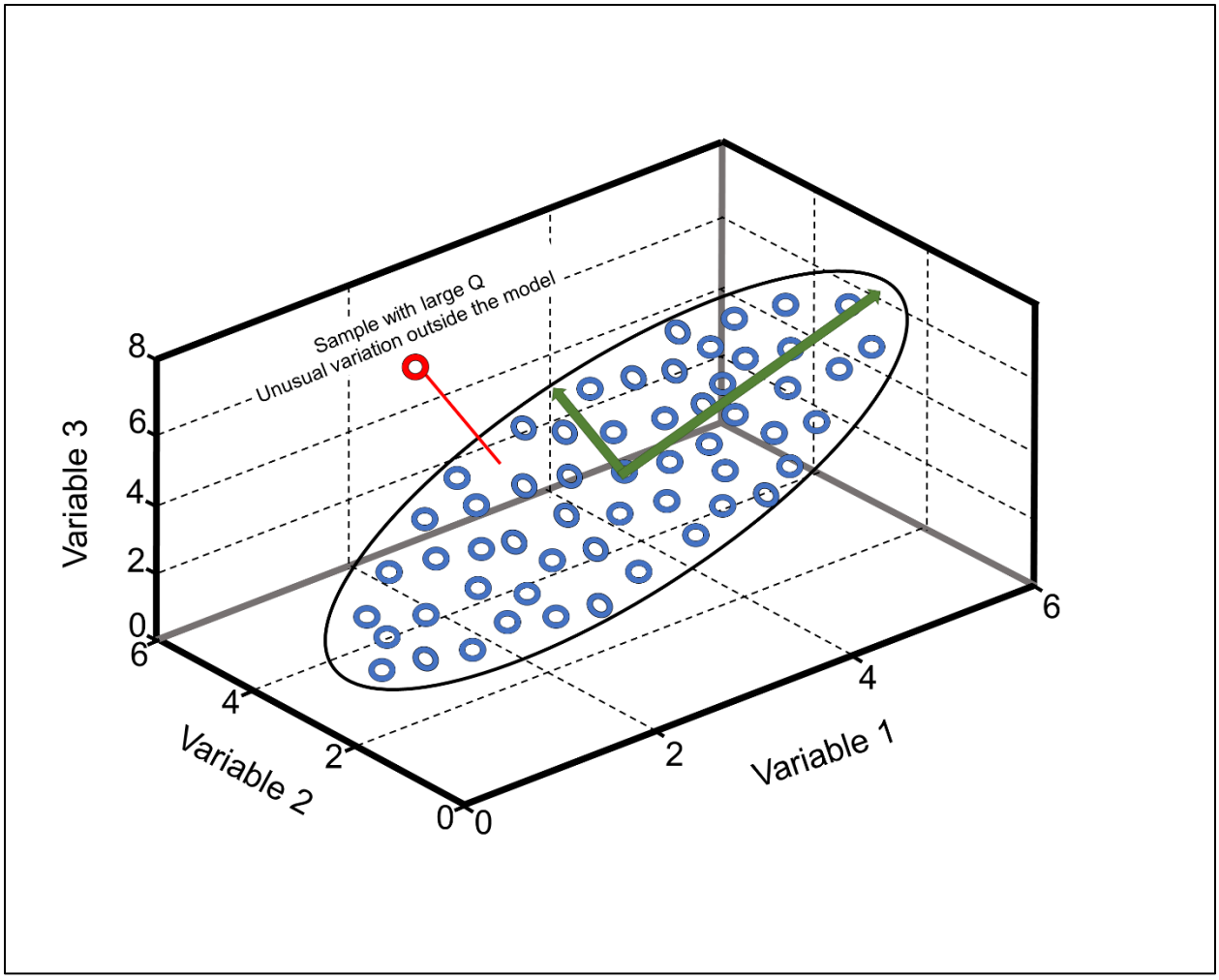

Figure 4.2 Schematic representation of the information obtained from the DModX

Robustness of the quantitative model was evaluated using the Hotelling's T^2Range (T^2R). T^2R displays a measure of how far each observation is from the center and was used as an evaluation tool before the NIR prediction (**Figure 4.3**). A pass result would lead the model to perform the NIR concentration prediction. T^2R was used as a second identification (ID) but based on the quantitative model. The use of T^2R gives assurance and reliability of the high quality the NIR predictions and is viewed as an additional control tool for the CM process. The T^2R values for observation i were calculated as [15]:

$$\boldsymbol{T_i^2 = \sum\left(t_{ia}^2 / s_{ta}^2\right)} \quad (2)$$

Where $\mathbf{S^2_{ta}}$ is the variance of $\mathbf{t_a}$ per the class model, and $\mathbf{t_{ia}}$ is the selected range of components of the scores.

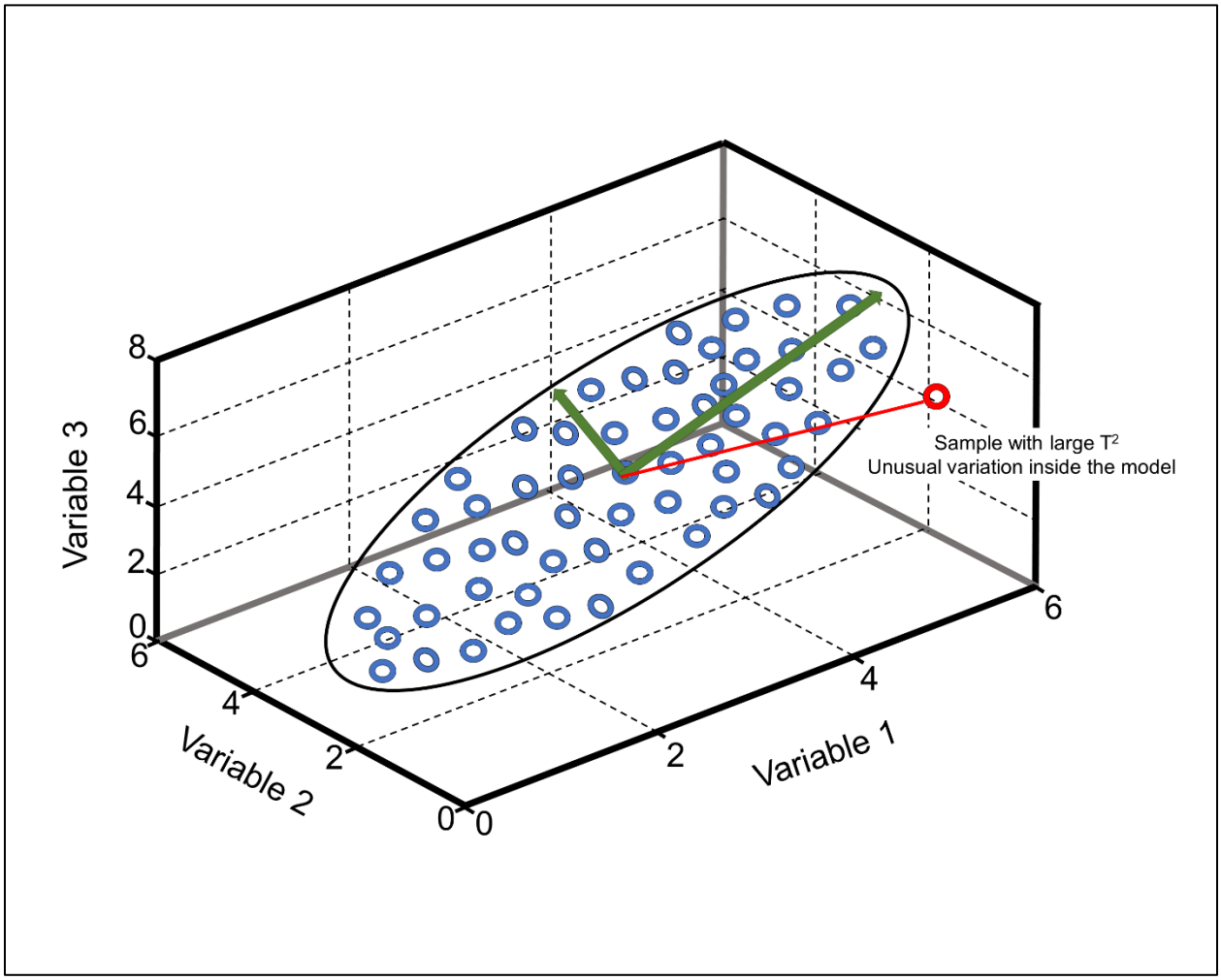

Figure 4.3 Schematic representation of the information obtained from the T^2Range

The quantitative model was developed using the PLS algorithm and was set to predict drug concentration of blend during the CM process. Accuracy, precision, linearity, robustness, and specificity were assessed as part of the quantitative model validation [16]. Accuracy, precision, and linearity were evaluated across the concentration range of the model (70% - 130% LC). The predictive performance of the quantitative model was evaluated in terms of the standard error of prediction (SEP) as per EMA guidelines [17]:

$$\mathbf{SEP} = \sqrt{\frac{\sum_{\mathbf{i=1}}^{\mathbf{n}}(\hat{\mathbf{y}} - \mathbf{Y_i})^2}{\mathbf{n}}} \quad (3)$$

Where $\hat{y}$ is the predicted value, y_i is the reference concentration, and n is the number of samples.

The qualitative and quantitative models are integrated in the SIPAT system (Siemens AG, Belgium) to evaluate blend spectra obtained in real time during commercial CM runs [18]. All blend spectra collected by the NIR spectrometers are sent to SIPAT where predictions are performed using the implemented models. SIPAT then communicates with the control system if an action needs to be taken (divert blend, stop the process, etc.) regarding the results obtained. Another evaluation (air diagnostic) is performed to the NIR spectra collected in the SIPAT system before the implemented models are applied. The air diagnostic evaluates each spectrum to ensure that spectra is not originate from the absence of sample in the sensing interface.

The air diagnostic was developed to detect when air spectra is collected due to the lack of blend in the interface. The spectral range 8880 – 8159 cm^{-1} was chosen for the air spectra evaluation since the API bands in this range are not observed in the air spectra or when there is fine powder stuck to the interface window. The air diagnostic test was performed with the absorbance (log 1/R) values without the use of spectral pretreatments. Three types of spectra were used to establish the air diagnostic limit: (a) spectra of blends at 70%, 100%, and 130% LC, (b) a spectrum acquired when no material is presented to the NIR spectrometers through the interface window (spectrum of air inside the interface), (c) and a spectrum acquired with fine powder residue left in the interface window (fine powder stuck to the interface window). The air spectrum was acquired with the CM line clean while the spectrum with powder stuck to the interface window was acquired with the CM line dirty, after the CM line was emptied. The three types of spectra (concentration blends, air, fine powder stuck to the interface window) were plotted and compared as shown in **Figure 4.4**. The air diagnostic value of each spectrum at 70%, 100%, and 130% LC was calculated as the average of the absorbance (log 1/R) values in the 8880 – 8159 cm^{-1} spectral range. All air diagnostic value calculated must yield absorbance values

above or equal to the blend spectra absorbance values but below the air spectrum absorbance values. Therefore, the air diagnostic limit was set as twice the average absorbance (log 1/R) value obtained for the blend spectra used (limit was set at 0.4). All spectra used for the validation of the NIR models complied with the air diagnostics.

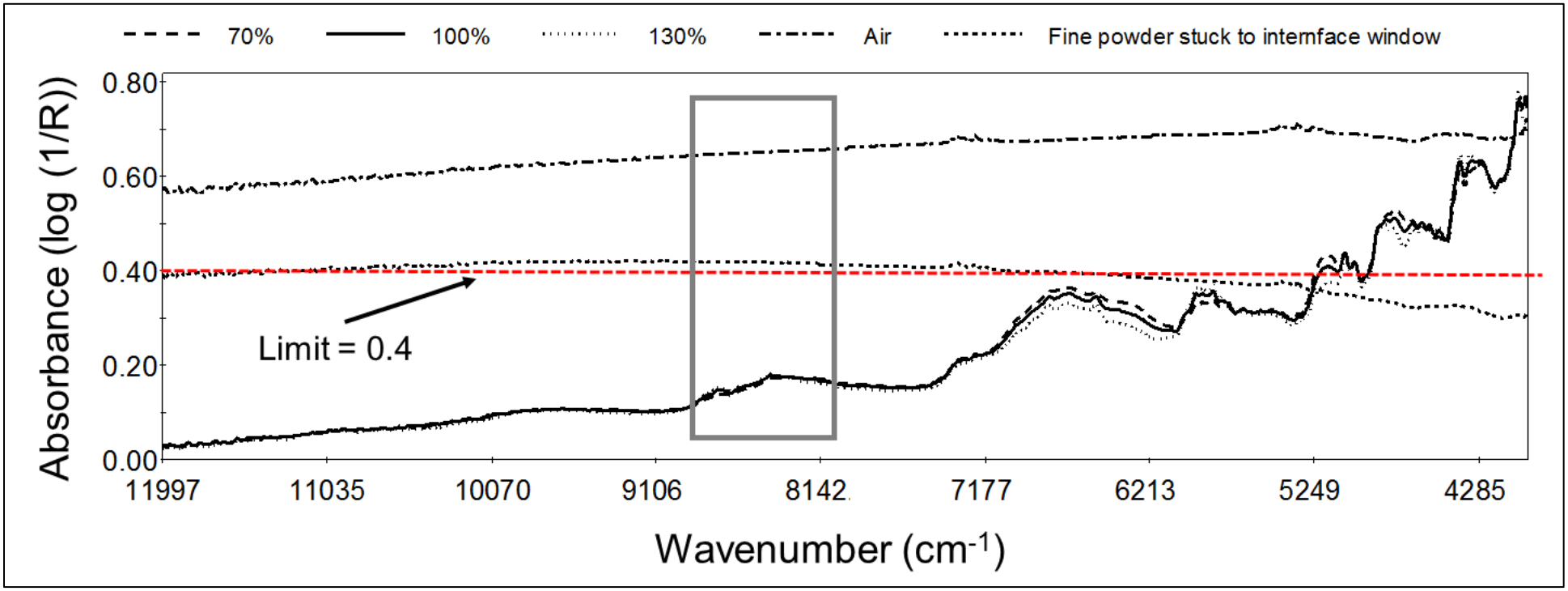

Figure 4.4 Plot for the air diagnostic evaluation using blend spectra at API target concentrations (70%, 100%, 130% LC), an air spectrum, and a spectrum of fine powder stuck to window, after the CM line was emptied. The spectral range usd for the air diagnostic (8880 – 8159 cm^{-1}) is shown in the boxed area. Limit was set as 0.4 absorbance value.

4.2.6. Variographic Analysis of Commercial CM Run

Variograms were calculated for a commercial CM run using a program developed with the MATLAB 2013b software (The MathWorks, Natick, MA) [19]. Eq. 4 shows the equation used to write the MATLAB code to calculate variograms.

$$V(j) = \frac{1}{2(Q_{total}-j)} \sum_{q=1}^{Q_{total}-j} (h_{q+j} - h_q)^2 \quad (4)$$

Where V(j) is the function of the distance between extracted increments, Q_{total} is the total number of analytical results, *j* is the *lag* and *h* is the heterogeneity contribution of the analyte measured in each increment.

The sill, nugget effect or minimum practical error (MPE), and the corrected sill were calculated using the variogram results. MPE is the estimate of the total sampling and analytical error, the sill gives the expected minimum sampling variance, and the corrected sill relates to the residual heterogeneity of the blends.

4.3 Results and Discussion

The qualitative model was developed and validated to determine whether the correct formulation was being prepared in the CM system. The model was implemented for the CM process to be located inside the SIPAT system and is applied before the quantitative model. The calibration set for the PCA model consisted of 60 spectra (five concentration levels, ten spectra per concentration level plus ten spectra from an additional API lot of the 100% target concentration) as indicated in **Table 4.1**. Two principal components (PCs - 98.2 % cumulative **X**-explained variance) described the spectral variation in the 6032 – 5710 cm^{-1} spectral range (**Figure 4.5**) when the SNV and first (1^{st}) derivative with a 25-point window data pretreatments were applied to NIR spectra. This spectral range was chosen to target bands associated to the API of interest. **Figure 4.6** shows the PCA score plot in the spectral region chosen for the model. Clearly defined clusters for all five CSS concentration levels are observed. The VSS projection in the PCA model ellipse shows that the validation set is distributed within the PCA scores plot.

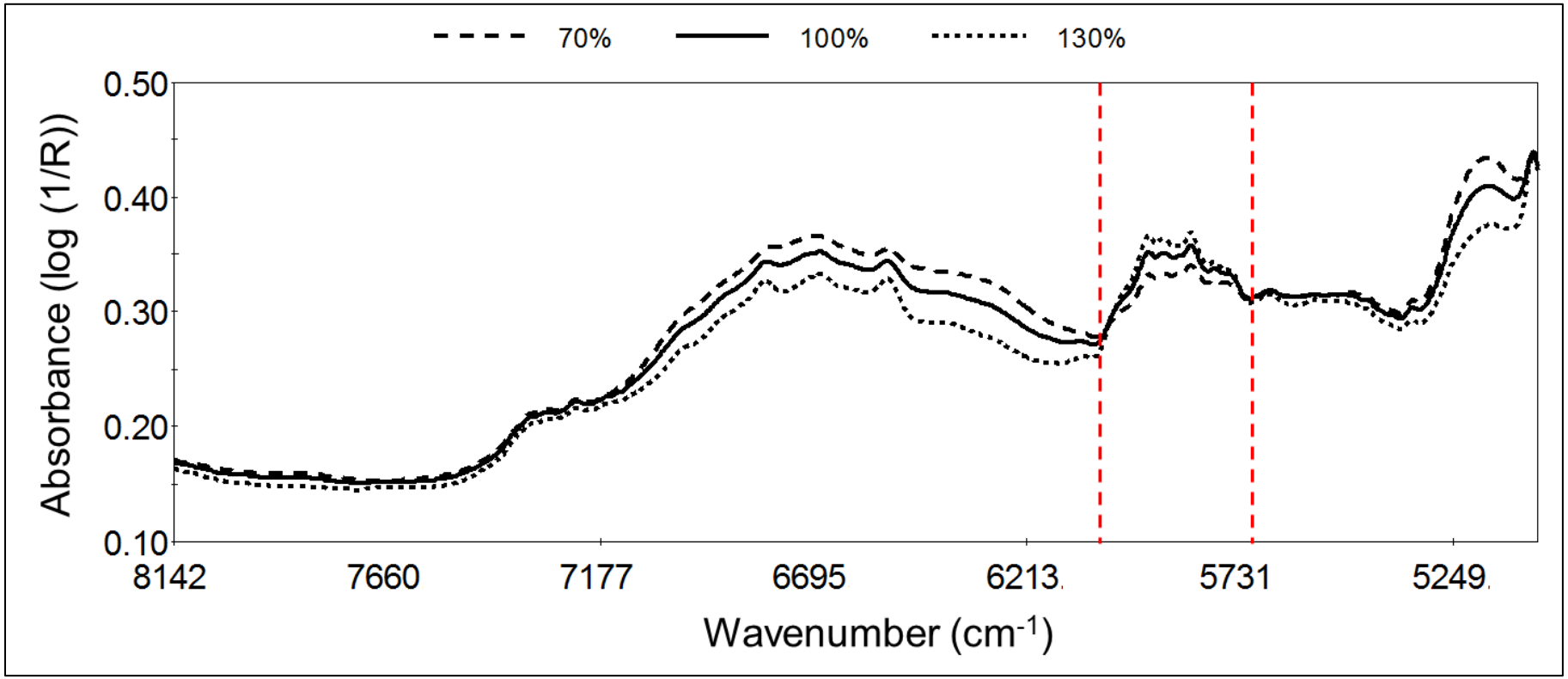

Figure 4.5 NIR spectra of the 70%, 100%, and 130% API concentration blends included in the CSS. The selected spectral range (6032 – 5710 cm^{-1}) used for the development of both models (qualitative and quantitative) is shown in the boxed area.

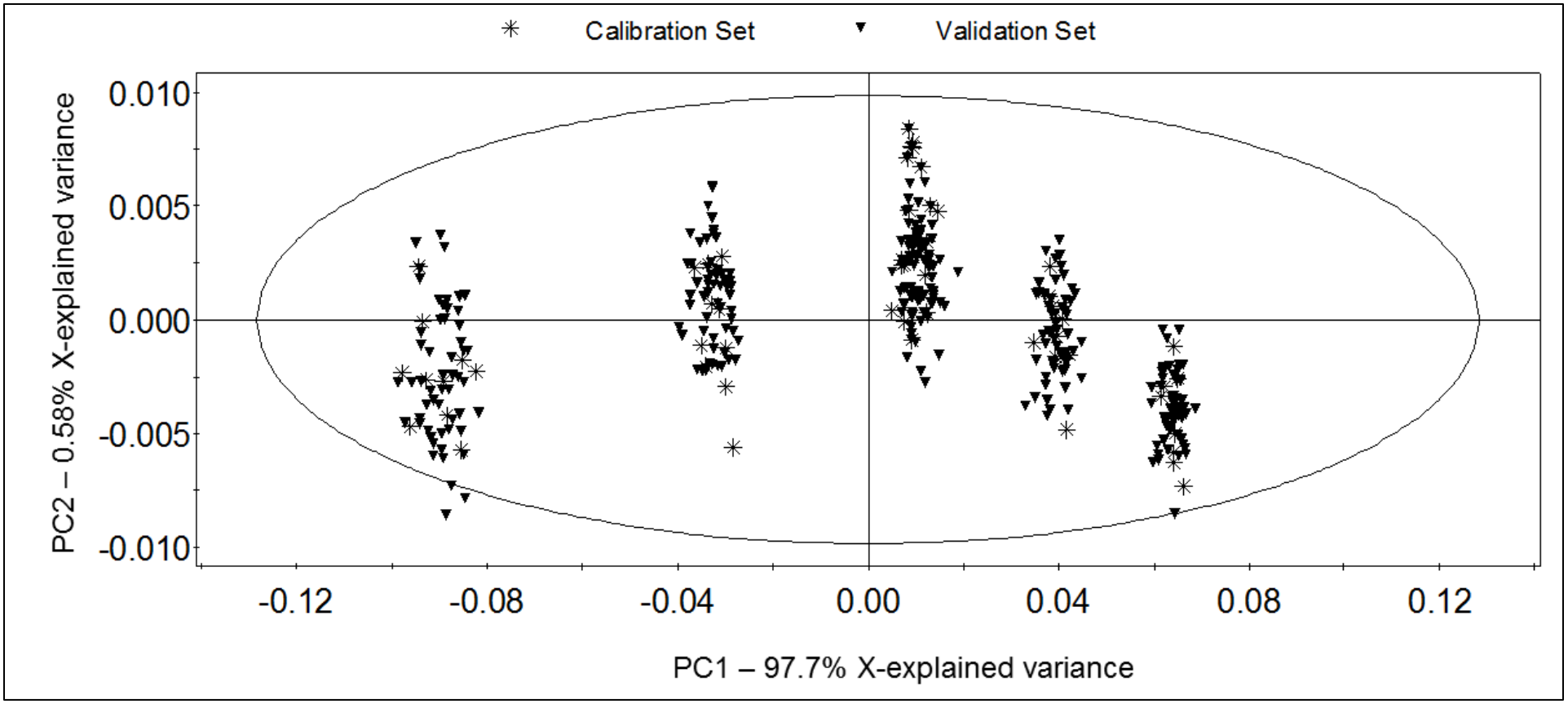

Figure 4.6 PCA scores plot overlay of the qualitative model CSS and VSS. The model was developed using 2 PCs in the spectral range: 6032 cm^{-1} – 5710 cm^{-1} using the SNV+1st derivative (25-point moving window) pre-treatment. PC1 explains 97.7% of the variation of the model while PC2 explains 0.58%.

An acceptance criterion was established for the DModX evaluation using the DModX values obtained for the CSS. The CSS DModX values were tested for normality to confirm if they followed a normal distribution before applying parametric calculations to establish a limit. Results showed that the DModX values were not drawn from a normal distribution and were then fit with a log-normal function to obtain a log-normal distribution. **Figure 4.7** shows the histogram plotted for the CSS and challenge blends DModX results. The mean plus 6σ of the log normalized DModX values was established as the DModX limit (2.6×10^{-3}). Six standard deviations were necessary because the CSS DModX values had a very narrow distribution and because of the high amount of data obtained from the CM process. If a lower limit had been established, it would have caused numerous process interruptions. However, this high limit did not compromise the ability of the model to reject the challenge blends which had DModX values 2.5 - 30 times higher than the established limit.

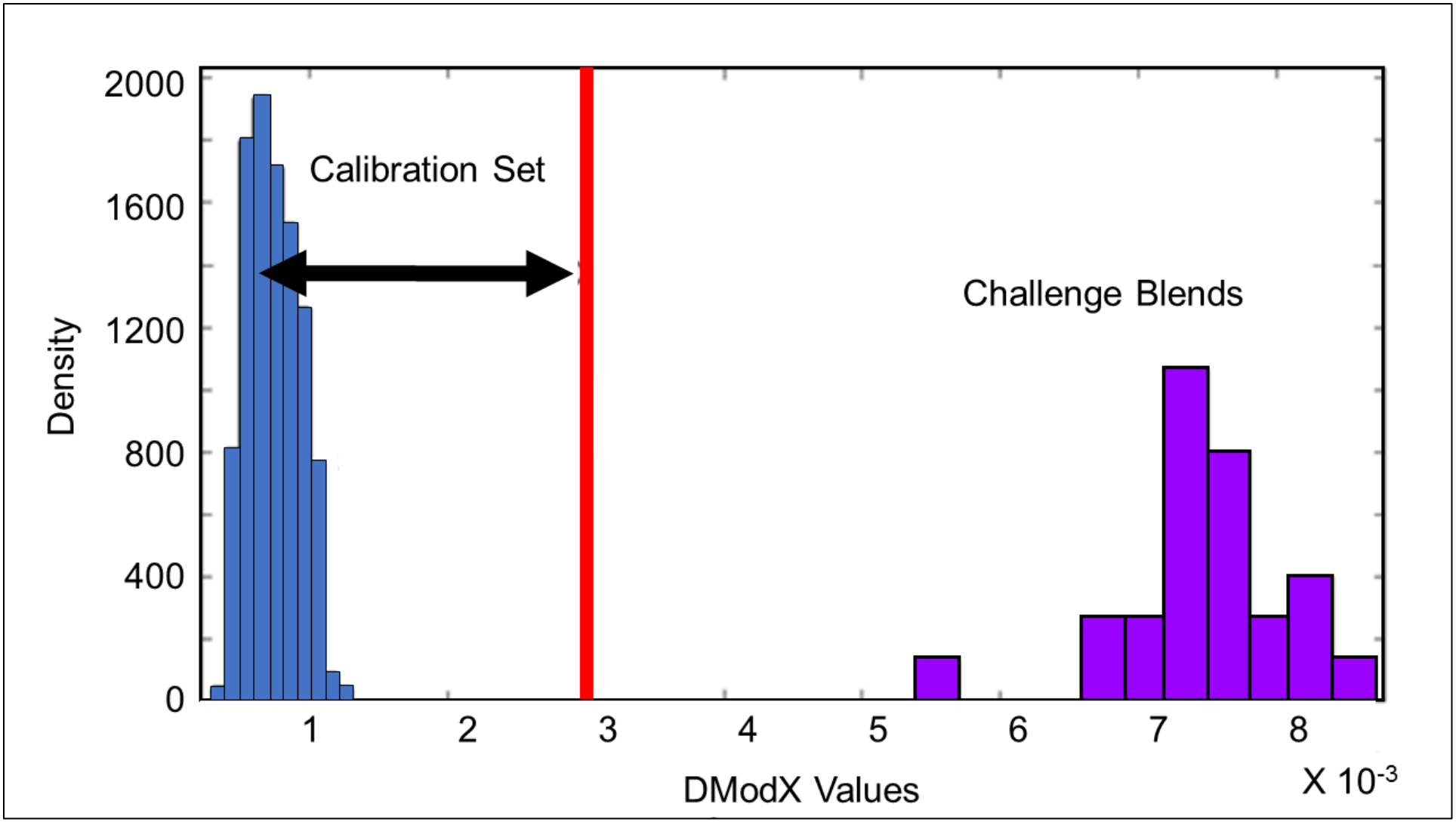

Figure 4.7 Histogram of the CSS and challenge blends DModX values. The red line shows the 6σ cutoff for the DModX limit.

Figure 4.8 shows the DModX results for the VSS. All DModX values were below the established limit (DModX limit = 2.6 x 10^{-3}) demonstrating the reliability of this qualitative model to confirm the correct API in the blend.

Specificity of the qualitative model was assessed with the VSS (**Figure 4.8**) and the challenge blends (**Figure 4.9**), as per the European Medicines Agency (EMA) guidelines [17]. The model was tested for specificity since this shows the ability of the method to detect the analyte of interest in the presence of other components in the formulation [20]. The challenge samples were compositionally incorrect formulations that should yield DModX results above the established limit for the qualitative model. The DModX results for the challenge blends were found to be between 2.5 and 30 times above the established limit (DModX limit = 2.6 x 10^{-3}), as shown in **Figure 4.9**. The challenge blends DModX results demonstrate the ability of the qualitative model to respond to blends prepared with incorrect components and the high capability of the model to identify as incorrect, blends containing the API of interest but with different filler (**Figure 4.9**, lactose DModX results).

Robustness of the qualitative model was evaluated using the VSS2. VSS2 was prepared varying both the API lot and the line throughputs (35, 40, and 45 kg/h) during the same CM run. DModX results were used to evaluate robustness. **Figure 4.10** shows the DModX plot for the robustness evaluation. Results show all DModX results below the established limit, confirming the high robustness and reliability of the qualitative model to confirm the correct API.

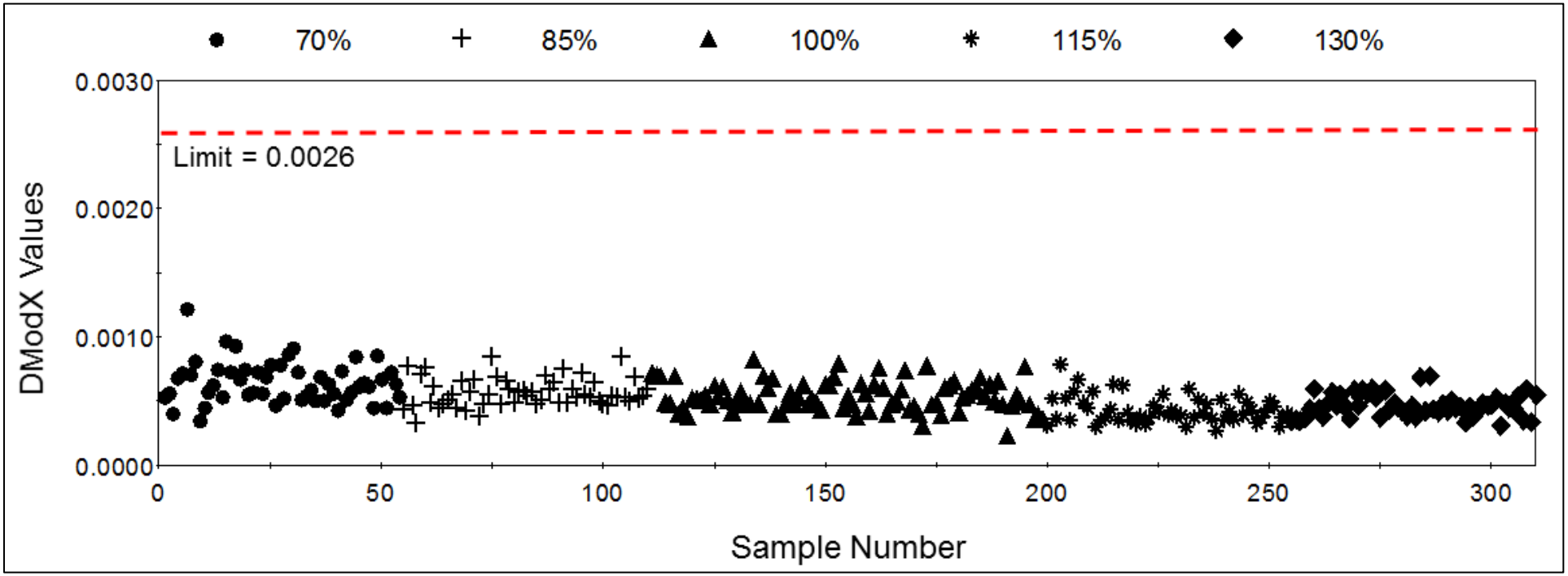

Figure 4.8 Plot for the VSS DModX results (DModX limit = 2.6 x 10^{-3})

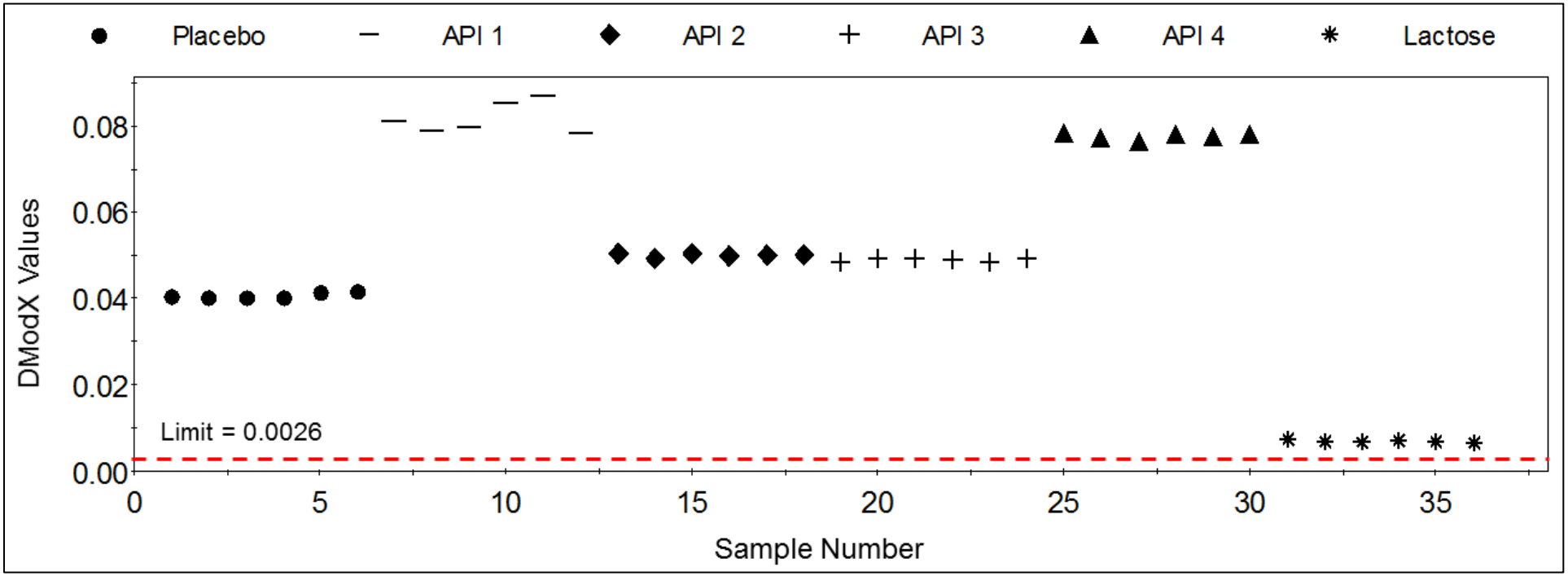

Figure 4.9 Plot for the challenge blends DModX results (DModX limit = 2.6 x 10^{-3})

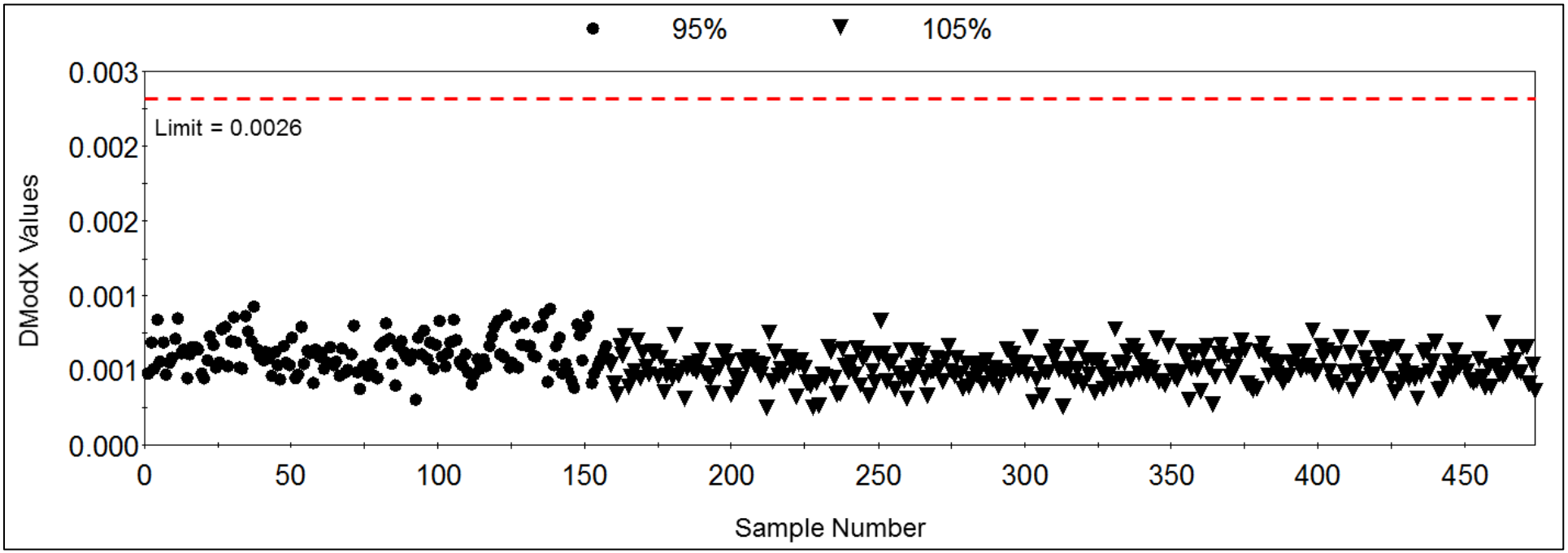

Figure 4.10 Plot for the DModX results for the robustness evaluation (DModX limit = 2.6 x 10^{-3})

4.3.1. Development and Validation of Quantitative Model

The PLS quantitative model was developed in the spectral range 6032 – 5710 cm^{-1} with two PLS factors and SNV and 1^{st} derivative with a 25-point window as pretreatment. The CSS consisted of 150 spectra (for all five concentration levels). NIR spectra were obtained in-line using the CM process. The reference method for the CSS and VSS concentrations were calculated from the mass flow data (obtained from the gravimetric feeders) as discussed in the Experimental section.

Robustness of the model was evaluated using T^2R. The T^2R acceptance criteria (limit = 6.2) was established using the PLS scores from the calibration set, based on a 95% confidence interval. T^2R values obtained for the VSS met the acceptance criteria established as shown in **Figure 4.11**.

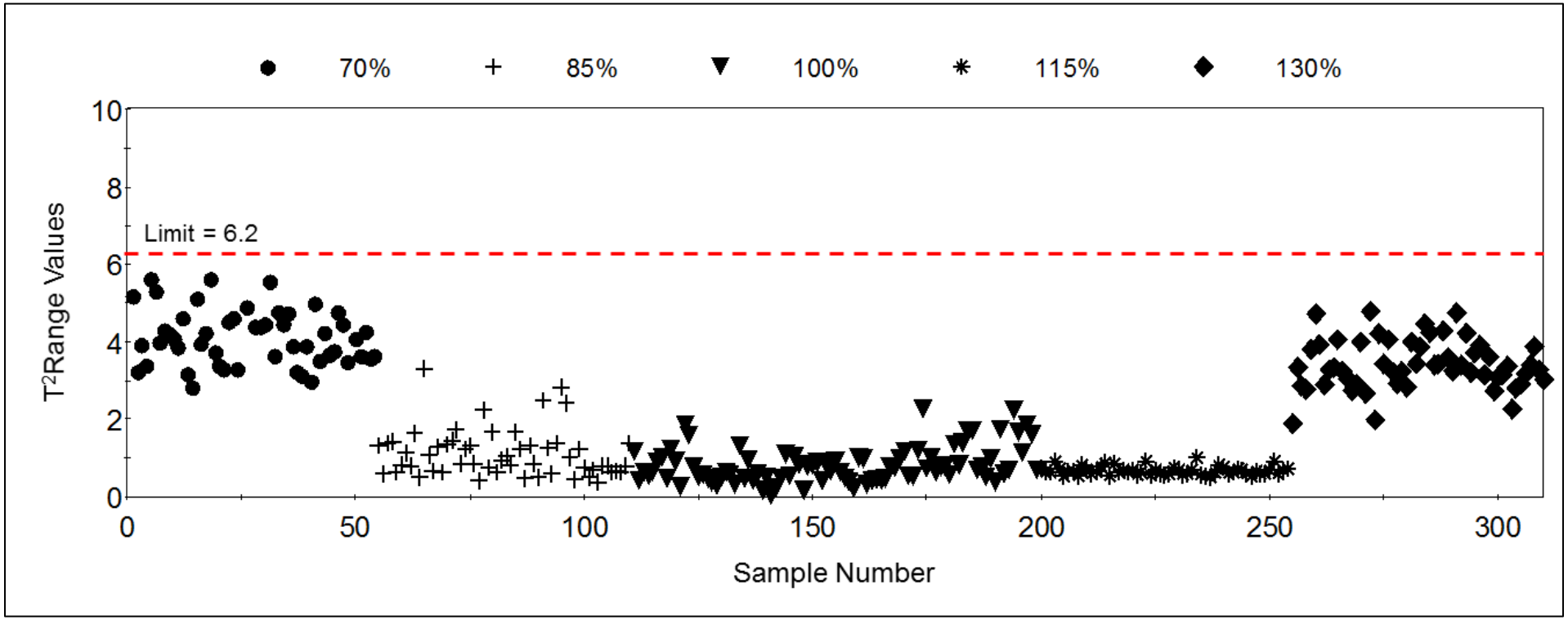

Figure 4.11 Plot for the VSS Hotelling's T^2Range results (T^2R limit = 6.2)

The quantitative model was validated by assessing the validation parameters identified in ICH Q2 guidelines [16, 17]. Accuracy, precision, and linearity were evaluated across the concentration range of the model. **Table 4.2** shows the results obtained for the quantitative model validation.

Accuracy was assessed across the CSS concentration range by comparing NIR predictions with the gravimetric concentrations (reference method). Accuracy was assessed in terms of SEP, RSEP (%), and bias as shown in **Table 4.2**. The highest bias for the validation observed for the validated set was 1.15% LC and RSEP values were below 0.22% LC. Previous studies have shown RSEP results between 0.8% and 3.93% [21, 22, 12, 23]. Therefore, the results obtained in this study demonstrate the high accuracy of the model to predict samples from a CM process. The validation of this model within a regulated environment required the establishment of an acceptance criterion for accuracy. This acceptance criterion was established using the calibration range expectation from the European Medicines Agency (EMEA) guidelines. The guideline states that the calibration range should be at least 10 x SEP [17]. Therefore, since the calibration samples were prepared at ±30% of the API target concentration (70% - 130%) the SEP was established as ≤ 6.0% (60%/10 = 6%). The criterion for the SEP was established as ≤ 4.5% based on a conservative approach of 75% of the maximum SEP limit. Results showed SEP values below the established limit (4.5%) with a maximum SEP value of 1.82% LC.

Precision was evaluated with the repeatability and the intermediate precision studies. Repeatability was performed using blend spectra obtained from one 100% API concentration sample. Six consecutive spectra were acquired, without moving the sample from its position. The standard deviation for the repeatability study was 0.23% showing the minimum standard deviation expected of the quantitative model and thus, the minimum variation of the CM process presented in this study. Two intermediate precision analyses were performed: IP1 and IP2. IP1 was performed using the NIR predictions of the validation set for the five API concentrations (70%, 85%, 100%, 115%, and 130% LC). Results ranged from 1.28% to 1.84%. IP2 was performed using spectra collected from five CM runs. The pooled standard deviation was calculated for a total of 20 sets of 60

spectra each, obtained from five CM runs performed on different days. The standard deviation varied from 1.30% to 5.52%. The pooled standard deviation yielded a value of 2.12%. Although this estimate of intermediate precision depends on the heterogeneity of the powder mixtures obtained in the CM system, it also provides an estimate of the variation under actual conditions of use. While intermediate precision can be measured in diverse ways, the approach followed for this study provides an estimate using a CM process. This information is needed for the future establishment of acceptance criteria in CM processes.

Linearity was evaluated based on the predictions of the VSS and the gravimetric concentrations (reference method). A plot of the NIR predictions versus the target concentration (**Figure 4.12**) yielded an R^2 of 0.99, showed excellent linearity across the prediction range.

Robustness was evaluated using the VSS2 which was prepared using API lot numbers different from the ones used for the CSS. Also, different line throughputs were used for the VSS2 preparation. T^2R was evaluated for 474 spectra collected from two independent CM runs at 95% and 105% LC. All T^2R results were below 6.2 with a minimum of 0.09 and a maximum of 3.89, meeting the established acceptance criterion. Robustness was also evaluated using SEP which results were below the limit established for this validation: ≤ 4.5% (1.94% for the CM blends at 95% LC and 1.64% for the CM blends at 105% LC).

Tablets compacted during the same validation exercise were also analyzed and results summarized in **Table 4.2**. A total of 50 tablets (five concentration levels, 10 tablets per level) were obtained from the validation run for spectra acquisition and analysis. The average NIR prediction obtained for the 100% target concentration was 100.6% LC with a SEP of 1.1%. The average NIR predictions for the blends 100% target concentration was 100.94% LC, very close to the value obtained for tablets.

Table 4.2 Validation results for the quantitative model including accuracy, intermediate precision, repeatability, robustness, and linearity. All values are reported in terms of % LC.

Evaluation	Validation parameter	Quantitative model results				
Accuracy	Number of spectra	54	56	89	55	56
	API target concentration (%)	70	85	100	115	130
	Average NIR prediction (%)	70.02	85.03	100.94	114.90	128.85
	SEP (%) (limit ≤ 4.5)	1.82	1.70	1.69	1.48	1.71
	Bias (%)	0.03	0.03	0.95	0.11	1.15
	RSEP (%)	0.22	0.18	0.17	0.14	0.15
Intermediate Precision 1	SD (%)	1.84	1.71	1.40	1.48	1.28
Intermediate Precision 2	Number of days	5				
	Number of sets per day	4				
	Total sets	20				
	Number of spectra per set	60				
	Pooled Standard Deviation (%)	2.12				
Repeatability	Number of spectra	6				
	SD (%) (limit ≤ 2.7)	0.23				
Robustness	Number of spectra	474				
	Max Hotelling's T^2Range (limit ≤ 6.2)	3.89				
	Min Hotelling's T^2Range	0.09				
	Number of spectra	158		316		
	API target concentration (%)	95		105		
	SEP (%) (limit ≤ 4.5)	1.94		1.64		
Linearity	Number of spectra	50				
	Target Concentration range (%)	70 – 130				
	Intercept	3.57				
	Slope	0.97				
	R^2	0.994				
Tablet Results	Number of tablets	10	10	10	10	10
	API target concentration (%)	70	85	100	115	130
	Average HPLC concentration (% LC)	70.1	85.2	99.6	113.6	127.7
	Average NIR prediction (% LC)	68.9	85.8	100.6	114.1	128.8
	SEP (%)	1.2	0.9	1.1	0.7	1.6
	Bias (%)	1.1	0.6	1.0	0.4	1.0
	SD (%)	0.5	0.8	0.4	0.6	0.7

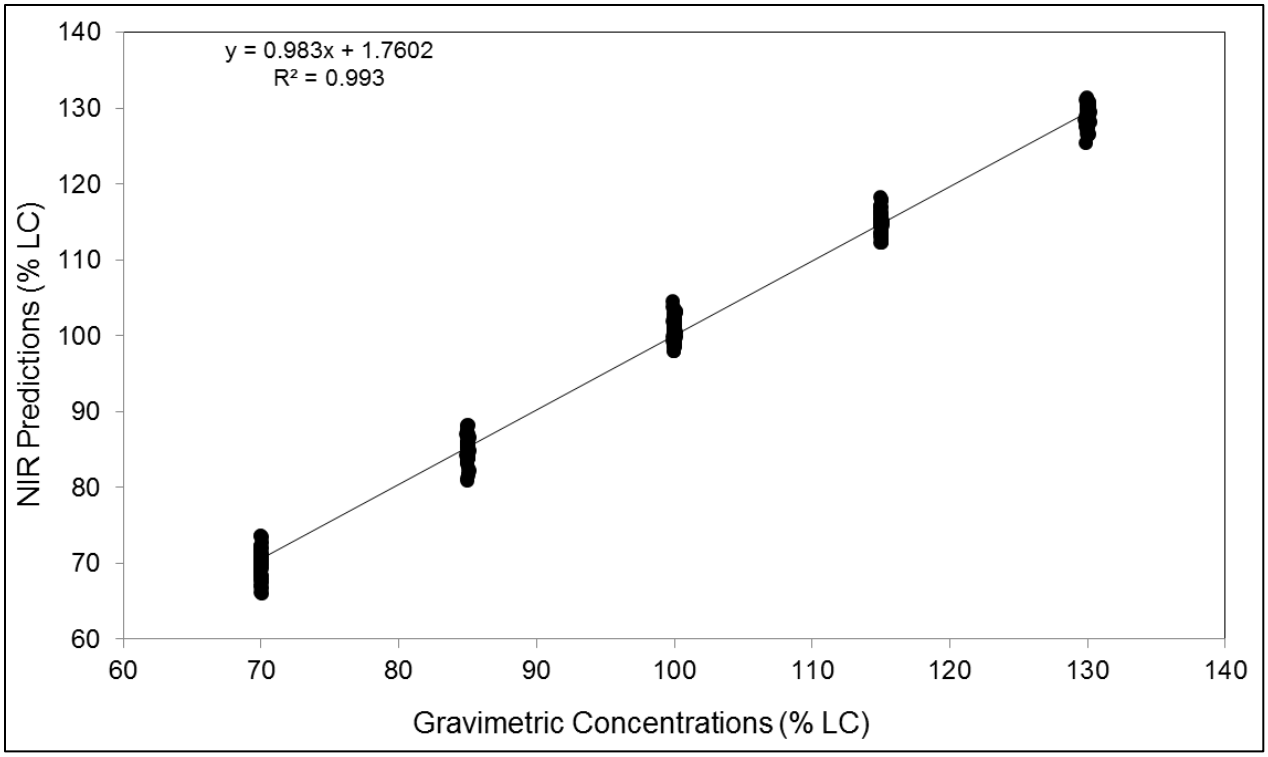

Figure 4.12 Regression plot for the linearity evaluation of the quantitative model NIR predictions

4.3.2. Implementation within Commercial Continuous Manufacturing

The validated qualitative model was implemented for routine use during commercial CM runs. During the beginning of one of the commercial runs, two blend ID failures were logged upon the initial blend testing performed with the qualitative model. A system alarm went off after two consecutive DModX values were obtained above the established limit (**Figure 4.13**). All CM processes were evaluated and it was concluded that the filler was spilling in the CM line, before the interface where NIR spectra of blends is acquired (Refer to **Figure 4.1**). NIR spectra were being collected of blends that contained approximately half of the filler that the formulation required. This event demonstrated the effectiveness of the qualitative model during a CM process to continuously monitor blends before applying the quantitative model and before tablet production.

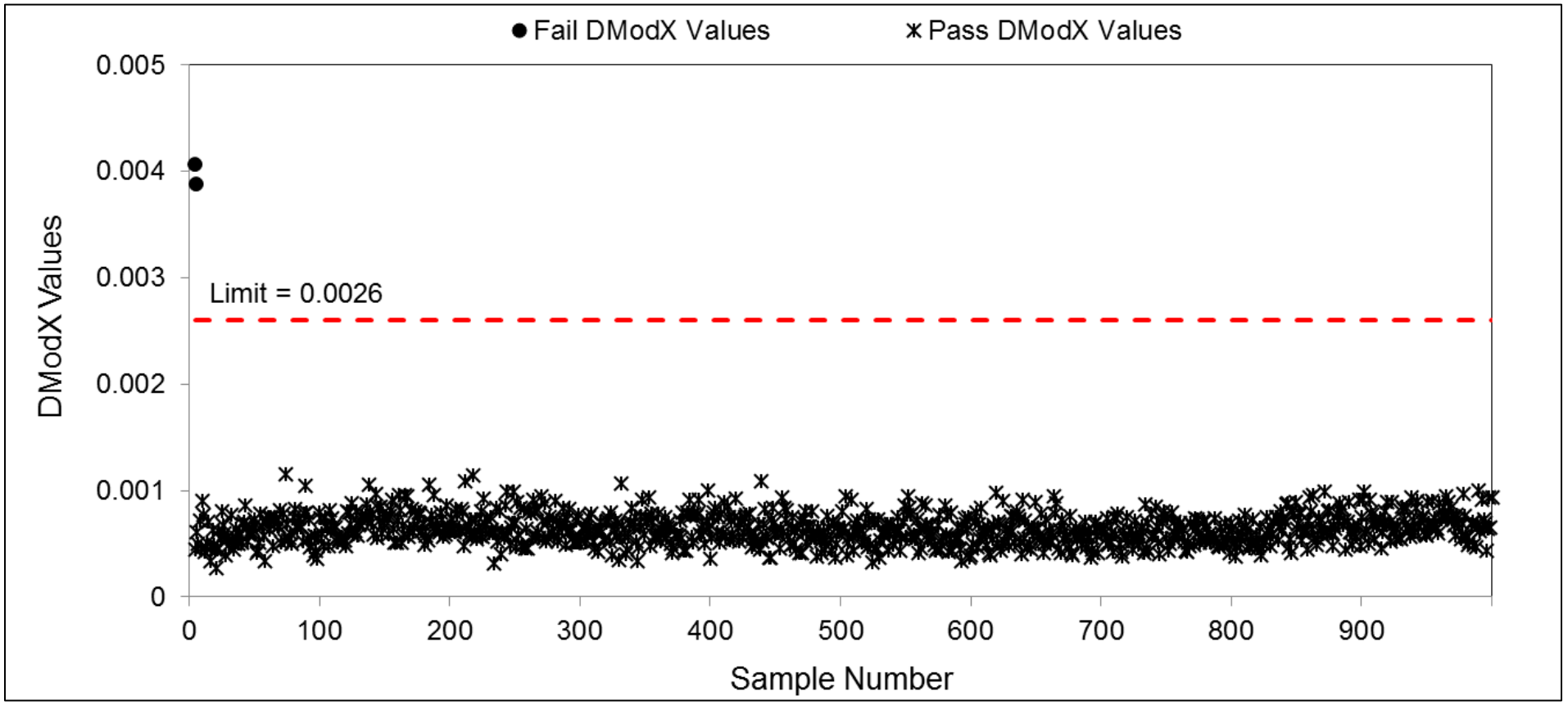

Figure 4.13 Plot of the failed DModX results obtained during the beginning of a commercial CM run due to a filler spill

The quantitative model was also implemented for routine use during commercial CM runs. **Figure 4.14** shows the NIR predictions obtained for a 28-hour commercial CM run. The run included a total of 12633 blend spectra. The average NIR prediction obtained was 101.17% LC with a standard deviation of 2.17%, a bias of 1.31% LC, and a SEP of 2.94% LC. The average NIR prediction for the tablets produced from these blends was 100.86% LC with a standard deviation of 0.4%, a bias of 0.86% LC, and a SEP of 0.95% LC, for 500 tablets analyzed by FT-NIR transmission spectroscopy. **Figure 4.15** shows NIR predictions obtained for the tablets prepared during the same CM process.

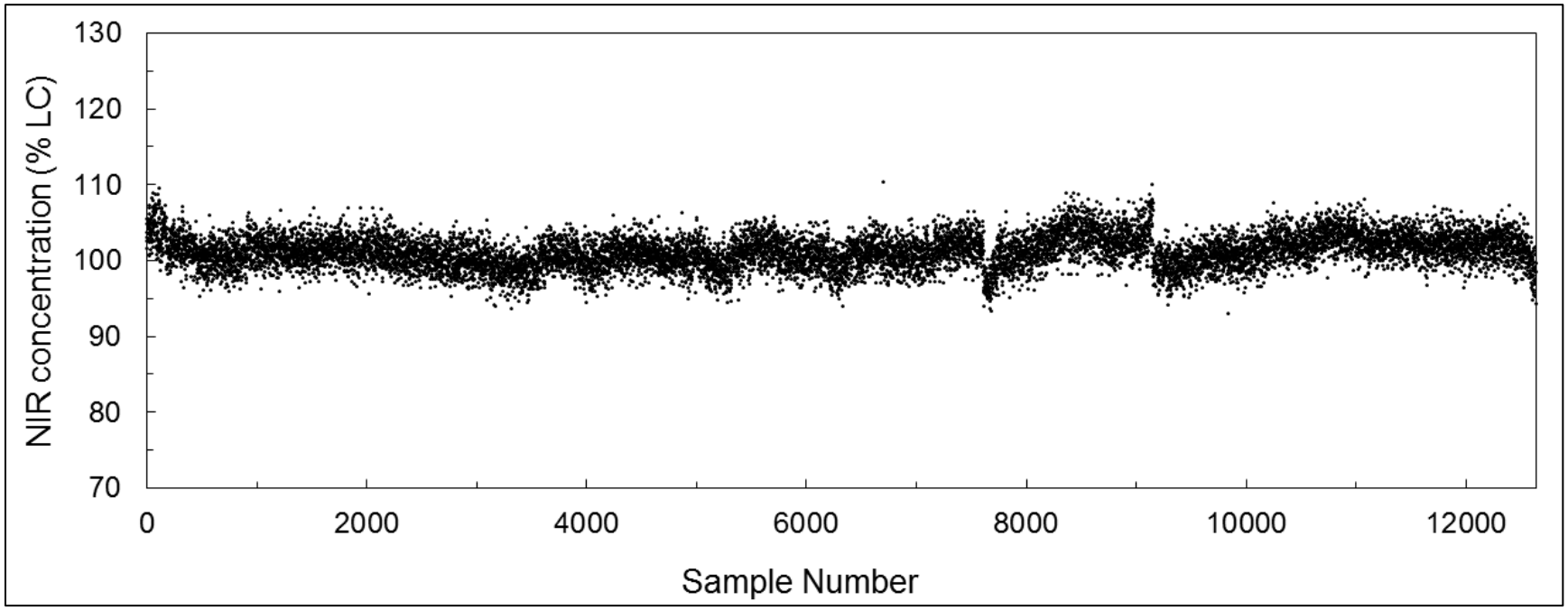

Figure 4.14 Plot of the NIR predictions obtained using the quantitative model during a commercial CM run. A total of 12,633 blend spectra were acquired

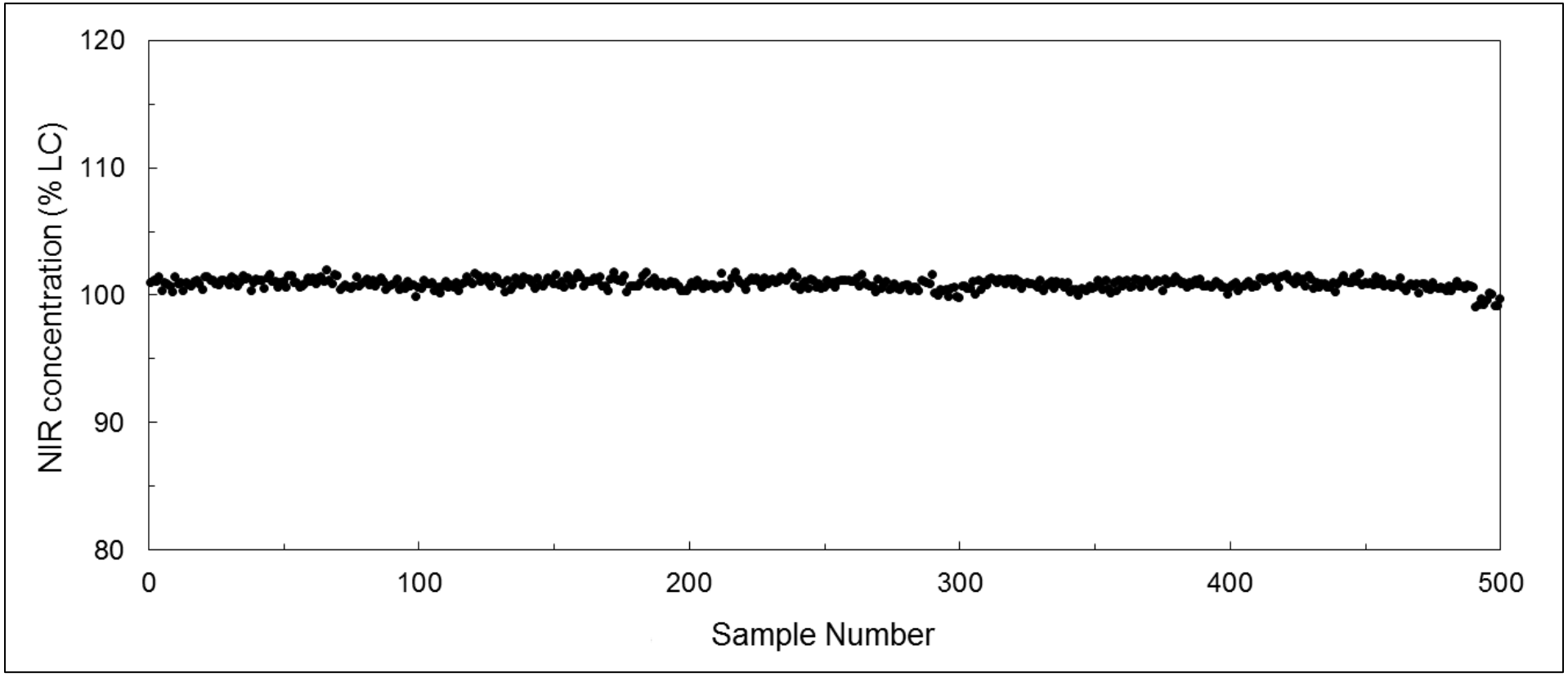

Figure 4.15 Plot of the CM tablet's NIR predictions obtained using a transmittance PLS model. A total of 500 tablet spectra were acquired

4.3.3. Variographic Analysis

Drug concentration results were further evaluated for the blend spectra collected from a commercial CM run using variograms [19]. Variographic analysis decomposes the effective total sampling and analytical error from the inherent process variation. Variograms were calculated from the individual and moving block predicted NIR concentrations. The moving block was performed for the blends analysis during the CM run due to the difference in sample mass analyzed between blends (~37 mg per spectrum) and tablets (>1000 mg). Subsets of three NIR predictions were used to calculate every moving block: samples 1, 2, 3 were averaged for the moving block #1; samples 2, 3, 4 were averaged for the moving block #2; samples 3, 4, 5 were averaged for the moving block #3, etc.

Figure 4.16 shows the variogram calculated using the NIR predictions obtained from a commercial CM run. The variogram plot shows the V(j) (variogram function) as a function of the lag (distance between concentration values reported in terms of % LC). A total of 12,633 spectra were used for the variographic analysis. This substantial number of samples was obtained since sampling was performed by acquiring in-line blend spectra for CM run of approximately 28 hours. The minimum practical error (MPE) or nugget effect, the sill, and the corrected sill were calculated from the variograms. MPE was calculated by extrapolating the first five V(j) values to the Y-axis to estimate “lag 0”. This “lag 0” is physically impossible since it would consist of a time difference of zero between the analytical results. However, this V(j) value at a lag (0) provides an estimate of the total sampling and analytical error. The range which is defined as the lag at which autocorrelation is no longer observed is also shown in **Figure 4.16**. Lags beyond the range shows the process variation. **Table 4.3** shows the sill, the minimum practical error (MPE) or nugget effect, and the corrected sill values for the commercial CM run for the individual and the moving block NIR predictions. The MPE (0.29) greatly improved in the moving block results due to the larger sample composite.

Figure 4.16 also shows the sill which provides the total process variation. The corrected sill shows the residual heterogeneity of the blend (calculated by subtracting the sill and MPE values) [19]. A cyclic behavior of the variogram is observed. Cyclic

variograms can be observed when cyclic fluctuations affect the process [24]. During the CM process, a rotary valve moves the blend from the sensing interface (where blend spectra were collected) to the tablet press, which may be the cause for the cyclic variogram. This cyclic behavior occurred approximately every 500 lags and the cyclic behavior is observed more clearly after the first 1000 lags. The variogram clearly indicates the low frequency cyclic variation. This shows the importance of using as many spectra as possible for the variographic analysis. If less than 1000 spectra had been used for this study, this cyclic behavior could have gone unnoticed.

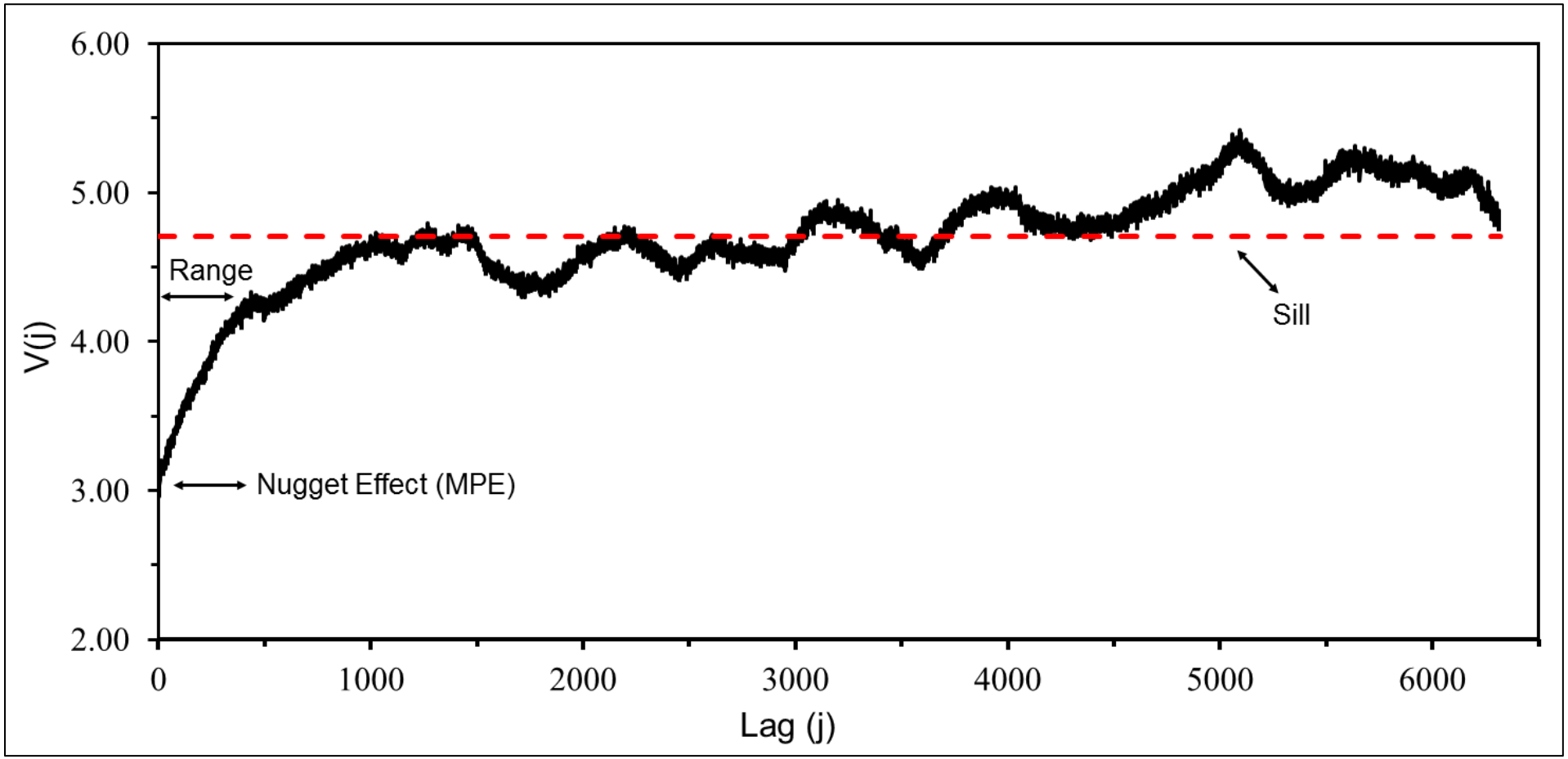

Figure 4.16 Variogram plot for the commercial CM run process. The plot includes the variograms calculated for the individual NIR predictions.

Table 4.3 Variographic analysis results for the commercial CM run, including the results for both the individual and moving block NIR predictions

NIR predictions	Individual spectra	Moving block
Sill	4.70	2.71
MPE	2.96	0.29
Corrected sill	1.74	2.42
Standard deviation (% LC) (n=12,633)	2.17	
Average NIR prediction (% LC)	101.17	

4.4 Conclusion

The qualitative and quantitative models validated as part of this study are currently being routinely used during commercial CM runs. Results showed the models to be fit for their intended purposes as they demonstrated to confirm the presence of the API of interest (qualitative model) as well as being accurate, precise, and linear (quantitative model). This work showed a modern way to prepare the CSS using the same CM process followed to manufacture commercial lots, ensuring the inclusion of variables inherent to the process to the model(s).

A cyclic behavior was observed for the variograms which was most likely induced by the rotary valve

Variograms showed a cyclic system more likely induced by the rotary valve found after the interface. The variographic results also showed the advantage of analyzing big sets of data as demonstrated by the variogram behavior observed after the first 1000 spectra.

This study demonstrates the benefits and advantages of using chemometric models during a CM as in-process control tools to assure the high quality of the final product. Continuous manufacturing along with the use of PAT techniques is an innovative way of working that allows the in-line monitoring of blends eliminating the need to use a sample thief. The monitoring of blends using qualitative and quantitative models proved to be an efficient indicator of the expected quality for tablets produced during the same CM process.

4.5 References

1. Lee SL, O'Connor TF, Yang X, Cruz CN, Chatterjee S, Madurawe RD et al. Modernizing pharmaceutical manufacturing: from batch to continuous production. Journal of Pharmaceutical Innovation. 2015;10(3):191-9.

2. Byrn S, Futran M, Thomas H, Jayjock E, Maron N, Meyer RF et al. Achieving continuous manufacturing for final dosage formation: challenges and how to meet them. May 20-21, 2014 Continuous Manufacturing Symposium. Journal of pharmaceutical sciences. 2015;104(3):792-802.

3. Allison G, Cain YT, Cooney C, Garcia T, Bizjak TG, Holte O et al. Regulatory and quality considerations for continuous manufacturing. May 20–21, 2014 Continuous Manufacturing Symposium. Journal of pharmaceutical sciences. 2015;104(3):803-12.

4. Schaber SD, Gerogiorgis DI, Ramachandran R, Evans JMB, Barton PI, Trout BL. Economic Analysis of Integrated Continuous and Batch Pharmaceutical Manufacturing: A Case Study. Industrial & Engineering Chemistry Research. 2011;50(17):10083-92.

5. Yu L. Continuous Manufacturing Has a Strong Impact on Drug Quality. In: FDA Voice. http://blogs.fda.gov/fdavoice/index.php/2016/04/continuous-manufacturing-has-a-strong-impact-on-drug-quality/. 2016. Accessed July 23, 2016.

6. Gray N. In first, FDA approves Janssen's switch to continuous manufacturing for HIV drug. In: BioPharma Dive. http://www.biopharmadive.com/news/in-first-fda-approves-janssens-switch-to-continuous-manufacturing-for-hiv/417460/. 2016. Accessed July 23, 2016.

7. Brennan Z. FDA Allows First Switch From Batch to Continuous Manufacturing for HIV Drug. In: Regularoty affairs professionals society. http://raps.org/Regulatory-Focus/News/2016/04/12/24739/FDA-Allows-First-Switch-From-Batch-to-Continuous-Manufacturing-for-HIV-Drug/. 2016. Accessed July 23, 2016.

8. Langhauser K. Janssen's Historic FDA Approval. The FDA has approved -- for the first time in history -- a manufacturer's production method change from "batch" to continuous manufacturing. In: Pharmaceutical Manufacturing. http://www.pharmamanufacturing.com/articles/2016/janssens-historic-fda-approval/. 2016. Accessed July 23, 2016.

9. MacDonald G. Janssen working on other continuous processes post US FDA OK for Prezista. In: in-Pharma Technologist. http://www.in-pharmatechnologist.com/Processing/Janssen-working-on-other-continuous-processes-post-US-FDA-OK-for-Prezista?utm_source=copyright&utm_medium=OnSite&utm_campaign=copyright. 2016. Accessed July 23, 2016.

10. Vargas, J. M.; Roman-Ospino, A. D.; Sanchez, E.; Romañach, R. J., Evaluation of Analytical and Sampling Errors in the Prediction of the Active Pharmaceutical Ingredient Concentration in Blends From a Continuous Manufacturing Process. J Pharm Innov 2017, 12 (2), 155–167. doi:10.1007/s12247-017-9273-1.

11. Bu D, Wan B, McGeorge G. A discussion on the use of prediction uncertainty estimation of NIR data in partial least squares for quantitative pharmaceutical tablet assay methods. Chemometrics and Intelligent Laboratory Systems. 2013;120:84-91.

12. Peinado A, Hammond J, Scott A. Development, validation and transfer of a near infrared method to determine in-line the end point of a fluidised drying process for commercial production batches of an approved oral solid dose pharmaceutical product. Journal of pharmaceutical and biomedical analysis. 2011;54(1):13-20.

13. Cogdill RP, Anderson CA, Drennen JK. Process analytical technology case study, part III: calibration monitoring and transfer. AAPS PharmSciTech. 2005;6(2):E284-E97.

14. García-Muñoz S, Kourti T, MacGregor JF, Apruzzese F, Champagne M. Optimization of batch operating policies. Part I. Handling multiple solutions#. Industrial & engineering chemistry research. 2006;45(23):7856-66.

15. Umetrics. User Guide to SIMCA-P+ Version 12. Kinnelon, NJ; 2008. p. www.umetrics.com.

16. International Conference on Harmonisation Guideline. Validation of analytical procedures: text and methodology Q2 (R1)2005.

17. European Medicines Agency. Guideline on the use of near infrared spectroscopy by the pharmaceutical industry and the data requirements for new submissions and variations. Westferry Circus, Canary Wharf, London 2014.

18. Markl D, Wahl PR, Menezes JC, Koller DM, Kavsek B, Francois K et al. Supervisory control system for monitoring a pharmaceutical hot melt extrusion process. AAPS PharmSciTech. 2013;14(3):1034-44.

19. Esbensen KH, Román-Ospino AD, Sanchez A, Romañach RJ. Adequacy and verifiability of pharmaceutical mixtures and dose units by variographic analysis (Theory of Sampling)–A call for a regulatory paradigm shift. International journal of pharmaceutics. 2016;499(1):156-74.

20. Inczedy J, Lengyel T, Ure A. International Union of Pure and Applied Chemistry, Compendium of Analytical Nomenclature, definitive rules. Blackwell Science, on-line version; 1997.

21. Colón YM, Florian MA, Acevedo D, Méndez R, Romañach RJ. Near Infrared Method Development for a Continuous Manufacturing Blending Process. Journal of Pharmaceutical Innovation. 2014;9(4):291-301.

22. Blanco M, Coello J, Eustaquio A, Iturriaga H, Maspoch S. Development and validation of a method for the analysis of a pharmaceutical preparation by near-infrared diffuse reflectance spectroscopy. Journal of pharmaceutical sciences. 1999;88(5):551-6.

23. Blanco M, Cruz J, Bautista M. Development of a univariate calibration model for pharmaceutical analysis based on NIR spectra. Analytical and bioanalytical chemistry. 2008;392(7-8):1367-72.

24. Esbensen KH, Paasch-Mortensen P. Process sampling: Theory of Sampling—the missing link in process analytical technologies (PAT). Process Analytical Technology. 2010:37-80.

Chapter 5

5 Assessment of Robustness for a Near Infrared Concentration Model for Real Time Release Testing in a Continuous Manufacturing Process

Published in Journal of Pharmaceutical Innovation, 2017, Issue 12, 14-25.

Yleana M. Colon, Jenny M. Vargas, Eric Sanchez, Gilfredo Navarro, Rodolfo J. Romañach

5.1 Introduction

Continuous Manufacturing (CM) is being studied to be implemented in the pharmaceutical industry for its potential, cost-efficacy, and quality advantages [1-3]. Recently, two continuous manufacturing processes were approved by the FDA [4, 5]. Previous publications have focused on evaluating the continuous manufacturing process and how process conditions such as feed rate, impeller rotation rate, shear intensity, total shear, and compression force could affect tablet properties [6-9]. Changes in the tablets properties could affect the near infrared (NIR) spectra which contains information related to the chemical and physical properties of the materials [10-13]. The understanding and use of NIR has increased in recent years until reaching a point where NIR is currently being used to monitor and control continuous manufacturing processes [3, 14-16]. However, there are still many challenges when NIR is used for real time release testing (RTRt) of a commercial pharmaceutical drug.

NIR spectroscopy is one of the principal analytical methods in RTRt and offers many advantages over traditional chemical methods. NIR is non-destructive, requires no sample preparation (no reagents), no waste is produced, and has a high precision. NIR spectroscopy is a cross-sensitive analytical technique that can provide essential information to RTRt application in CM processes since it allows the determination of moisture, drug concentration, and tablet hardness from one single spectrum [17, 18].

NIR calibration models can be developed to monitor continuous manufacturing processes. The current industry approach is to develop NIR calibration models using calibration sets prepared in laboratory scale [19-22]. The calibration set must represent all significant sources of variability that will be found in future samples [19]. Variations in concentration levels, excipients, and the process must be included. Therefore, NIR calibration models that will be used in a continuous manufacturing line must include a calibration set prepared using the same CM process. The preparation of calibration sets using a continuous manufacturing process can be expensive and time consuming [13]. However, the development of the NIR calibration models must be done including the necessary sources of variability to obtain a robust calibration model. Therefore, identifying the sources of variability (physical and chemical) is very important.

This study shows the results obtained during the adaptation of a NIR spectroscopic calibration model to a pharmaceutical RTRt process. RTRt offers many advantages to the pharmaceutical manufacturing process such as a reduced operational cycle time, enabling real time control to improve quality, and assessment based on a large set of measurements.

This investigation describes the implementation of RTRt using NIR spectroscopy for a continuous manufacturing process. The active pharmaceutical ingredient (API) used for this study exchanges solvate molecules with water from the environment. This exchange could affect the NIR spectra and thus, the NIR predictions of concentration. However, the exchange does not affect product quality. Several NIR calibration models have been previously developed to determine drug concentration in tablets. However, none of these models were developed using compounds that exchanged solvate molecules with the water from the environment [23-33]. Therefore, the effect on the NIR predicted concentrations of tablets exposed to the environment was investigated through the assessment of robustness for a NIR calibration model developed. This study is applicable to many other situations since screening studies have found that 80-90% of the organic compounds tested were capable of existing in polymorphic or solvatomorphic forms [34, 35].

Tablet relaxation was also investigated for this study since spectra acquisition of tablets might not occur immediately, right after compaction. The effect of relaxation could affect the drug concentration results. In this study, the drug concentration of tablets was determined at different time points after tablet compaction. Tablet relaxation has been previously studied to understand formation of pores (porosity) [36], assess viscoelastic properties of materials [37-41], and understand relaxation behavior during the ejection phase [42, 43] or throughout time [44, 45]). The effect of tablet relaxation on NIR predicted concentrations has not been previously studied.

5.2 Materials and Methods

5.2.1. Materials

The formulation used for this study was composed of an API (more than 50% LC of the formulation) and three excipients (filler, disintegrant, and lubricant).

5.2.2. Sample Preparation

Laboratory, pilot plant, and continuous manufacturing equipment were employed to prepare the different sample sets used to develop the NIR calibration models, as outlined in **Table 5.1** and **Table 5.2**. Tablets were prepared across the 70 - 130 % LC concentration range including seven concentration levels with three tablets per concentration level. The CM Line was used to prepare the sample set used to optimize the calibration model. All tablets used for this study (lab scale, pilot scale, and CM Line equipment) were matched for thickness, weight, and hardness, to the best capability possible since lab and pilot scale tablets were prepared manually.

Table 5.1 Summary of sample sets prepared

API concentration (% LC)	Sample preparation
Calibration sample set (CSS)	
70	Laboratory scale
85	
95	
100	
105	
115	
130	
Calibration test sample set (CTSS)	
71	Laboratory scale
98	
102	
129	
Robustness sample set	
100	Pilot plant
Sample set used to update the model	
90	CM line
100	
110	

Table 5.2 Laboratory, pilot-plant, and CM equipment description

Description	Equipment
Weighing of all raw materials and blends	Mettler Toledo Analytical Balance
Manual Compression	Enerpac P142 from GlobePharma Tablet Press
Pilot Scale Operation	Pilot Scale Equipment
Weighing of minor excipients	Mettler Toledo Analytical Balance
Weighing of major excipients	Mettler Toledo Loading Balance
Blending	Bohle LM- bin Blender with 40 l bin
Compression	Korsch KM12 Tablet Press
Process Operation	CM Line Equipment Train
Weighing of raw materials	Mettler Toledo Loading Balance
Loading/Feeding	K-Tron Volumetric/Gravimetric Feeders
Milling	In-line Quadro Comil U10
Blending	Glatt GCG 70 Continuous Blender
Compression	Korsch KM12 Tablet Press

5.2.3. Tablet Preparation using Laboratory Scale Equipment

The calibration sample set (CSS) and the calibration test sample set (CTSS) were prepared using laboratory scale equipment [46]. The CSS consisted of tablets prepared using seven blends (one blend per concentration level). A total of seven concentration levels were prepared for the CSS including 70%, 85%, 95%, 100%, 105%, 115% and 130% LC of the API target concentration. Three tablets were prepared per concentration level for the CSS and the CTSS.

CTSS provided the first challenge of the calibration model and consisted of tablets prepared using four blends (one blend per concentration level). A total of four concentration levels were prepared for the CTSS including 71%, 98%, 102% and 129% LC of the API target concentration. An experimental design was performed to reduce the correlation between the concentrations of the API and the main excipient using the Excel Solver tool. The CSS and CTSS blends were prepared individually by weighing the raw materials for a total of 100 g per blend except for the 100% LC CSS blend for which 500 g were prepared. All raw materials were passed through a sieve before mixing (USA Standard Test Sieve No. 25: 0.0278 Inches, from the Fisher Scientific Company) to remove large aggregates. Once all raw materials were weighed, the blends were transferred to plastic bottles and placed inside a bin blender (Bohle LM-40 bin blender). The blender was operated at 20 rpm for four minutes.

An analytical balance was used to weigh the correct quantities of blend to prepare each tablet. Tablets were compressed using a hand press tablet compaction equipment (Enerpac P142 from GlobePharma) and thickness was measured using a Mitutoyo calibrated caliper. Tablets were compacted at a pressure of 3,800 psi (26.2 MPa) to match final average weight, thickness, and hardness of the formulation tablets.

5.2.4. Tablet Preparation using Pilot Scale Equipment

The tablets used for the robustness study were prepared at 100% LC API concentration using the pilot scale equipment. Raw materials were weight and place inside a bin blender (Bohle LM-40; filled to 60% capacity) set at 20 rpm for four minutes. After mixed, blends were poured through a hopper into a Korsch XM-12 tablet press to prepare the tablets matching the weight and thickness of the target commercial tablets.

5.2.5. Tablet Preparation using the Continuous Manufacturing Process

The tablets used to challenge the NIR calibration model developed were prepared using the CM line. These tablets were prepared at 90%, 100%, and 110% LC API concentration. The CM process included the use of four gravimetric feeders which delivered each material at its own set point into an in-line conical mill. After, the material enters an in-line continuous paddle blender which then directs it to the Korsch XM-12 Tablet Press. All compressed tablets were analyzed using NIR spectroscopy.

5.2.6. Tablet Spectra Acquisition

NIR transmission spectra of tablets were acquired using a Bruker multi-purpose analyzer (MPA). The spectrometer has an indium gallium arsenide (InGaAs) detector with a useful wavenumber range of 12500 cm^{-1} to 5800 cm^{-1}. Spectra were acquired using a resolution of 64 cm^{-1} with 32 spectra average scans (scan time = 5.8 secs). Background spectra were always measured before the tablet spectra acquisition.

5.2.7. NIR Calibration Model Development

The Umetrics software prediction engine SIMCA P+12 was used to develop the NIR calibration model, using the partial least squares (PLS) algorithm. Several spectral regions, data pretreatments, and PLS components were analyzed before developing the NIR calibration model. Performance of the model was evaluated in terms of the root mean standard error of prediction (RMSEP) and the fraction of the Y-variation modeled by the PLS component ($R2Y_{cum}$), using the CTSS. The RMSEP equation used was:

$$RMSEP = \sqrt{\frac{\sum_{i=1}^{m}(\hat{y}_i - y_i)^2}{n}} \quad (1)$$

where, $\hat{y}_i$ is the API concentration predicted by the NIR calibration model, y_i is the reference (gravimetric) concentration, n is the number of samples in the prediction. All spectra were mean centered. Pretreatments such as first derivative, second derivative, and standard normal variate (SNV) were analyzed for the development of the NIR calibration model. Derivatives were calculated using a 15-point window with a distance of one.

5.2.8. API HPLC Method

The reference method used to quantify the API in tablets was the high-performance liquid chromatography (HPLC). Each tablet collected was weighed and transferred to a 50-mL volumetric flask using a solution of 50% acetonitrile: 50% distilled water as diluent. After sample preparation, the solution was analyzed using an HPLC equipped with a variable wavelength UV detector, column oven, and auto-sampler.

5.3 Results and Discussion

5.3.1. Development of the NIR Calibration Model

The NIR calibration model was prepared using the CSS consisting of 21 tablets (7 concentration levels, 3 tablets per concentration level). The seven concentration levels included tablets at 70%, 85%, 95%, 100%, 105%, 115% and 130% LC of API concentration. The CTSS was composed of 12 tablets (4 concentration levels, 3 tablets per concentration level) including API target concentrations of 71%, 98%, 102% and 129% LC. Variables associated with the molecular vibrations of the API (third overtones of C-H aromatic bands {11760 – 11630 cm^{-1}} and the C-H stretching from methyl groups {11110 – 10990 cm^{-1}}) were used to develop the calibration model. **Figure 5.1** shows the spectra of tablets at 70%, 100%, and 130% LC API concentration. Low wavenumbers (10100 - 5800 cm-1) were not used for model development since the absorbance values obtained at these wavenumbers are associated with noise related to the low amount of radiation reaching the detector [47-49] . Variables corresponding to water bands (10260-10150 cm^{-1}) were also excluded since they could affect the accuracy of the NIR predicted concentration because the API used exchanges solvate molecules with water from the environment.

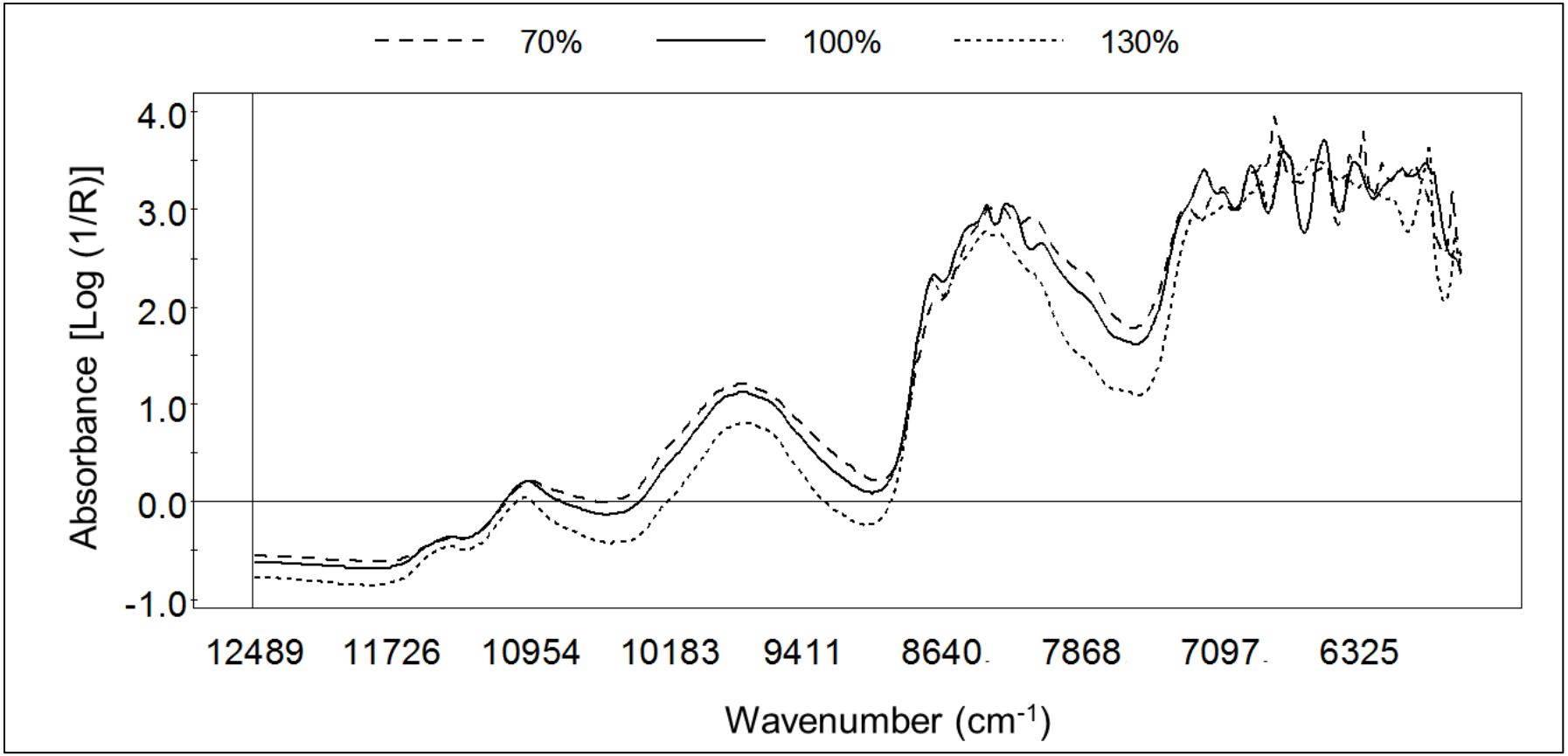

Figure 5.1 Spectra of tablets at 70%, 100%, and 130% LC API concentration

Several pretreatments and PLS factors were evaluated to develop the NIR calibration model. The evaluation was performed using RMSEP (eq. 1) and was based on the ability of the model to predict the CTSS. The spectral region chosen for the calibration model was 12034-10592 cm^{-1} using one PLS factor and SNV + 1^{st} derivative as the pretreatment. **Figure 5.2** shows the spectrum of placebo, API, and a 100% LC tablet with the 2^{nd} derivative pretreatment applied. The plot shows the selectivity of the method to the used API in the presence of excipients in the chosen spectral range. **Figure 5.3** shows the CSS tablets at 70% (low), 100% (middle), and 130% (high) LC API concentration with the chosen spectral pretreatment applied (SNV+1^{st} derivative). The plot shows that as the API concentration increases, the response (absorbance) of the bands around 11800 - 11400 cm^{-1} and 11320–10954 cm^{-1}, increases. The cross validation statistical results and the calibration and CTSS NIR predicted concentrations, using one and two PLS factors, are shown in **Table 5.3**.

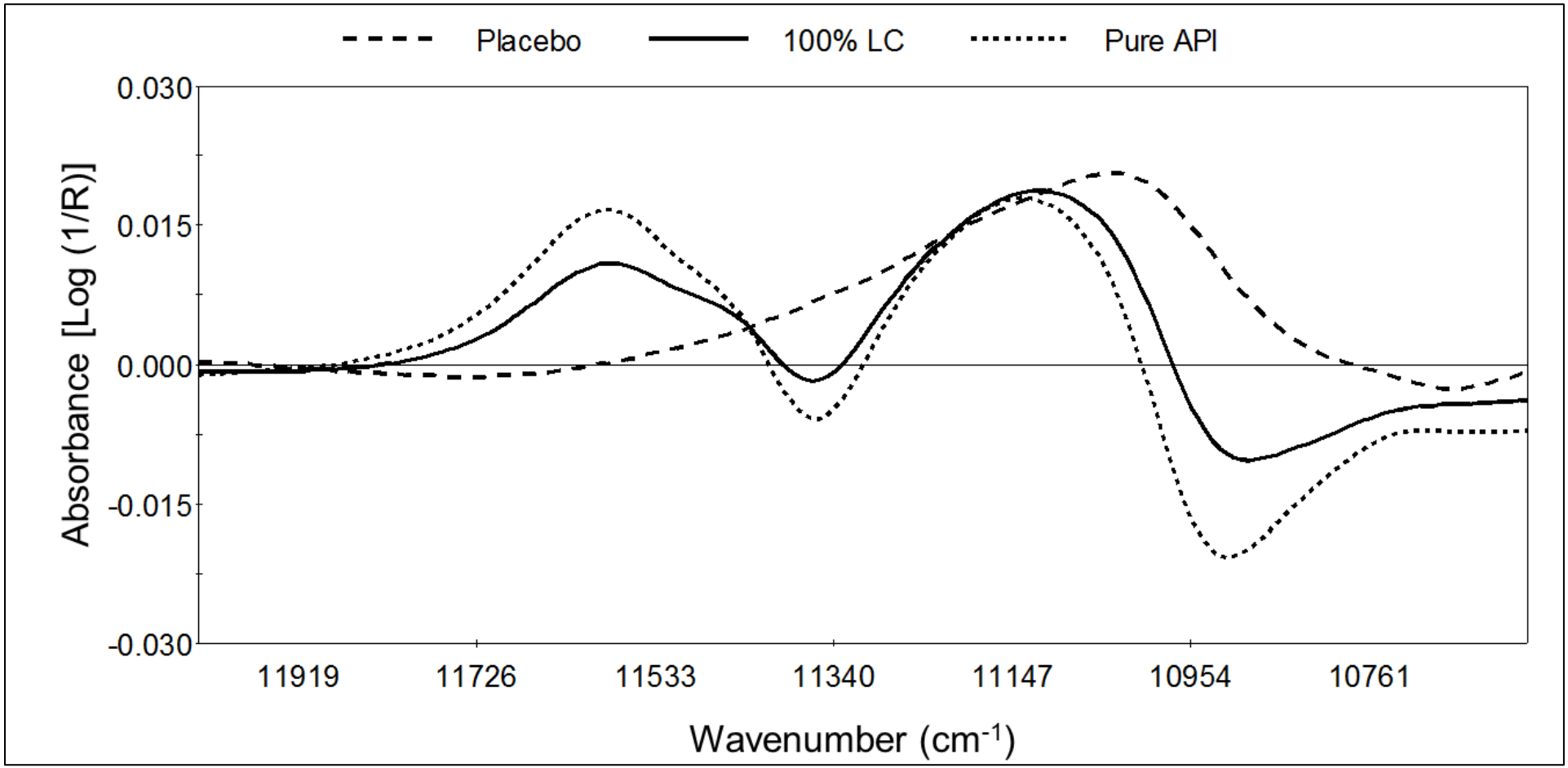

Figure 5.2 Plot of the placebo, API, and a 100% LC tablet spectra with the second derivative (15-point window) pretreatment applied in the spectral range 12034-10592 cm^{-1}

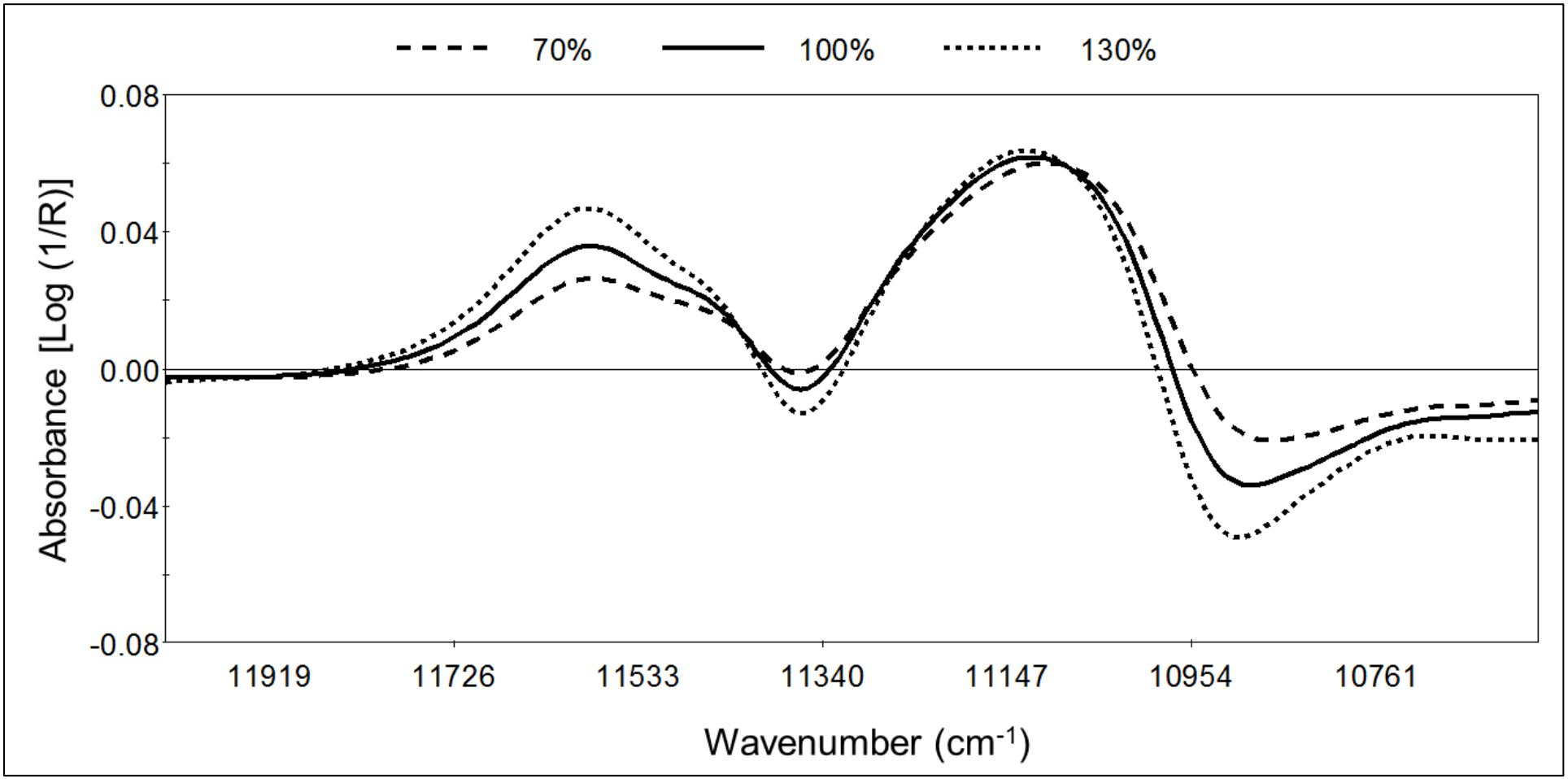

Figure 5.3 Plot of tablet spectra at 70%, 100%, 130% LC with the SNV+ 1st derivative (15-point window) pretreatment applied in the spectral range 12034-10592 cm^{-1}

Table 5.3 Calibration, cross-validation statistics and CTSS results

PLS factors	SEC	CV parameters	SECV	*Intercept	*Slope	RMSEP (%) n=12
1	0.9	Leave 1 out	0.89	0.0	1.0	1.0
		Leave 3 out	0.92			
		Leave 7 out	0.91			
2	0.7	Leave 1 out	0.78	0.0	1.0	1.1
		Leave 3 out	0.84			
		Leave 7 out	0.80			

*Intercept and slope values were obtained from the regression between the HPLC values and the NIR predicted concentrations.

Results show that SEC, SECV, the intercept, and the slope yield similar results when using 1 or 2 PLS factors. However, differences were found in the RMSEP results. NIR predicted concentrations for the CTSS were lower using 1 PLS factor. **Figure 5.4** shows the PLS scores plot for the CSS. Pretreatments SNV+1st derivative (15-point window) were applied to the CSS for this figure. The plot shows that the 1st PLS factor explains most of the variation of the PLS model (99.7% R2Ycum). In addition, defined clusters, based on the API concentration, are observed. The 2nd PLS factor only explains 0.2% of the variation in the PLS model. However, the NIR calibration model was evaluated using 2 PLS factors but the results obtained were similar to the model using 1 PLS factor. Therefore, the model with 1 PLS factor was chosen for further evaluation.

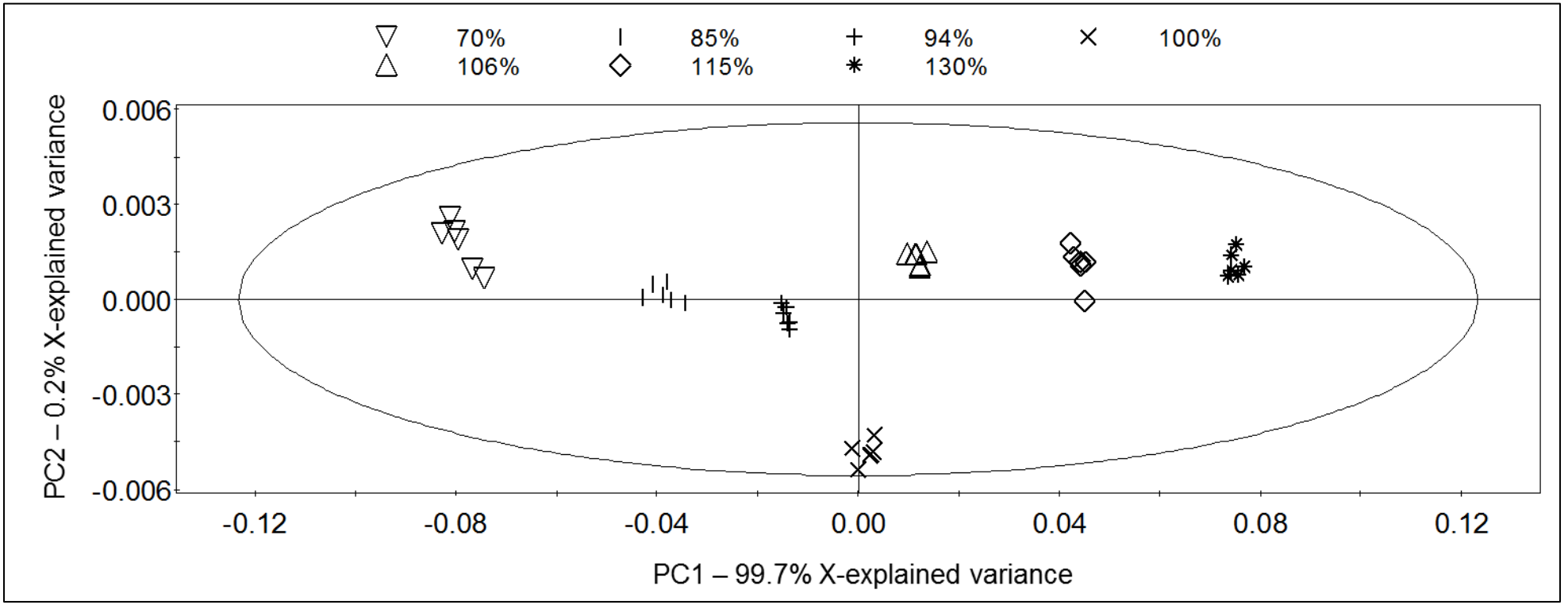

Figure 5.4 PLS score plot of the calibration sample set (CSS)

5.3.2. Evaluation of Accuracy and Precision

CTSS tablets were used for the accuracy and precision evaluation. A total of twelve tablets (four concentration levels, three tablets per level) prepared using lab scale equipment, were used. Tablet compression was performed manually by placing powder in a die while manual force was applied through the pressure of another die. Both sides of the tablets were analyzed since the embossing on the dies are different and this could have an impact on the NIR scattering. Six spectra per concentration level (one spectra per tablet side) were acquired. **Table 5.4** shows the accuracy and repeatability results for the CTSS using 1 and 2 PLS factors. HPLC API concentrations and RMSEP results were also included in the table. For the repeatability study, ten consecutive spectra were acquired from tablet #1, without moving the tablet.

RMSEP results were found to be below 1.5% for all the concentrations evaluated. Repeatability was ≤ 0.1%. No statistical differences were obtained between the spectra collected from each side of the tablets. These results indicate that NIR spectra can be acquired to either side of the tablet.

Table 5.4 Accuracy and repeatability results for the CTSS using 1 and 2 PLS factors

API target conc. (% LC)	Tablet	HPLC API conc. (% LC)	NIR conc. prediction (% LC) (Side 1)	NIR conc. prediction (% LC) (Side 2)	NIR SD (both sides combined)	RMSEP (%)	Repeatability (SD %)
1 PLS factor							
71	1	72.16	72.48	72.04	1.1	0.6	0.1
	2	73.14	73.35	73.13			
	3	73.75	74.90	74.47			
98	1	98.26	98.12	98.02	1.4	1.2	0.1
	2	99.25	100.56	100.01			
	3	99.10	101.14	100.75			
102	1	104.02	103.88	103.76	0.4	0.6	0.1
	2	104.07	104.56	104.39			
	3	103.23	104.48	103.76			
129	1	128.30	126.62	126.83	1.1	1.4	0.1
	2	128.67	128.99	128.19			
	3	128.26	127.05	126.16			
2 PLS factors							
71	1	72.16	73.04	72.53	1.3	1.2	0.1
	2	73.14	74.05	73.78			
	3	73.75	75.80	75.35			
98	1	98.26	97.01	96.92	1.5	1.0	0.1
	2	99.25	99.77	99.25			
	3	99.10	100.28	99.86			
102	1	104.02	103.52	103.36	0.5	0.7	0.1
	2	104.07	104.51	104.39			
	3	103.23	104.43	103.73			
129	1	128.30	126.44	126.73	1.2	1.3	0.1
	2	128.67	129.36	128.58			
	3	128.26	127.38	126.50			

5.3.3. Robustness Study

The NIR calibration model was evaluated for robustness. Tablet relaxation and exposure to the environment were evaluated. Spectra were collected from ten 100% LC tablets, right after compaction. After spectra collection, tablets were left on the NIR carrousel, exposed to the environment, (room temperature, RH 56%) until NIR spectra was measured again after 2, 3, 4, 5, 9, 19, 77, and 99 hours of being compressed. **Table 5.5** shows the results for the robustness evaluation. Results show that NIR predicted concentrations of tablets from hour 1 through hour 5 are statistically similar (p-value < 0.300). However, after five hours, the NIR predicted concentrations are statistically different (95% confidence interval) with a p-value < 0.003. These results demonstrate that the developed NIR calibration model is not suitable to be used in an environment where certain events could delay the analysis of tablets for more than five hours, after compaction. Therefore, the model required an optimization to extend the time range where the model could accurately predict the API concentration of tablets.

Table 5.5 Robustness evaluation results: tablets exposed to the environment

Time interval (hours)	Average NIR conc. prediction (% LC) n=10	Standard deviation (%)
	1 PC	
1	97.21	0.67
2	97.59	0.65
3	97.47	0.72
4	97.23	0.60
5	97.22	0.82
9	96.48	0.60
19	95.39	0.28
77	93.92	0.67
99	93.61	0.62

Relative humidity was maintained within limits throughout the experiment since this was performed in a controlled production environment. Hours 1-5: p-value < 0.297 / Hours 1-9: p-value < 0.002 / Hours 1–99: p-value < 0.000

A second study was designed to evaluate the NIR predicted concentrations of tablets protected from the environment after compaction and between analyses. Spectra were

collected from a new set of ten 100% LC tablets, right after compaction. After spectra collection, tablets were placed inside sealed bags and re-measured after 2, 4, 8, 18, 25, 48, and 113 hours of being compressed. **Table 5.6** shows the results of the NIR predicted concentrations obtained for the protected tablets. Results showed no statistical difference up to 25 hours with a p-value < 0.200. The tablets NIR predicted concentrations started to decrease after 25 hours of being compressed, even if protected from the environment. These results indicate that tablets predictions will be accurate for approximately 20 hours after compaction if the tablets are stored in sealed bags. However, this practice of placing tablets in sealed bags is not practical during RTRt activities. Therefore, the NIR calibration model developed was optimized.

Table 5.6 NIR predicted concentrations of stored tablets

Time interval (hours)	Average NIR conc. prediction (% LC) n=10	Standard deviation (%)
	1 PC	
1	97.46	0.58
2	97.81	0.97
4	97.82	1.00
8	97.32	0.79
18	97.42	1.21
25	97.00	0.53
48	96.05	0.46
113	96.55	0.90

Hours 1-25: p-value < 0.2 / Hours 1-48: p-value < 0.001 / Hours 1–113: p-value < 0.001

5.3.4. NIR Calibration Model Optimization #1: Spectral Range

A spectra comparison was performed using tablet spectra collected at the beginning of the study (1 hour) and at the end of the study (113 hours) to understand why the API concentration decreased with time. **Figure 5.5** shows the spectra compared. Differences between the spectra were observed in the free OH second overtone (10900 – 10592 cm^{-1}) spectral region. These differences could be related to the exchange of solvate molecules with water in the environment [50]. The spectral range of the NIR calibration model developed was optimized to reduce the effect that tablet humidity has on the NIR

predicted concentration. The spectral range was optimized from 12034 – 10592 cm^{-1} to 12034 – 10900 cm^{-1}.

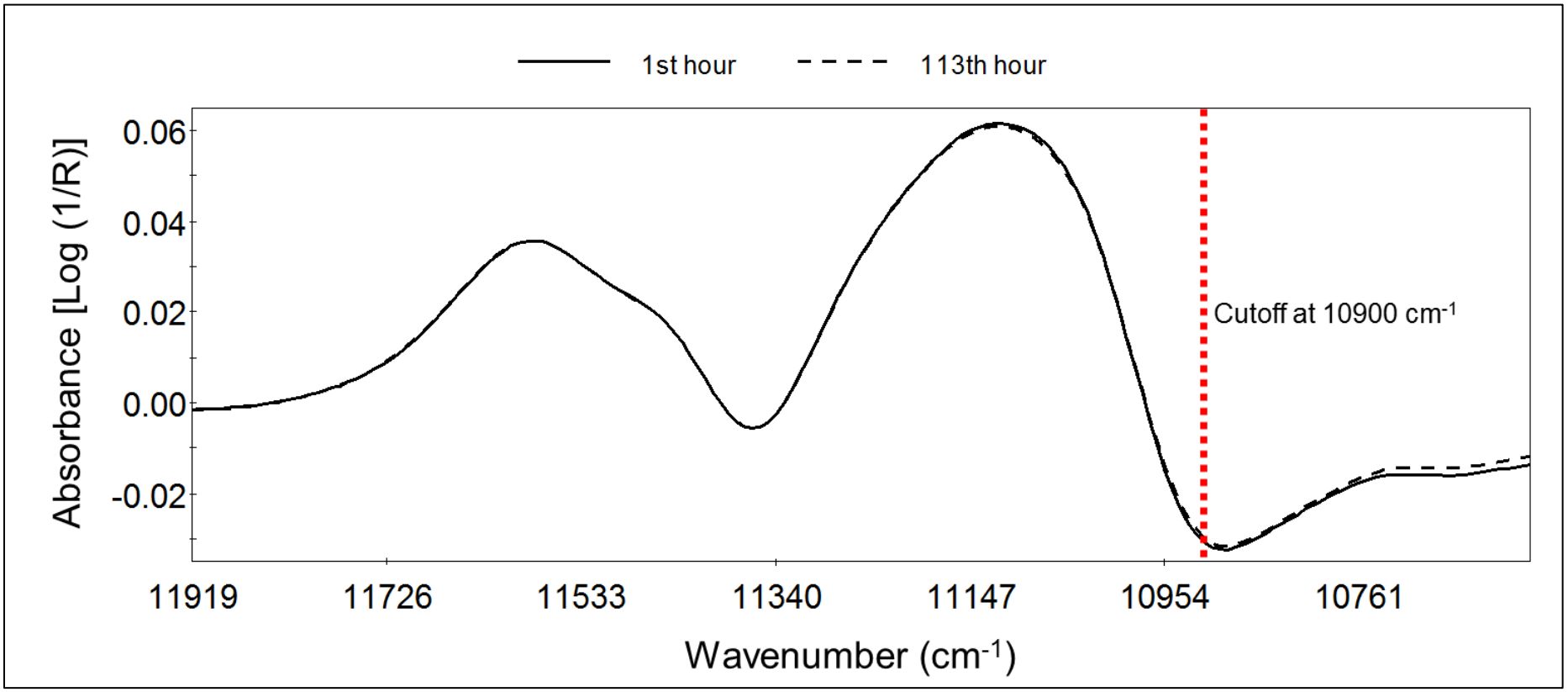

Figure 5.5 Comparison of spectra of tablet(s) stored for the 1st and the 113 hours.

The spectra acquired of tablets under controlled storage conditions were also predicted using the optimized NIR calibration model. **Table 5.7** shows the NIR predicted concentrations of the ten stored tablets (same from **Table 5.6**). Results showed that the NIR predicted concentrations remained statistically similar throughout 113 hours (p-value < 0.130). This demonstrates that the optimized NIR calibration model yields more robust results than the ones obtained prior to performing the spectra optimization. More accurate and precise results were obtained when using the optimized NIR calibration model.

Table 5.7 NIR predicted concentrations of tablets under controlled storage conditions

Time interval (hours)	Average NIR conc. prediction (% LC) n=10	Standard deviation (%)	Bias (% LC) n=10
1	99.23	0.46	0.77
2	99.36	0.81	0.64
4	99.32	0.95	0.68
8	99.07	0.58	0.93
18	99.31	1.13	0.69
25	98.89	0.43	1.11
48	98.52	0.44	1.48
113	98.78	0.84	1.22

Hours 1-113: p-value < 0.130. Bias based on 100% API target concentration.

Robustness of the optimized NIR calibration model was also evaluated using tablets undergoing elastic recovery post-compaction. Previous studies have evaluated the dimensional changes of tablets resulting of the elastic recovery that occurs after tablet compaction [51-53]. Elastic recovery post-compaction could affect the NIR concentration results due to physical changes in the tablets. It has been previously published that differences in tablet compaction are observed in baseline and slope changes in the NIR spectra [54]. Therefore, tablets were collected immediately after compression and spectra was acquired immediately after ejecting from the press. Spectra acquisition was continuously performed (tablets 1-10) for 1 hour. A total of 28 spectra per tablet were obtained during this first hour.

Table 5.8 shows the NIR predicted concentrations for the spectra obtained during the first hour of the study. The average NIR predicted concentration was 99.11% LC with an

RMSEP of 0.89 and a p-value < 1.001 (variability within the time interval is much larger than the variability between time intervals). Results demonstrated the robustness of the optimized model within this first hour, as predictions are not statistically different throughout this time range evaluated. Therefore, tablet relaxation (elastic recovery) effects during this first hour do not affect the NIR predicted concentration.

Table 5.8 NIR predicted concentrations of the tablet relaxation study (Elastic recovery)

Tablet collection interval	Average NIR conc. prediction %LC (n=10)	Tablet collection interval	Average NIR conc. prediction %LC (n=10)
1	99.26	15	99.07
2	99.26	16	99.10
3	99.21	17	99.14
4	99.25	18	99.14
5	99.19	19	99.09
6	99.05	20	99.09
7	99.02	21	99.01
8	99.08	22	99.13
9	99.17	23	99.14
10	99.09	24	99.05
11	99.14	25	99.14
12	99.11	26	99.00
13	99.10	27	99.02
14	99.08	28	98.99

5.3.5. NIR Calibration Model Optimization #2: CSS

Samples representative of the CM process were included in the CSS of the developed NIR calibration model to include the inherent process variations and thus increase robustness of the model. **Figure 5.6** shows the PCA scores plot of the CM tablet samples (90%, 100%, and 110% LC) projected onto the optimized NIR calibration model ellipse. The CSS and the CM tablets are aligned in increasing API concentration. The variation observed in the second factor could be due to the different preparation equipment used (e.g. lab scale and CM process). Process differences such as compaction force, hardness, and thickness could affect the NIR predicted concentrations. Therefore, spectra of CSS tablets prepared using lab-scale equipment (95%, 100%, and 105% LC) were substituted with spectra of tablets prepared using the CM process (three

concentration levels - 90%, 100%, and 110% LC). The lab-scale tablets were substituted instead of keeping them in addition to the CM tablets to reduce the effect that could happen if a lot of weight is applied to the target or near the target concentration (center of model).

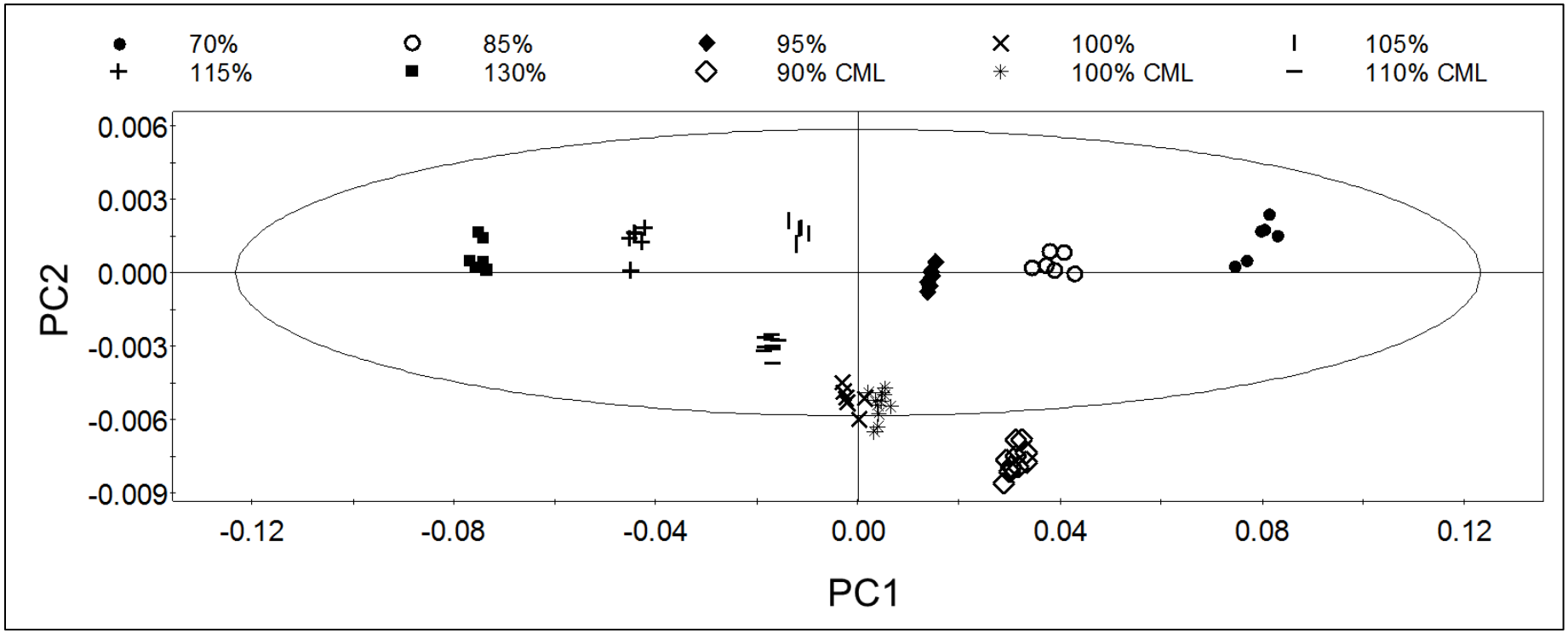

Figure 5.6 PCA scores plot of the CM tablet samples projected onto the optimized NIR calibration model ellipse. *CML* indicates samples prepared using the continuous manufacturing line

The accuracy of both optimized NIR calibration models (spectral range and CSS optimizations) was evaluated using five independent tablet sets prepared using the CM process. These independent runs were performed on different days using different API and excipient lot numbers, not included in the model. **Table 5.9** shows the results obtained using both NIR calibration model optimizations (spectral range and CSS). Run #5, shown under optimization #2, shows the results obtained two years after the NIR calibration model was optimized. Results showed that the overall NIR predicted concentrations of the five CM runs. obtained with the optimized NIR calibration model (CSS optimization), yielded RMSEP and bias values of less than 2.0% with standard deviations of less than 1.0%, improving the RMSEP by 50% when compared to the spectral range optimized model. The low bias obtained from the CSS optimized model demonstrates the suitability of the NIR calibration model performance. The low standard deviations demonstrate the high precision of the model. Therefore, the addition of CM line samples improved the accuracy of the model predictions, without jeopardizing its precision.

A paired t-test was performed to determine if there was a statistically significant mean difference between the results obtained using the spectral range optimized model and the CSS optimized model. Statistical differences were found between both optimizations with p-values < 0.005 (p-value of 0.000) for all four CM runs. In addition, a paired-sample t-test was performed between the HPLC results and the NIR predicted concentration obtained from both optimized models. **Table 5.9** shows the HPLC results and the predicted concentrations obtained using both optimized models. None of the NIR predicted concentrations obtained with the spectral range optimized model were statistically similar (p-values < 0.005); however, NIR predicted concentrations obtained with the CSS optimized model were statistically similar for Run #1 and Run #3 (target API concentrations of 90% and 100% LC) with p-values < 0.060 and 0.400, respectively. These results confirm that including CSS samples prepared using the CM process increases the accuracy of the predictions.

Table 5.9 Comparison of results obtained from both NIR calibration model optimizations (spectral range and CSS)

Run #	Average HPLC conc. (% LC) n=10	Average NIR API prediction (% LC) n=10	SD (%)	RMSEP	Bias (%)
Optimization #1: spectral range					
1	90.1	88.3	0.8	2.0	1.9
2	97.2	94.8	0.4	2.4	2.4
3	100.0	98.4	0.4	1.6	1.5
4	109.7	106.6	0.9	3.2	3.1
Optimization #2: CSS					
1	90.1	89.6	0.8	1.0	0.6
2	97.2	96.2	0.4	1.1	1.0
3	100.0	99.8	0.5	0.5	0.2
4	109.7	108.0	0.9	1.9	1.7
5	100.1	100.2	0.4	0.4	0.1

Run # 1 p-value < 0.05 / Run # 3 p-value < 0.30

5.4 Conclusion

This study provides additional evidence of the high accuracy provided by NIR spectroscopy when used to predict drug concentration in tablets. An excellent agreement of results was obtained between HPLC and the CSS optimized model. The importance of including the expected process variability in the calibration model, was demonstrated. Results demonstrated that including CSS samples prepared using the CM process, added enough process variation to the model leading to more accurate predictions of CM tablets. This work also demonstrated the importance of selecting the correct spectral range for model development based on the analyte (API) of interest to avoid the effect of water bands associated with the exchange of solvate molecules with water in the environment.

5.5 References

1. Ierapetritou M, Ramachandran R, editors. Process Simulation and Data Modeling in Solid Oral Drug Development and Manufacture. 1 ed., 2016.

2. Singh R, Román-Ospino AD, Romañach RJ, Ierapetritou M, Ramachandran R. Real time monitoring of powder blend bulk density for coupled feed-forward/feed-back control of a continuous direct compaction tablet manufacturing process. International journal of pharmaceutics. 2015;495(1):612-25.

3. Colón YM, Florian MA, Acevedo D, Méndez R, Romañach RJ. Near Infrared Method Development for a Continuous Manufacturing Blending Process. Journal of Pharmaceutical Innovation. 2014;9(4):291-301.

4. Langhauser K. Janssen's Historic FDA Approval. The FDA has approved -- for the first time in history -- a manufacturer's production method change from "batch" to continuous manufacturing. In: Pharmaceutical Manufacturing. http://www.pharmamanufacturing.com/articles/2016/janssens-historic-fda-approval/. 2016. Accessed July 23, 2016.

5. Thayer AM. Continuous drug production advances. AMER CHEMICAL SOC 1155 16TH ST, NW, WASHINGTON, DC 20036 USA. 2016. Accessed November 2, 2016.

6. Vanarase AU, Osorio JG, Muzzio FJ. Effects of powder flow properties and shear environment on the performance of continuous mixing of pharmaceutical powders. Powder technology. 2013;246:63-72.

7. Mehrotra A, Llusa M, Faqih A, Levin M, Muzzio FJ. Influence of shear intensity and total shear on properties of blends and tablets of lactose and cellulose lubricated with magnesium stearate. International journal of pharmaceutics. 2007;336(2):284-91.

8. Llusa M, Levin M, Snee RD, Muzzio FJ. Shear-induced APAP de-agglomeration. Drug development and industrial pharmacy. 2009;35(12):1487-95.

9. Järvinen MA, Paaso J, Paavola M, Leiviskä K, Juuti M, Muzzio F et al. Continuous direct tablet compression: effects of impeller rotation rate, total feed rate and drug content on the tablet properties and drug release. Drug development and industrial pharmacy. 2013;39(11):1802-8.

10. Gupta A, Peck GE, Miller RW, Morris KR. Nondestructive measurements of the compact strength and the particle-size distribution after milling of roller compacted powders by near-infrared spectroscopy. Journal of pharmaceutical sciences. 2004;93(4):1047-53.

11. Barajas MJ, Cassiani AR, Vargas W, Conde C, Ropero J, Figueroa J et al. Near-Infrared Spectroscopic Method for Real-Time Monitoring of Pharmaceutical Powders During Voiding. Appl Spectrosc. 2007;61(5):490-6.

12. Mateo-Ortiz D, Colon Y, Romañach RJ, Méndez R. Analysis of powder phenomena inside a Fette 3090 feed frame using in-line NIR spectroscopy. Journal of pharmaceutical and biomedical analysis. 2014;100:40-9.

13. Blanco M, Peguero A. Influence of physical factors on the accuracy of calibration models for NIR spectroscopy. Journal of pharmaceutical and biomedical analysis. 2010;52(1):59-65.

14. Singh R, Velazquez C, Sahay A, Karry KM, Muzzio FJ, Ierapetritou MG et al. Advanced Control of Continuous Pharmaceutical Tablet Manufacturing Processes. In: Ierapetritou MG, Ramachandran R, editors. Process Simulation and Data Modeling in Solid Oral Drug Development and Manufacture. Methods in Pharmacology and Toxicology, 2016. p. 191-224.

15. Martínez L, Peinado A, Liesum L, Betz G. Use of near-infrared spectroscopy to quantify drug content on a continuous blending process: Influence of mass flow and rotation speed variations. European Journal of Pharmaceutics and Biopharmaceutics. 2013;84(3):606-15.

16. Shi Z, McGhehey KC, Leavesley IM, Manley LF. On-line monitoring of blend uniformity in continuous drug product manufacturing process—The impact of powder flow rate and the choice of spectrometer: Dispersive vs. FT. Journal of pharmaceutical and biomedical analysis. 2016;118:259-66.

17. Pasikatan MS, JL; Spillman, CK; Haque, E. Near Infrared Reflectance Spectroscopy for online particle size analysis of powders and ground material. J Near Infrared Spectrosc. 2001;9:153-64.

18. Alcala M, Blanco M, Bautista M, Gonzalez JM. On-line monitoring of a granulation process by NIR spectroscopy. Journal of pharmaceutical sciences. 2010;99(1):336-45.

19. Romañach R, Román-Ospino A, Alcalà M. A Procedure for Developing Quantitative Near Infrared (NIR) Methods for Pharmaceutical Products. In: Ierapetritou MG, Ramachandran R, editors. Process Simulation and Data Modeling in Solid Oral Drug Development and Manufacture. Methods in Pharmacology and Toxicology: Springer New York; 2016. p. 133-58.

20. Shi Z, Cogdill RP, Short SM, Anderson CA. Process characterization of powder blending by near-infrared spectroscopy: blend end-points and beyond. Journal of pharmaceutical and biomedical analysis. 2008;47(4):738-45.

21. Liew CV, Karande AD, Heng PW. In-line quantification of drug and excipients in cohesive powder blends by near infrared spectroscopy. International journal of pharmaceutics. 2010;386(1-2):138-48.

22. Càrdenas V, Blanco M, Alcalà M. Strategies for selecting the calibration set in pharmaceutical near infrared spectroscopy analysis. A comparative study. Journal of Pharmaceutical Innovation. 2014;9(4):272-81.

23. Alcala M, Leon J, Ropero J, Blanco M, Romanach RJ. Analysis of low content drug tablets by transmission near infrared spectroscopy: selection of calibration ranges according to multivariate detection and quantitation limits of PLS models. Journal of pharmaceutical sciences. 2008;97(12):5318-27.

24. Boiret M, Meunier L, Ginot YM. Tablet potency of Tianeptine in coated tablets by near infrared spectroscopy: model optimisation, calibration transfer and confidence intervals. Journal of pharmaceutical and biomedical analysis. 2011;54(3):510-6.

25. Blanco M, Alcalá M. Content uniformity and tablet hardness testing of intact pharmaceutical tablets by near infrared spectroscopy: a contribution to process analytical technologies. Analytica Chimica Acta. 2006;557(1):353-9.

26. Pieters S, Saeys W, Van den Kerkhof T, Goodarzi M, Hellings M, De Beer T et al. Robust calibrations on reduced sample sets for API content prediction in tablets: definition of a cost-effective NIR model development strategy. Anal Chim Acta. 2013;761:62-70.

27. Aldridge P, Mushinsky R, Andino M, Evans C. Identification of tablet formulations inside blister packages by near-infrared spectroscopy. Applied spectroscopy. 1994;48(10):1272-6.

28. Blanco M, Coello J, Iturriaga H, Maspoch S, Serrano D. Near-infrared analytical control of pharmaceuticals. A single calibration model from mixed phase to coated tablets. Analyst. 1998;123(11):2307-12.

29. Blanco M, Eustaquio A, Gonzalez J, Serrano D. Identification and quantitation assays for intact tablets of two related pharmaceutical preparations by reflectance near-infrared spectroscopy: validation of the procedure. Journal of pharmaceutical and biomedical analysis. 2000;22(1):139-48.

30. Chen Y, Thosar SS, Forbess RA, Kemper MS, Rubinovitz RL, Shukla AJ. Prediction of drug content and hardness of intact tablets using artificial neural network and near-infrared spectroscopy. Drug development and industrial pharmacy. 2001;27(7):623-31.

31. Broad NW, Jee RD, Moffat AC, Smith MR. Application of transmission near-infrared spectroscopy to uniformity of content testing of intact steroid tablets. Analyst. 2001;126(12):2207-11.

32. Ebube N, Thosar S, Roberts R, Kemper M, Rubinovitz R, Martin D et al. Application of near-infrared spectroscopy for nondestructive analysis of Avicel® powders and tablets. Pharmaceutical development and technology. 1999;4(1):19-26.

33. Blanco M, Cruz J, Bautista M. Development of a univariate calibration model for pharmaceutical analysis based on NIR spectra. Analytical and bioanalytical chemistry. 2008;392(7-8):1367-72.

34. Brittain HG. Polymorphism and Solvatomorphism 2007. Journal of pharmaceutical sciences. 2009;98(5):1617-42.

35. Variankaval N, Sheth A. Physical Stability of Crystal Forms-Implications in Drug Development. AMERICAN PHARMACEUTICAL REVIEW. 2007;10(6):96.

36. Van Veen B, Van der Voort Maarschalk K, Bolhuis G, Visser M, Zuurman K, Frijlink H. Pore formation in tablets compressed from binary mixtures as a result of deformation and relaxation of particles. European journal of pharmaceutical sciences. 2002;15(2):171-7.

37. Rehula M, Adamek R, Spacek V. Stress relaxation study of fillers for directly compressed tablets. Powder technology. 2012;217:510-5.

38. Armstrong N, Haines-Nutt R. Elastic recovery and surface area changes in compacted powder systems. Powder Technology. 1974;9(5-6):287-90.

39. David S, Augsburger L. Plastic flow during compression of directly compressible fillers and its effect on tablet strength. Journal of pharmaceutical sciences. 1977;66(2):155-9.

40. Rees J, Rue P. Time-dependent deformation of some direct compression excipients. Journal of Pharmacy and Pharmacology. 1978;30(1):601-7.

41. Ebba F, Piccerelle P, Prinderre P, Opota D, Joachim J. Stress relaxation studies of granules as a function of different lubricants. European journal of pharmaceutics and biopharmaceutics. 2001;52(2):211-20.

42. Anuar M, Briscoe B. The elastic relaxation of starch tablets during ejection. Powder Technology. 2009;195(2):96-104.

43. Anuar MS, Briscoe B. Interfacial elastic relaxation during the ejection of bi-layered tablets. International journal of pharmaceutics. 2010;387(1):42-7.

44. Baily E, York P. An apparatus for the study of strain recovery in compacts. Journal of Materials Science. 1976;11(8):1470-4.

45. Picker KM. The automatic micrometer screw. European journal of pharmaceutics and biopharmaceutics. 2000;49(2):171-6.

46. European Medicines Agency. Guideline on the use of near infrared spectroscopy by the pharmaceutical industry and the data requirements for new submissions and variations. Westferry Circus, Canary Wharf, London 2014.

47. Sanchez-Paternina A, Roman-Ospino AD, Martinez M, Mercado J, Alonso C, Romanach RJ. Near infrared spectroscopic transmittance measurements for pharmaceutical powder mixtures. Journal of pharmaceutical and biomedical analysis. 2016;123:120-7.

48. Meza CP, Santos MA, Romanach RJ. Quantitation of drug content in a low dosage formulation by transmission near infrared spectroscopy. AAPS PharmSciTech. 2006;7(1):E29.

49. Xiang D, Lobrutto R, Cheney J, Wabuyele BW, Berry J, Lyon R et al. Evaluation of Transmission and Reflection Modalities for Measuring Content Uniformity of Pharmaceutical Tablets with Near-Infrared Spectroscopy. Appl Spectrosc. 2009;63(1):33-47.

50. Weyer LG, Lo SC. Spectra– Structure Correlations in the Near-Infrared. Handbook of Vibrational Spectroscopy. John Wiley & Sons, Ltd; 2006.

51. Picker KM. Time dependence of elastic recovery for characterization of tableting materials. Pharmaceutical development and technology. 2001;6(1):61-70.

52. Ropero J, Colon Y, Johnson-Restrepo B, Romanach RJ. Near-infrared chemical imaging slope as a new method to study tablet compaction and tablet relaxation. Applied spectroscopy. 2011;65(4):459-65.

53. Macias K, Jayawickrama D, McGeorge G. The Impact of Elastic Recovery on Near- Infrared Tablet Predictions. American Pharmaceutical Review. 2011;14(7).

54. Kirsch JD, Drennen JK. Nondestructive tablet hardness testing by near-infrared spectroscopy: a new and robust spectral best-fit algorithm. Journal of pharmaceutical and biomedical analysis. 1999;19(3):351-62.

6 Concluding Remarks

6.1 Contributions

The studies presented under this dissertation were part of the investigations performed for the implementation of the first commercial FDA approved continuous manufacturing line in Puerto Rico. Throughout the years, chemistry and chemists have been linked to laboratory work, analytical testing of manufacturing products, and quality assurance, after production is completed. However, this dissertation demonstrates the need of chemists in the manufacturing process to develop innovative ways to monitor chemical and physical properties of materials during pharmaceutical productions.

The implementation of continuous manufacturing processes delivers high quality end products. However, this is not the only advantage. **Figure 6.1** shows some of the benefits that accompany the implementation of continuous manufacturing processes. These percentages are based on the actual benefits achieved due to the implementation of the CM process discussed in this dissertation.

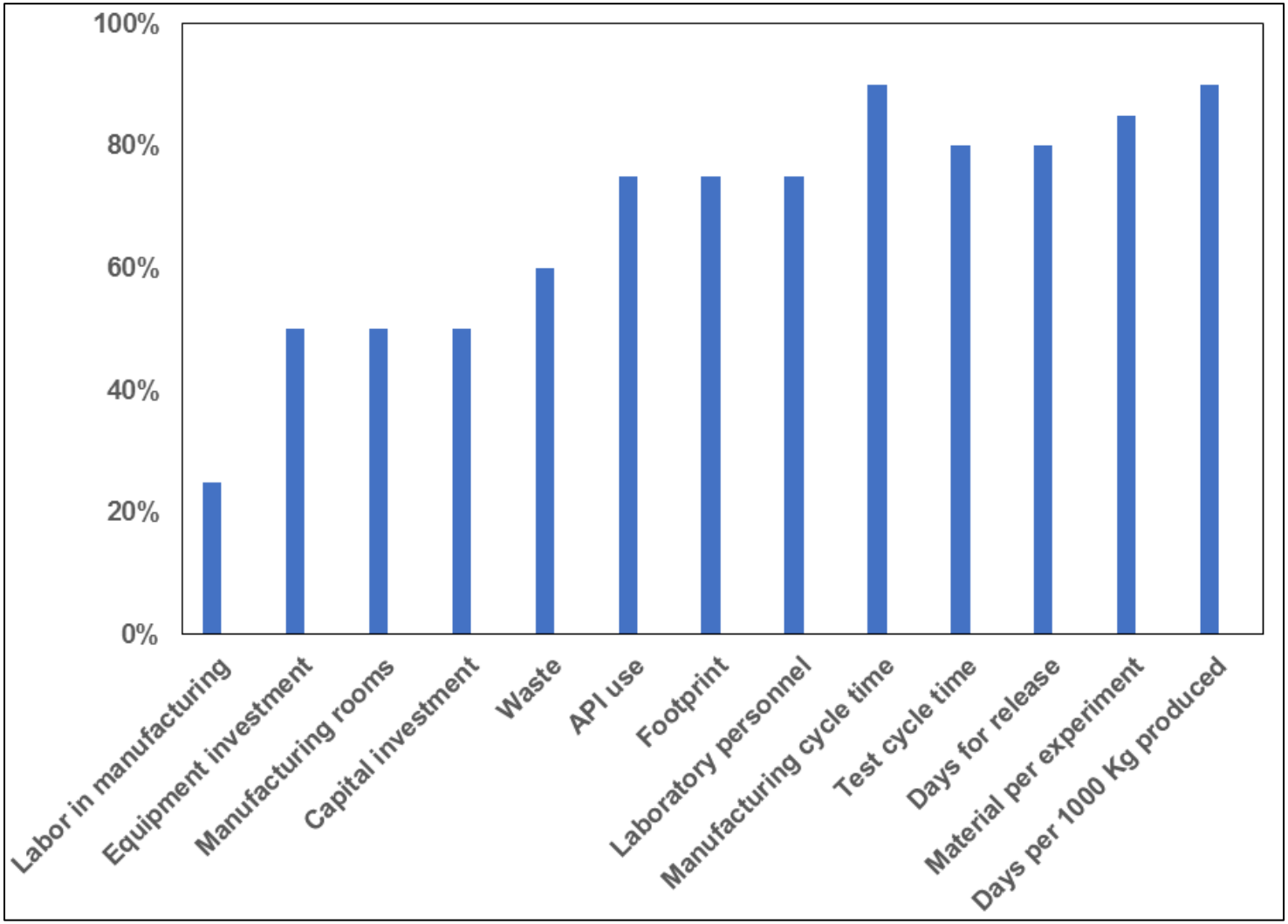

Figure 6.1 Plot of the reduction (in percentage, %) achieved due to the implementation of a continuous manufacturing process